AD_____

Award Number: DAMD17-99-1-9560

TITLE: Genetic Evaluation of Peripheral Nerve Sheath Tumors in Neurofibromatosis Type I

PRINCIPAL INVESTIGATOR: David H. Viskochil, M.D., Ph.D.

CONTRACTING ORGANIZATION: University of Utah
Salt Lake City, Utah 84102-1870

REPORT DATE: October 2002

TYPE OF REPORT: Annual

PREPARED FOR: U.S. Army Medical Research and Materiel Command
Fort Detrick, Maryland 21702-5012

REPORT DOCUMENTATION PAGE

Form Approved
OMB No. 074-0188

1. AGENCY USE ONLY (Leave blank)	2. REPORT DATE	3. REPORT TYPE AND DATES COVERED
	October 2002	Annual (1 Oct 01 - 30 Sep 02)

4. TITLE AND SUBTITLE
Genetic Evaluation of Peripheral Nerve Sheath Tumors in Neurofibromatosis Type I

5. FUNDING NUMBERS
DAMD17-99-1-9560

6. AUTHOR(S):
David H. Viskochil, M.D., Ph.D.

7. PERFORMING ORGANIZATION NAME(S) AND ADDRESS(ES)
University of Utah
Salt Lake City, Utah 84102-1870

E-Mail: dave.viskochil@hsc.utah.edu

8. PERFORMING ORGANIZATION REPORT NUMBER

9. SPONSORING / MONITORING AGENCY NAME(S) AND ADDRESS(ES)
U.S. Army Medical Research and Materiel Command
Fort Detrick, Maryland 21702-5012

10. SPONSORING / MONITORING AGENCY REPORT NUMBER

11. SUPPLEMENTARY NOTES
report contains color

12a. DISTRIBUTION / AVAILABILITY STATEMENT
Approved for Public Release; Distribution Unlimited

12b. DISTRIBUTION CODE

13. Abstract ***(Maximum 200 Words)*** *(abstract should contain no proprietary or confidential information)*

The goal of this research project is to identify molecular changes that are associated with the progression of a peripheral nerve sheath tumor (PNST) from benign to malignancy. Archival and prospectively acquired benign PNSTs and malignant PNSTs are collected, and molecular changes at the *NF1* locus and throughout the genome are assessed. In addition, immunohistological evaluations of benign plexiform neurofibromas and malignant peripheral nerve sheath tumors are performed. We have begun preliminary analyses of immunohistochemical phenotypes of the tumors and genome-wide screen tetra-nucleotide screen for allelic imbalance, as a marker for accumulation of somatic mutations in PNSTs. In addition to the genome-wide screen, we have evaluated high-grade MPNSTs that have aberrant p53 immunoreactivity for *TP53* mutations. Other candidate genes have not been screened as rigorously for somatic mutations. Tumor heterogeneity has been assessed for benign and malignant PNSTs, and appears to be somewhat stable in benign tumors versus those undergoing malignant transformation. In addition to mutation analysis of PNSTs, we have developed high-throughput germline *NF1* mutation screening.

14. SUBJECT TERMS	15. NUMBER OF PAGES
tumor suppressor gene, p53, immunohistochemistry, LOH, mutations	125
	16. PRICE CODE

17. SECURITY CLASSIFICATION OF REPORT	18. SECURITY CLASSIFICATION OF THIS PAGE	19. SECURITY CLASSIFICATION OF ABSTRACT	20. LIMITATION OF ABSTRACT
Unclassified	Unclassified	Unclassified	Unlimited

TABLE OF CONTENTS

INTRODUCTION

Peripheral nerve sheath tumors (PNSTs) are soft tissue tumors that are associated with neurofibromatosis type 1 (NF1). These tumors can undergo malignant transformation, however the mechanisms that are involved in this process are not known. The goal of this research project is to identify the molecular changes that are associated with the progression of a PNST from a benign to a malignant state. To carry out this project, archival and prospectively acquired PNSTs from NF1 individuals are examined for consistent immunohistochemical and genetic abnormalities. The samples are examined for expression of a set of informative immunologic markers in multiple sites of the tumor, if available. Relatively routine histologic analysis enables one to distinguish benign plexiform neurofibromas from high-grade MPNSTs. It does not easily determine diagnosis of benign plexiform neurofibroma with atypia versus low-grade MPNST. Special immunohistochemical stains are being applied to PNSTs, especially those that are low-grade MPNSTs, to define immunophenotypes that could prove helpful for pathologists to assess malignant transformation. In addition, genetic analysis of corresponding immunostained sections is performed. Genetic analysis includes screening for constitutional *NF1* mutations in white blood cells (if available) of patients with NF1-related PNST, identification of somatic loss of the normal *NF1* allele in tumor specimens, and allelic imbalance analysis of a subset of genomic markers representing each of the chromosome arms. Differences between benign PNSTs (plexiform neurofibromas) and malignant PNSTs are duly noted, and provide relevant data helpful in the identification of potential candidate genes that could play a role in the process of malignant transformation. As candidate genes, genetic analyses of the *TP53* and *INK4A/CDKN2A* genes are now being performed to identify somatic mutations in tumor tissue.

BODY

ARCHIVAL SPECIMENS

Identify genetic changes associated with malignant transformation in archival specimens

Task 1: Months 1-15 Obtain tumor specimens and perform pathology studies
Comment: Tumor collection still in progress. Some results are pending.

The University of Utah and Department of the Army provided human subjects approval for this study in August 2000. Tumor specimens are still currently being identified and collected. Pathology sections from several archived blocks of malignant PNSTs (MPNSTs) have been prepared for immunohistochemistry analysis of p53, p16, p27, Bcl-2, CD57 (Leu7), S100, CD34, Mib-1, topoisomerase I (TOPO1) and topoisomerase II-alpha (TOPO2). The immunohistochemical stains for 46 archival tumor specimens have been evaluated by our collaborators, Dr. Cheryl Coffin and Dr. Holly Zhou (pathologists at the University of Utah). There were 19 plexiform neurofibromas and 27 MPNSTs. Our work was initially presented at the United States and Canadian Academy of Pathology (Chicago, IL, 2/25/02). This is the first report comparing this set of immunohistochemical markers between benign, low-grade and high-grade peripheral nerve sheath tumors. The details of this work are provided in the appendix as a manuscript that has been prepared and submitted for peer review. We concluded that p53, p16, and p27 immunohistochemical staining is associated with tumor progression, however they do not distinguish low-grade MPNST from benign plexiform neurofibromas. Nevertheless, p53 expression is a consistent marker for high tumor grade. There was also a higher frequency of p53 expression in NF1-related versus sporadic high-grade MPNSTs. This observation supports published work by Liapis *et al.* (1999), which is in contrast to Halling *et al.* (1996).

Additional studies on this same set of archived peripheral nerve sheath tumors are underway with different antibodies directed against epidermal growth factor receptor (EGFR) and mast cells. In previous work, increased immunoreactivity of EGFR has been shown to be associated with PNST progression (DeClue *et al.* 2001) (appended). An abstract regarding the EGFR immunohistochemical staining patterns of this set of tumors has been submitted to the United States and Canadian Academy of Pathology for presentation at its annual meeting in February 2003 (see appendix). Mast cell infiltration in PNST formation has been proposed to play a central role in the initiation of neurofibromas (Zhu *et al.*, 2002), therefore we have embarked on mast cell immunohistochemical staining of this same set of archived tumors.

The findings that p53 immunoreactivity is abnormal in high-grade MPSNTs coupled with the *Nf1/Tp53* double mutant mouse model for high-grade, triton-like MPNSTs (Cichowski *et al.*, 1999; Vogel *et al.*, 1999) suggests that abnormal *TP53* is potentially the most important somatic mutation that leads to tumor progression in NF1-related MPNSTs. These observations refocused our efforts toward the dual analysis of the *TP53* locus for somatic mutations in DNA extracted from tumors (see tasks 6 and 20) and the detailed immunohistochemical staining for p53 and p16 in multiple sections of PNST

tissue blocks. We have submitted a proposal to the US Army Medical Research and Materiel Command NFRP02 (Log#NF020074; September, 17, 2002) to expand these studies with respect to p53 analysis. The technical abstract for this submission is appended.

Task 2: Months 1-24 Select and begin microdissection across transition zones
Comment: This task is in progress, and has been modified according to the amount of tissue in an individual section.

Microdissection experiments have been carried out to determine the robustness of the technique to obtain DNA template for allelic imbalance analysis. These experiments have been carried out on a prospectively acquired MPNST, and on several dermal neurofibromas that were mentioned in the previous annual report. In the last report we noted that the amount of DNA used in the genotyping and allelic imbalance analysis is critical to the reproducibility of the data. Therefore, two strategies have since been implemented. The first is to harvest as much tissue from the section of interest as possible. This is accomplished by either harvesting more tissue by laser capture microdissection (LCM), or if the section appears homogeneous, by simply scraping off the section of tissue with a clean sterile syringe needle. The second strategy that has been implemented is the technique of primer-extension pre-amplification polymerase chain reaction (PEP-PCR) according to Paulson et al., (1999) [1]. This technique amplifies the whole genome using random oligomers 15 nucleotides in length. This second strategy is outlined in task 3.

We have identified 24 archived tumors that clearly show clonal areas of mitoses and nuclear atypia that signify high-grade MPNST. Likewise, we have identified tumors that have benign-appearing foci in the context of an MPNST (see figures 3 and 4 in the appended Zhou *et al* manuscript). These sections will be microdissected and assayed for genomic imbalances indicative of somatic mutation.

Task 3: Months 4-30 Genotyping and allelic imbalance analysis of microdissected DNA
Comment: This task is in progress, and has been modified by the addition of another method.

In order to have reproducible microdissection data, the method of PEP-PCR has been implemented. Microdissected DNA is purified using the Puregene® DNA isolation kit from Gentra Systems. 500µl of cell lysis solution from the kit is added to 100µl of crude DNA extract. This is mixed by pipetting, 200µl of protein precipitation solution is added and vortexed for 20sec. The mixture is placed on ice for 5min, then centrifuged at 12000g for 3min at room temperature in a microfuge. 600µl of isopropanol is added to the supernatant and mixed gently by inverting the tube 50 times to precipitate the DNA. The DNA is then collected by centrifugation at 12000g, for 5min at 4°C in a microfuge. The DNA pellet is washed using 75%(v/v) ethanol, air-dried for 5min and resuspended in 30µl sterile H_20.

The isolated DNA serves as template in the PEP-PCR. The DNA is mixed with 400μM random 15mer random primers (Operon), 1×PCR buffer, 300μM dNTP mixture, 2.5mM $MgCl_2$, and 5U of *Taq* DNA polymerase (Gibco-BRL). Cycling conditions are 1min at 95°C, 2min at 37°C, ramp up to 55°C at 10sec/degree, hold at 55°C for 4min and repeat cycling for 49 cycles with a final hold at 4°C. The resulting product is subjected to specific PCR reactions for each marker. There is a size limitation associated with this method, and the largest product we can amplify is in the range of 300 base pairs. This has limited our ability to use the ABI automated genotype analyzer for allelic imbalance studies. Therefore, PEP-PCR products from microdissected samples are limited in the number of genetic loci that can be tested. We have applied the technique to direct mutation analysis of TP53 from a subset of high-grade MPNSTs shown to have high p53 immunostaining.

Figure 1 shows the microdissected H&E section for tumor #1949713 and the *TP53* PCR-based single strand conformation polymorphism (SSCP) analysis of exon 5 to examine for somatic mutation of the *TP53* gene in a specimen that has aberrant p53 staining. This section corresponds to the tumor represented as figures 3 and 4 in the appended Zhou *et al.* manuscript. This analysis enables us to screen for TP53 mutations in areas of the tumor that show high immunoreactivity for p53. In addition to SSCP analysis, we have been able to DNA sequence individual *TP53* exons. Figure 2 shows PCR products for *TP53* exons 4 – 8, and figure 3 shows the DNA sequence generated from the respective PCR products.

Task 4: Months 12-30 Statistical analysis of allelic imbalance analysis in genomic regions that are candidates for harboring genes important in malignant transformation
Comment: This task has not been initiated.

The statistical analysis has not yet begun. We now recognized that tumor material from paraffin blocks is not adequate for robust genome-wide allelic imbalance studies. This material has been used to analyze specific loci. Archival samples that have been frozen are adequate for allelic imbalance studies, but the number of archival tumors that we have collected which were initially frozen are too few to perform detailed statistical analysis. We have obtained permission to extend our study to obtain more archival samples.

Task 5: Months 18-34 Expand allelic imbalance analysis in candidate regions
Comment: This task is in progress.

We have found that the genomes of the dermal neurofibromas and benign PNSTs appear very stable, and allelic imbalance at any given genomic locus is rare. On the other hand, MPNSTs demonstrate a number of marker loci that are in imbalance. Consistent loci demonstrating imbalances have not been identified, however 2 potential candidate regions (17p for *TP53*; 9p21 for *INK4A/CDKN2A*) in MPNSTs have been identified from published work (Berner *et al*, 1999; Kourea *et al*, 1999; Nielson *et al*, 1999). We are in process of screening each locus in detail (see tasks 6 and 20). We have not yet identified

another locus that merits detailed expansion of the genetic marker analysis. Potential candidates are any loci that show allelic imbalance. One such candidate locus is the *EGFR* gene. The finding of over-expression of EGFR in MPNSTs (DeClue *et al*, 2000; appended) suggests that the gene could be amplified in genomic DNA. The closest genetic marker for the EGFR locus on the short arm of chromosome 7 has not demonstrated allelic imbalance in our set of PNSTs. This suggests that the overexpression is not due amplification of the genome harboring the *EGFR* gene. Other regulatory processes likely play a significant role in EGFR over-expression.

Once consistent allelic imbalance has been demonstrated at genetic marker locus, our intention is to use additional genetic markers on the same chromosome arm to delineate potential transitions from allele balance to allelic imbalance. Our genotyping core at the University of Utah has developed an adequate number of genetic loci for each chromosome arm, which will enable us to provide them samples for further analysis, after loci are identified as having consistent allelic imbalance in high-grade tumor tissue.

Task 6: Months 6-18 Screen known candidate genes for mutations
Comment: Most of the work is still in progress.

One candidate gene that we investigated involved the t(X;18) chromosomal translocation, commonly observed in synovial sarcomas (Dos Santos *et al.* 2001). The breakpoint genes have been identified as *SYT* from chromosome 18, and *SSX* from the X chromosome (deLeeuw *et al.*, 1994; Clark *et al.*, 1994). However, it was recently reported that this chromosomal translocation was also observed in MPNSTs [2]. We determined that the t(X;18) chromosomal translocation could not be found in dermal neurofibromas, benign PNSTs or MPNSTs from patients with NF1. Our results have been published in the journal Pediatric and Developmental and Pathology (see Appendix).

The assays for candidate genes *TP53* and *INK4A/CDKN2A* are currently being optimized. As was mentioned in the first annual report, it was planned that a PCR product would be generated from genomic DNA for exons 4-8 of *TP53*, which could then be sequenced to find mutations. At this stage, the PCR reaction works well for genomic DNA derived from tumor tissue, and we have sequenced some PCR products without identification of *TP53* mutations. We are presently screening DNA extracted from adjacent slide sections of high-grade MPNSTs that demonstrated abnormal p53 immunoreactivity (see task 3). This has turned out to be more challenging, because it is difficult to amplify large PCR products from the genomic DNA extracted from paraffin-embedded tissue. We have re-designed the primers used in the *TP53* screen to make several smaller PCR products spanning individual *TP53* exons instead of one large product. Figure 4 in Zhou et al. (appended manuscript) shows a high-grade MPNST in which an adjacent section was microdissected (figure 1) and its DNA screened for *TP53* mutations by SSCP (single-strand conformation polymorphism) and direct DNA sequencing (figures 2 and 3). These finding are consistent with Lothe et al (2001) who failed to identify *TP53* mutations in 16 PNSTs. The association of p53 immunoreactivity and lack of mutations of TP53 in high-grade MPNSTs has yet to be explained.

Deletions of the *INK4A/CDKN2A* locus, also known as the *p16* gene, have been implicated in MPNST development (Kourea *et al.*, 1999). We have synthesized primer

sets for 4 genetic markers that span the *P16* locus; *D9S274* (151-171bp), *D9S137* (133-149bp), *D9S156* (133-155bp), and *D9S162* (172-186bp). Three blood-MPNST (archived tumor tissue) pair DNA samples have been analyzed for allelic imbalance by denaturing gel electrophoresis of end-labeled PCR products. Only one of the blood samples was heterozygous (at *D9S137* and *D9S162*) and neither marker demonstrated allelic imbalance. Microdissection of this sample was not performed, but our demonstration that these markers are robust on tumor tissue enables us to apply this marker set to other archived PNST samples.

In summary, we have completed screening of RNA samples collected from frozen MPNSTs for the t(X;18) chromosomal translocation, however none show such an abnormality (see appended manuscript, Liew *et al*, 2002). We have designed rigorous screening techniques for *NF1* gene mutation analysis by high-throughput DNA sequencing. We have designed primer sets to screen the *P16* locus for allelic imbalance and we have screened the *TP53* locus for somatic mutations in peripheral nerve sheath tumors.

Task 7: Months 24-36 Screen candidate genes identified in this proposal
Comment: This task is in progress.

Apart from the known candidate genes being tested, no others have yet been identified experimentally, so screening of other genes has not yet begun.

Establish the degree of tumor heterogeneity in archival PNSTs

Task 8: Months 1-15 Obtain specimens and select foci for microdissection
Comment: This task is in progress.

We are continuing to select foci from the appropriate archival bank of tumors to complete this task. We are using immunohistochemical phenotyping of different sites in single tumors to determine areas that may be most informative in linking the immunophenotype with genetic studies. We recognize that having blood DNA from patients in whom we are dissecting foci is most informative for the genetic studies.

Task 9: Months 4-12 Perform genotyping and allelic imbalance analysis
Comment: This task is in progress.

Genotyping and allelic imbalance analysis is currently underway on an expanded set of tumors, including prospectively acquired samples with matched blood DNA from the subject. Blood/tumor genotype analysis is also covered in task 14. We now have data from 19 dermal neurofibromas, 7 benign PNSTs and 3 MPNSTs. These samples have been screened for allelic imbalance at a subset of genomic loci representing different chromosomal arms. These data show few markers with allelic imbalance in benign PNSTs, suggesting that these tumors are, in general, stable throughout the genome (see

Table 1). Only 1 of the benign PNSTs (36670) demonstrates LOH in this set of genetic markers (see table 2). These data are comparable to the results from the dermal neurofibromas, which were also very stable as stated in the previous report (see summary table 3). The more interesting data come from high-grade MPNSTs, which clearly show allelic imbalance at a number of genetic marker loci.

Genotyping of the *NF1* locus has been initiated on the archival tumors. We have started genotyping these tumors at the markers *GXAlu*, *D17S960*, $(GATN)_n$, a CA/GT repeat in intron 38, a CA/GT repeat in intron 27b, and single nucleotide polymorphic markers found at positions *NF1* cDNA 702, 2034, and 10647. Our results indicate that the genomic DNA extracted from many PNSTs clearly undergo loss of heterozygosity at *NF1* genetic marker loci (see figure 4).

Task 10: Months 12-18 Compare foci to establish the degree of tumor heterogeneity
Comment: This task is in progress.

To determine the degree of tumor heterogeneity, different pieces from the same tumor have been analyzed. This analysis has been extended into the other 6 benign PNSTs, and we have preliminary data from one of the MPNSTs (Table 1). The data demonstrate that in the benign PNSTs there are subtle signs of tumor genetic heterogeneity based on differential allelic imbalances between 5 different sampled sites in single PNSTs. Some of the markers have allelic imbalance in all of the sites sampled, while other markers have only a couple of sites with allelic imbalance. The best example of this experiment is shown for tumor 708429 (see table 1 and figure 5), whereby this benign PNST had but a few genetic loci demonstrating differences of allelic imbalance. Only genetic markers on chromosome 10p demonstrated allelic imbalance at all sampled sites. It implies that the somatic genetic mutation on 10p originated early in the clonal proliferation of Schwann cells, whereas other somatic genetic changes arise later in this particular tumor progression. In summating with other benign PNST data (table 1), there is only a mild degree of tumor heterogeneity in the benign plexiform neurofibromas.

In MPNST 306595, there are clear signs of intra-tumor genetic heterogeneity. Two markers have some sites that demonstrate allelic imbalance, whereas others are normal. The strongest evidence can be seen in the 2 markers with LOH, as there is only 1 site out of the 4 in each case that has LOH. There are 2 caveats to this data. The first is that there is presently no blood DNA data available to enable us to make a comparison with the tumor data. The second is that it is only 1 MPNST, and more tumors are needed to undergo this substantial analysis before genetic heterogeneity can be definitely concluded for malignant PNSTs.

PROSPECTIVE SPECIMENS

Identify common genetic alterations in prospectively acquired benign and malignant PNSTs

Task 11: Months 1-24 Obtain tumor/blood pairs
Comment: This task is in progress.

Tumor/blood pairs are still currently being collected. This has been difficult given the issues related to inter-institutional review board approval to collect and send pathologic specimens between non-affiliated academic centers. We are continuing our recruitment of other Centers, and we are also working with a consortium to develop a tissue core facility for collection of MPNSTs as part of a multi-center project to integrate Sarcoma Centers with NF Centers in the diagnosis and treatment of MPNSTs in individuals with NF1. A summary of the consortium meeting at Aspen in 2002 and a manuscript (Ferner and Gutmann, 2002) summarizing the first consortium meeting are appended.

Task 12: Months 1-24 Perform pathology analysis on PNSTs
Comment: This task has not yet been initiated.

Immunophenotyping has been performed on two prospectively acquired PNSTs (figures 6 and 7). Results from the immunohistochemical staining profiles of archived PNSTs (Zhou et al, appended manuscript) enabled us to select Mib-1, Topo IIa, p53, p16 and p27 as discriminating immunohistochemical markers in addition to the routine H&E and S100 stains used for every tumor specimen. Tumor 36670 (figure 6) has typical features of benign plexiform neurofibroma, and the allelic imbalance studies demonstrate that it has a very stable genome. Tumor 38628 (figure 7) shows a potential transition to malignancy, whereby increased p53 staining and nuclear atypia suggest changes associated with low-grade MPNST. Allelic imbalance studies performed on this tumor showed loss of heterozygosity for a number of genetic marker loci (table 1), which alerted us to the possibility that this otherwise benign-appearing PNST could be different that other plexiform neurofibromas. In reviewing the clinical pathology report, this tumor has been classified on clinic-pathologic criteria as a low-grade MPNST.

Now that immunohistochemical techniques have been developed, all prospectively acquired PNSTs will undergo an expanded set of antibody staining protocols as part of their assessment for correlation to genetic abnormalities.

Task 13: Months 1-34 Perform *NF1* germline mutation analysis on blood samples from prospectively enrolled subjects who have a PNST
Comment: This task is in progress.

Currently, we still evaluate cDNA PCR products from *NF1* mRNA extracted from white blood cells. Since the previous report, the new primers have been designed, and appear to work better. We continue to have problems amplifying product 1 from *NF1* cDNA. In addition to sequencing the coding region of *NF1*, we are also attempting to sequence the promoter region. This is turning out to be very difficult, as designing primers for this region is even more difficult than the coding region.

There is a risk in screening cDNA for mutations; some mutations result in mRNA instability leaving only 1 normal allele in the analysis. Our laboratory has moved to a new location adjacent to the University of Utah Genome Center directed by Professor Robert Weiss, which has provided us with an opportunity to develop a genomic DNA

sequencing protocol for *NF1* mutation detection. Dr. Weiss' laboratory team has established methodology for high throughput DNA sequencing for the detection of mutations in the Duchenne Muscular Dystrophy gene. With this success, his team agreed to collaborate on an effort to develop a genomic DNA mutation screen for germline *NF1* mutations in NF1 patients. This process was begun in Spring of 2002. We have designed primer sets that generate 1-kb fragments specific for the *NF1* locus from genomic DNA template. Automated, high-throughput sequencing has been performed on control DNA and 9 individuals with NF1 (see table 4).

NF1 mutations have been detected in 5 of the 9 individuals; 2 of which were know mutations used as a positive control. The five purported mutations include a frame-shift single-basepair deletion in exon 21, a frame-shift single-basepair deletion in exon 12b, nonsense mutation in exon 23-1, a frame-shift single-base deletion in exon 16 (corresponds to tumor 38628; see figure 8), and a frame-shift single-base deletion of exon 10a (corresponds to tumor 36670). These purported mutations detected by a high-throughput screen are now in the process of adjudication by focused DNA sequence analysis. This is proof of principle that high-throughput DNA sequence analysis can detect mutations, even in the presence of a normal allele.

In addition to mutations, this technique is robust in the detection of polymorphisms that may prove useful in other genetic studies. As shown in table 4, each subject's *NF1* genome has between 6 and 14 sequence variants that could represent polymorphisms. Each exon is spanned by approximately 800 basepairs of intron sequence in each PCR product that is sequenced, therefore potential functional polymorphisms may be detected that could modify the expression of *NF1* transcripts.

This technique has been included in the proposal submitted to the US Army MRMC NFRP02 Program (see technical abstract in the appendix). We hope to extend these studies to determine if there is a genotype-PNST phenotype correlation.

Task 14: Months 1-30 Genotype and perform allelic imbalance analysis blood/tumor pairs
Comment: This task is in progress.

Some genotyping or allelic imbalance analysis has been performed on prospectively acquired PNSTs (Tables 1 and 2). Results from other tumors that have been collected are currently being processed.

Of keen interest is tumor 38628, which appears low-grade by immunophenotype and had 10/36 genetic markers with LOH. The other MPNST 306595 had 2 sites of LOH when compared to other areas of the same tumor. There could be complete LOH at all four sampled sites for a number of loci that are presently scored as uninformative, but defining these additional sites requires a comparison to blood DNA to determine heterozygosity at such loci from constitutional genomic DNA.

Task 15: Months 1-18 Perform differential display by microarray analysis of PNST RNA
Comment: This task has been delayed.

No further microarray analysis has been performed. However, we are currently looking into modifying the current protocol, to compare tumors to a MPNST cell line. This would provide a more stable control in order to make comparisons. The original chips used for microarray at the University of Utah are specific for certain cancers, not sarcomas. We could not compare our data with other investigators using other chips. Approximately 2 years ago, Dr. Lor Randall began using an Alphametrix chip for all sarcomas collected at the University of Utah. He has analyzed the data in 4 MPNSTs in addition to other soft tissue tumors. In a collaborative effort, Dr. Randall has agreed to perform microarray analysis as part of a sarcoma center service for those tumors that we use for immunohistochemical and genomic allelic imbalance studies. We have isolated RNA from all prospectively acquired PNSTs, and cDNA has been synthesized for long-term storage. Likewise, Dr. Randall has collected a large percentage of MPNSTs that have been surgically resected at the University of Utah. This joint endeavor will ensure that tumor tissue is collected and is now available for this new microarray service provided by laboratory personnel affiliated with the sarcoma center.

Task 16: Months 12-30 Identify candidates by combining allelic imbalance/differential display
Comment: This task has not yet been initiated.

We have not linked our genomic allelic imbalance data with Dr. Randall's data on differential expression of genes in MPNSTs versus the standard fibroblast cell line genes. Since Dr. Randall is evaluating differences between sarcomas, he will likely identify genes that are specifically associated with Schwann cell proliferation in MPNSTs versus other soft tissue tumors. The analysis of MPNST microarray gene expression data is presently being performed on jointly acquired tumors samples. We meet with Dr. Randall approximately once a month to review the sarcoma center projects, and gene expression microarray data is presented only after it has been evaluated by his laboratory personnel. We have not compared data sets for the prospectively acquired tumors obtained under our protocols.

Task 17: Months 12-36 Compare allele imbalance differences of benign versus malignant PNSTs
Comment: This task has not yet been initiated.

More PNSTs are to be collected before statistically significant conclusions can be determined. In review of the data at hand, it appears that benign dermal and plexiform neurofibromas have few loci with allelic imbalance, whereas MPNSTs have much higher levels of allelic imbalance, including complete loss of heterozygosity. This is an expected result, as we suspect that benign tumors are genomically stable and malignant PNSTs accumulate a number of somatic mutations in the process of tumor progression.

Determine the level of *Ras*-activation in prospectively acquired PNSTs

Task 18: Months 3-30 Perform *Ras*-activation assays on frozen samples of PNSTs
Comment: This task has begun.

Nine tumor samples have been assayed in the last year (see table 5). Of these, 3 are prospectively acquired PNSTs of which 2 were processed into liquid nitrogen immediately upon collection.

Task 19: Months 12-36 Compare Ras GTP/GDP levels between benign and malignant PNSTs
Comment: This task has been delayed, pending more tumors to be collected.

The range of GTP/(GTP + GDP) ratios is quite variable. As a measure of ras activation, the data are not consistent. One MPNST (306595) is 3%, whereas a benign plexiform neurofibroma is 30%. We initially hypothesized that there would be higher GTP to (GTP+GDP) ratios for higher-grade PNSTs, even though it is known that benign plexiform neurofibromas have double inactivation of *NF1*. This data suggest that ras signaling may be influenced substantially by other genetic loci or gene expression patterns. We have a number of frozen samples that have not yet been analyzed, and before making any conclusions regarding this aberrance in expected data we will complete the studies on additional samples.

Determine somatic mutation status of candidate genes in PNST progression
Task 20: Months 1-30 Perform mutation analysis on known candidate genes
Comment: This task is in progress for *TP53*, but has not been initiated for *Nras*, *Hras* and *KRas*.

The mutation analysis will be performed on *TP53* as the PNSTs are acquired. In addition, we are developing primer sets to screen for mutations in *INK4A/CDKN2A*, also known as the *p16* gene. We are in process of designing primers to amplify each of the *P16* gene exons. Mutations will be screened by using a combination of single stranded conformational polymorphism (SSCP) analysis and direct sequencing. We have developed primer sets to screen for mutations in the gene known to cause Noonan syndrome, *PTPN11*. Individuals with NF1 who have a more remarkable phenotype, including higher numbers of dermal neurofibromas, sometimes fit a diagnosis of Noonan-NF syndrome. Likewise, individuals with Noonan syndrome have physical features found in NF1, and visa versa. This connection has suggested an overlapping biochemical pathway with neurofibromin and the *PTPN11* gene product, protein tyrosine phosphatase SHP-2. Noonan syndrome patients have recently been shown to have missense mutations in exon 3 (2/3 of all detectable mutations in Noonan syndrome patients), that lead to gain-of-function changes and excessive SHP-2 activity (Tartaglia et al, 2001). For this reason, tumor DNA has been screened for mutations in exon 3 of the *PTPN11* gene as a candidate modifier gene of proliferating Schwann cells. We developed PCR primers

(L:51211 and R:51748) to amplify a 537-bp product spanning the 207-bp exon. Using internal primers, DNA sequence analysis was carried out on both strands in 7 archived frozen PNST specimens. No *PTPN11* exon 3 mutations were identified.
Task 21: Months 18-36 Perform mutation analysis on candidate genes identified in this study
Comment: This task has not yet been initiated.

Once identified the candidate genes will be analyzed.

Task 22: Months 12-36 Compare mutation status of candidate genes in benign versus MPNSTs
Comment: This task has not yet been initiated.

Once acquired, the mutation status of candidate genes in benign versus MPNSTs will be compared.

Develop future NF1 investigators

Task 23: Months 1-18 Trainee develops, revises and streamlines protocols
Comment: This task is completed.

Dr. Michael Liew started work on this project, June 1st, 2000. He attended the NNFF, Inc Consortium meeting in June, 2000, and he has developed collaborations at the University of Utah to undertake additional techniques. He regularly attends seminar series at the Eccles Institute of Human Genetics and the Huntsman Cancer Institute. His protocols are continually being developed and streamlined. Last year, he attended the 51st Annual Meeting of the American Society of Human Genetics at San Diego, CA, from the 12th-16th of October, 2001. He presented a talk at the Neurofibromatosis symposium before the meeting, as well as a poster at the actual meeting. Finally, he completed a manuscript that was published in the journal Pediatric Development and Pathology. He attended the NNFF Consortium Meeting in June, 2002 and presented a poster entitled, a comparison of cell cycle/growth activation marker expression in plexiform neurofibromas and malignant peripheral nerve sheath tumors in NF1. Dr. Liew submitted 3 grant proposals during his tenure as trainee under this award. One proposal was funded by the Shriners Research Foundation (June, 2002). It is entitled, Immunohistochemical and Genetic Analysis of Tibial Pseudarthorsis in NF1 (Total amount of award - $16,500). Work outlined in the proposal was a continuation of the molecular techniques that he had applied to the peripheral nerve sheath tumors in NF1. Dr. Liew completed his fellowship July 12th, 2002. This was about 9 months premature because he obtained a position as staff scientist at ARUP (Associated Regional University Pathologists), which is an affiliated Laboratory of the Department of Pathology at the University of Utah. His training, with respect to the molecular biology of tumors associated with NF1, is now being applied in a research and development laboratory at ARUP. He satisfied the goals of the traineeship award, although Dr. Viskochil had hoped he would have pursued an independent academic career evaluating the link between growth factor receptors

(epidermal growth factor and insulin-like growth factor receptors) and cellular responses in cells derived from individuals with NF1.

In addition to work with a postdoctoral trainee, a dermatologist from Japan, Dr. Katsumi Tanito, has been training with David Viskochil and Michael Liew since September 2000. He is using similar techniques to screen a set of peripheral nerve sheath tumors from Japan.

David Viskochil has devoted a significant portion of his time developing a consortium with other investigators to address a number of issues with respect to MPNSTs in NF1. The consortium met in May, 2001 in London and June 2002 in Aspen Colorado as a satellite meeting to the annual NNFF-sponsored Consortium meeting. David Viskochil was designated as the organizer of the June, 2002 meeting, and a copy of the executive summary statement is provided in the appendix.

Task 24: Months 12-36 Trainee analyzes likelihood of non-NF1 loci role in PNSTs
Comment: This task is in progress.

Dr. Michael Liew has initiated studies into the likelihood of non-*NF1* loci being involved in the development of PNSTs. So far he has ruled out the t(X;18) chromosomal translocation as having a role in the development of PNSTs. The preliminary data he has on the role of IGF-IR is interesting, and will require more work to determine whether it is causative or a result of tumor development.

KEY RESEARCH ACCOMPLISHMENTS

- Determined that, in addition to the dermal neurofibromas being stable across the genome, benign PNSTs (plexiform neurofibromas) are also very stable across the genome with few and inconsistent somatic changes in genetic marker loci.
- Early data suggests that MPNSTs, including low-grade MPNSTs are genetically unstable at selected genetic loci across the genome.
- Different foci in benign PNSTs harbor similar, and stable, genomic signatures.
- Different foci in benign PNSTs have similar immunohistochemical staining patterns.
- Mib-1, TopoII, and P53 are the most informative immunohistochemical markers for the distinction between benign and low-grade PNSTs.
- Genetic heterogeneity can be detected in different sites from within one MPNST.
- Have developed a robust protocol for the amplification of DNA from tissue sections suitable for genotyping.
- Developed primer sets for *NF1* cDNA sequence mutation screening.
- Developed primer sets for *NF1* genomic DNA sequence mutation screening and identification of single nucleotide polymorphisms upstream and downstream of intron-exon boundaries.
- Developed primer sets for *TP53* exons for gene mutation screening of DNA extracted from paraffin-embedded PNSTs.
- Developed primer sets *P16* genetic markers to detect allelic imbalance in PNSTs.
- Developed and screened PNST DNA for missense mutations in the Noonan gene, *PTPN11*. No mutations were found in plexiform neurofibromas.
- Developed a standard set of genetic markers to determine the size of *NF1* microdeletions with respect to the repetitive sequences that are associated with approximately half of *NF1* microdeletions.
- Contributed to the establishment of a working group focused on the detection and treatment of MPNSTs in individuals with NF1.
- Could not establish a specific Ras-GTP/Ras-GDP ratio indicative of malignant transformation in peripheral nerve sheath tumors.

REPORTABLE OUTCOMES

Manuscripts

PERIPHERAL NERVE SHEATH TUMORS FROM PATIENTS WITH NEUROFIBROMATOSIS TYPE 1 (NF1) DO NOT HAVE THE CHROMOSOMAL TRANSLOCATION t(X;18)

Michael A. Liew, Cheryl M. Coffin, Jonathan A. Fletcher, Minh-Thu N. Hang, Katsumi Tanito, Michihito Niimura , David Viskochil

Pediatric and Developmental Pathology, April/May (2002). 5;165-169.

INTERNATIONAL CONSENSUS STATEMENT ON MALIGNANT PERIPHERAL NERVE SHEATH TUMORS IN NEUROFIBROMATOSIS 1

Rosalie Ferner and David Gutmann.

Cancer Research (2002).62;1573-1577

David Viskochil attended a Conference in London, UK that led to this consensus report. He chaired the Clinical Group Section.

PLEXIFORM NEUROFIBROMAS IN NF1: TOWARDS BIOLOGIC-BASED THERAPY

Roger Packer, David Gutmann, Alan Rubenstein, David Viskochil, Robert Zimmerman, Gilbert Vezina, Judy Small, and Bruce Korf

Neurology (2002).58;1461-1470.

David Viskochil chaired a session on clinical trials and contributed to the synopsis of the Clinical Trial Design section, an he reviewed the consensus report prior to submission.

C TO U RNA EDITING OF NEUROFIBROMATOSIS 1 mRNA OCCURS IN TUMORS THAT EXPRESS THE TYPE II TRANSCRIPT AND THAT ALSO EXPRESS APOBEC-1, THE CATALYTIC SUBUNIT OF THE APOLIPOPROTEIN B mRNA EDITING ENZYME

Debnath Mukhopadhyay, Shrikant Anant, Robert Lee, Susan Kennedy, David Viskochil, and Nicholas Davidson

American J Human Genetics. (2002).70;38-50.

Some of the retrospectively acquired PNSTs in Dr. Viskochil's lab were tested in the assays performed in this work. Dr. Viskochil also provided intellectual effort in the review and discussion of pertinent data.

Poster presentations

51st Annual Meeting of the American Society of Human Genetics, San Diego CA, October 12th-16th, 2001.

GENOME-WIDE SCREEN WITH TETRA-NUCLEOTIDE REPEATS DEMONSTRATES INFREQUENT ALLELIC IMBALANCE IN BENIGN PERIPHERAL NERVE SHEATH TUMORS IN NF1.

Michael Liew, Katsumi Tanito, Yan Zhang, Minh-Thu Hang, Linda Ballard, Shunichi Sawada, Michihito Niimura and David Viskochil

ABSTRACT

Approximately 20-25% of patients with neurofibromatosis type 1 (NF1) have benign peripheral nerve sheath tumors (PNSTs), also known as plexiform neurofibromas. Some of these tumors undergo transformation into malignant PNSTs (MPNSTs), however pathogenesis of malignant transformation has not been determined. Stable benign PNSTs have double inactivation of NF1, therefore we hypothesize that additional genetic changes must occur to lead to malignant transformation. A genome-wide tetra-nucleotide genotyping screen was implemented to evaluate allelic imbalance in DNA derived from different sites within 8 benign PNSTs from 8 individuals with NF1. Using GenotyperTM software the area under the allele-specific peaks and the ratio of the areas for two alleles were compared between blood and tumor DNA to estimate allelic imbalance in tumor-derived DNA template. A ratio of peak areas for informative alleles that was either less than 0.75 or greater than 1.25 in tumor versus blood DNA samples was scored as allelic imbalance. Loss of heterozygosity (LOH) was scored by a ratio less than 0.2, or greater than 5.0. This allele imbalance could reflect either LOH or extensive amplification of one allele.

39 tetra-nucleotide markers from the distal arms of 22 chromosomes were genotyped. 2/8 PNSTs had LOH, one with one marker demonstrating LOH and 3 markers with allelic imbalance, while the other had 9 markers with LOH and 12 markers with allelic imbalance. The latter tumor is currently under re-evaluation, and is not included in this current study. The remaining PNSTs had 1-8 sites of allelic imbalance. These data were unable to identify common markers that have LOH in PNSTs, but possibly could be used to potentially classify the malignant state of a tumor based on the number of markers that show a change. Use of these markers with adjacent sets of markers in an extended set of tumors would better define candidate genes that might contribute to NF1-related tumor formation, growth and transformation.

CONCLUSIONS

Since the previous report we have implemented some of the protocols developed, as well as refining others. Our main accomplishment this year has been in the realm of immunolohistochemical phenotyping of benign plexiform neurofibromas, low-grade MPSNTs, and high-grade MPNSTs. We have developed a set of antibodies that when applied in a standardized way could lead to more uniform analysis of PNSTs. As before, our analysis of the coding region of *NF1* and now the promoter region, has been slowed by the difficulties faced in designing primer sets for the PCR reactions from cDNA transcribed from *NF1* mRNA. We have worked with the genome center at the University of Utah to develop a screen to detect *NF1* mutations from genomic DNA by direct sequencing.

In addition, the protocols for DNA extraction and genome-wide screen we have developed are robust and informative. We now have more results that support our data from the previous annual report that genetic heterogeneity can be detected in benign and malignant PNSTs. The data also indicates that benign PNSTs are very stable across the genome, like the dermal neurofibromas. However, from the MPNST data, it appears that once malignant transformation occurs the genome of these tumors becomes very unstable. This probably means that there are other genetic changes outside of *NF1* that may lead to their development, and that some of the markers could indicate a progression in the tumor. It must be stressed however, that, at this point, the data for the MPNSTs are not sufficient to make statistically valid conclusions. We have developed assays to screen for somatic mutations of *TP53*, *P16*, and *PTPN11* in addition to *NF1*. We are now assessing the correlations between immunohistochemical staining, *TP53* mutations, and genome screening for allelic imbalance in an attempt to decipher the role p53 plays in tumor progression in NF1-related MPNSTs.

REFERENCES

Berner J, Sorlie T, Mertens F, et al. Chromosome band 9p21 is frequently altered in malignant peripheral nerve sheath tumors: studies of CDKN2A and other genes of the pRB pathway. Genes Chromosomes Cancer 1999; 26:151-160.

Cichowski K, Shih T, Schmitt E, Santiago S, Reilly K, McLaughlin M, Bronson R, Jacks T. Mouse models of tumor development in neurofibromatosis type 1. Science 1999;286:2172-2176.

Clark J, Rocques PJ, Crew AJ, et al. Identification of novel genes SYT and SSX, involved in the t(X;18)(p11.2;q11.2) translocation found in human synovial sarcoma. Nat Genet 1994; 7: 502-508.

DeClue J, Heffelfinger S, Benvenuto G, Ling B, Li S, Rui W, Vass W, Viskochil D, Ratner N. Epidermal growth factor receptor expression in neurofibromatosis type 1-related tumors and NF1 animal models. J Clin Invest 2000;105:1233-1241.

de Leeuw B, Balemans M, Olde Weghuis D, et al. Molecular cloning of the synovial sarcoma-specific translocation (X;18)(p11.2;q11.2) breakpoint. Hum Mol Genet 1994; 3: 745-749.

Dos Santos NR, De Bruijn DRH and Van Kessel AG. Molecular mechanisms underlying human synovial sarcoma development. Genes Chrom Cancer 2001; 30: 1–14.

Ferner R, Gutmann D. Meeting Report; International consensus statement on malignant peripheral nerve sheath tumors in neurofibromatosis 1. Cancer Research 2002:62;1573-1577.

Halling K, Scheithauer B, Halling A, et al. p53 expression in neurogivroma and malignant peripheral nerve sheath tumor. An immunohistochemical study of sparadic and NF1-associated tumors. Am J Clin Pahtol 1996;106:282-288.

Kourea HP, Orlow I, Scheithauer BW, Cordon-Cardo C and Woodruff JM. Deletions of the *INK4A* gene occur in malignant peripheral nerve sheath tumors but not in neurofibromas. Am J Path. 1999; 155: 1855-1860.

Liapis H, Marley E, Lin Y, et al. p53 and Ki-67 proliferating cell nuclear antigen in benign and malignant peripheral nerve sheath tumors in children. Pediatr Dev Pathol 1999:2;377-384.

Lothe R, Smith-Sorensen B, Hektoen M, Stenwig A, Mandahl N, Saeter G, Mertens F. Biallelic inactivation of TP53 rarely contributes to the development of malignant peripheral nerve sheath tumors. Genes, Chromosomes & Cancer 2001;30:202-206.

Nielson G, Stemmer-Rachamimov A, Ino Y, et al. Malignant tranformation of neurofibromas in neurofibromatosis 1 is associated with CDKN2A/p16 inactivation. Am J Pathol 1999; 155:1879-1884.

Paulson TG, Galipeau PC and Reid BJ. Loss of heterozygosity analysis using whole genome amplification, cell sorting, and fluorescence-based PCR. Genome Res. 1999; 9: 482-491.

Tartaglia M, Mehler E, Goldberg R, Zampino G, Brunner H, Kremer H, van der Burgt I, Crosby A, Ion A, Jeffery S, Kalidas K, Patton M, Kucherlapati R, Gelb B. Mutations in PTPN11, encoding the protein tyrosine phosphatase SHP-2, cause Noonan syndrome. Nature Genetics 2001:29;465-468.

The Utah Marker Development Group. A collection of ordered tetranucleotide-repeat markers from the human genome. Am. J. Hum. Genet. 1995; 57: 619-628.

Vogel K, Klesse L, Belasco-Miguel S et al. Mouse tumor model for neurofibromatosis type 1. Science 1999;286:2176-2179.

Zhu Y, Ghosh P, Charnay P, Burns D, Parada L. Neurofibromas in NF1: Schwann cell origin and role of tumor environment. Science 2002:296;920-922.

APPENDICES

Submitted manuscript: Zhou H, Coffin C, Perkins S, Tripp S, **Liew M, Viskochil D.** Malignant Peripheral Nerve Sheath Tumor (MPNST): A comparison of grade, immunophenotype, and cell cycle/growth activation marker expression in sporadic and neurofibromatosis 1 (NF1)-related lesions. **(PREPRINT, NOT FOR DISTRIBUTION)**

Published manuscript: DeClue J, Heffelfinger S, Benvenuto G, Ling B, Li S, Rui W, Vass W, **Viskochil D**, Ratner N. Epidermal growth factor receptor expression in neurofibromatosis type 1-related tumors and NF1 animal models. J Clin Invest 2000;105:1233-1241.

Submitted abstract: Zhou H, **Viskochil D**, Perkins S, Tripp S, Coffin C. Expression of epidermal growth factor receptor and vascular endothelial growth factor receptor in plexiform neurofibroma, and malignant peripheral nerve sheath tumors. to the United States and Canadian Academy of Pathology Meeting 2003.

Technical Abstract in proposal to the US Army Medical Research and Materiel Command NFRP02 (Log#NF020074; September, 17, 2002; PI: **David H. Viskochil)**

Published manuscript: **Liew M**, Coffin C, Fletcher J, Hang M-T, Tanito K, Niimura M, and **Viskochil D**. Peripheral nerve sheath tumors from patients with neurofibromatosis type 1 do not have the chromosomal translocation t(X;18). Pediatric and Developmental Path 2002:5;165-169.

Published manuscript: Ferner R and Gutmann D. Meeting Report; International consensus statement on malignant peripheral nerve sheath tumors in neurofibromatosis 1 Cancer Research 2002:62;1573-1577. (Contribution by **David Viskochil**

Executive summary statement: MPNST symposium, Aspen 06/2002 (organizer, **David Viskochil)**

Published manuscript: Muknopadhyay D, Anan S, Lee R, Kennedy S, **Viskochil D**, Davidson N. C-> U Editing of neurofibromatosis 1 mRNA occurs in tumors that express both the type II transcript and aobec-1, the catalytic subunit of the apolipoprotein B mRNA-editing enzyme. Am J Hum Genet. 2002:70;38-50.

Published manuscript: Packer R, Gutmann D, Rubenstein A, **Viskochil D**, Zimmerman R, Vezina G, Small J, Korf B. Plexiform neurofibromas in NF1. Toward biologic-based therapy. Neurology 2002:58;1461-1470.

Figure 1. Analysis of tumor specimen from patient #1949713. A) An H&E section showing the area that was scraped and DNA extracted for genetic analysis. B) SSCP results of human *tP53* exon 5 from DNA extracted from H&E paraffin section. The asterik denotes the sample that was part of the manuscript submitted for publication and the immunohistochemical staining shown in Figure 2 of the manuscript.

A)

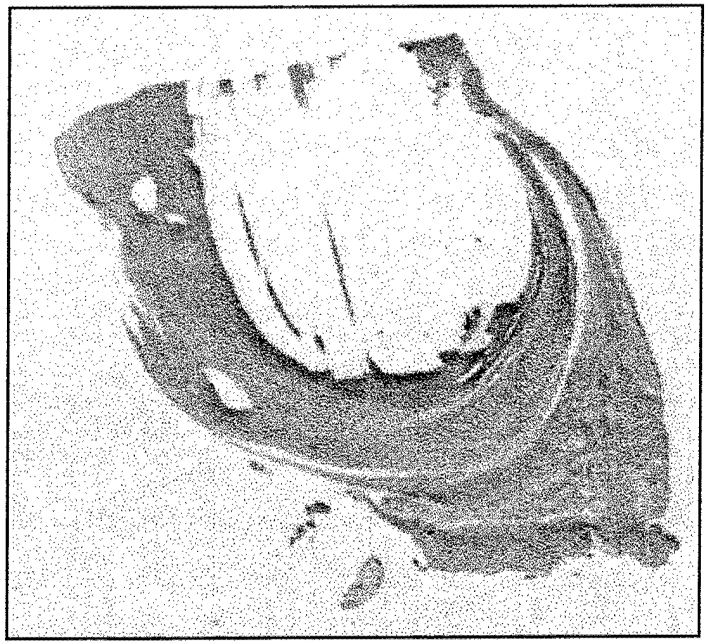

B)

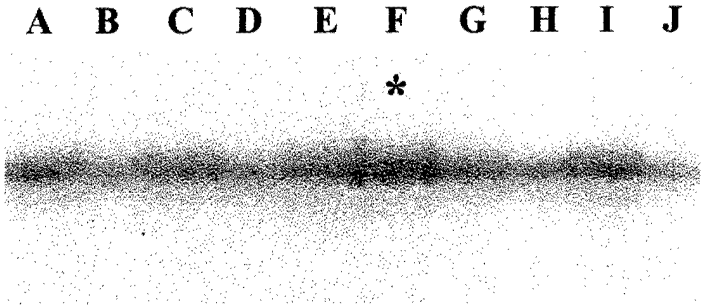

A)	500-068751F	E)	501-05042	I)	42730
B)	PS278-830	F)	1949713 *	J)	1972-931A
C)	48299012	G)	P309		
D)	89575400	H)	U135		

Figure 2. Exon 4 to 8 of the *tP53* gene was amplified with specific primers. The first sample in each group is a water control (*). The remaining samples are PCR products from DNA template extracted from H&E tumor sections. Each lane contains 5µl of PCR product + 2µl of sample buffer. The samples were separated on a 1% agarose gel containing EtBr.

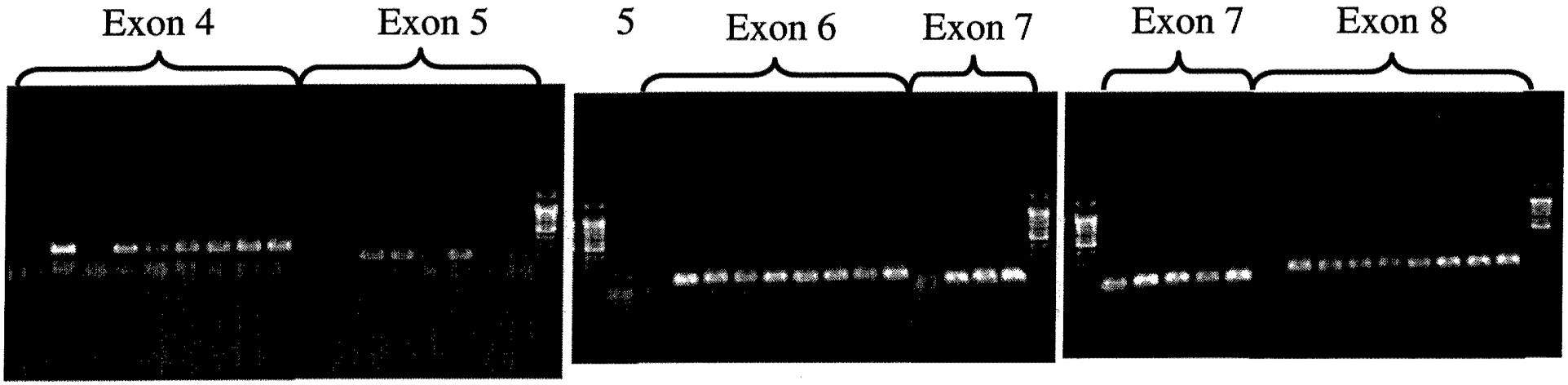

Figure 3. Sequencing results from PCR products for exon 4-8 of human *tP53*. Sequencing was carried out at core facility in the University Hospital.

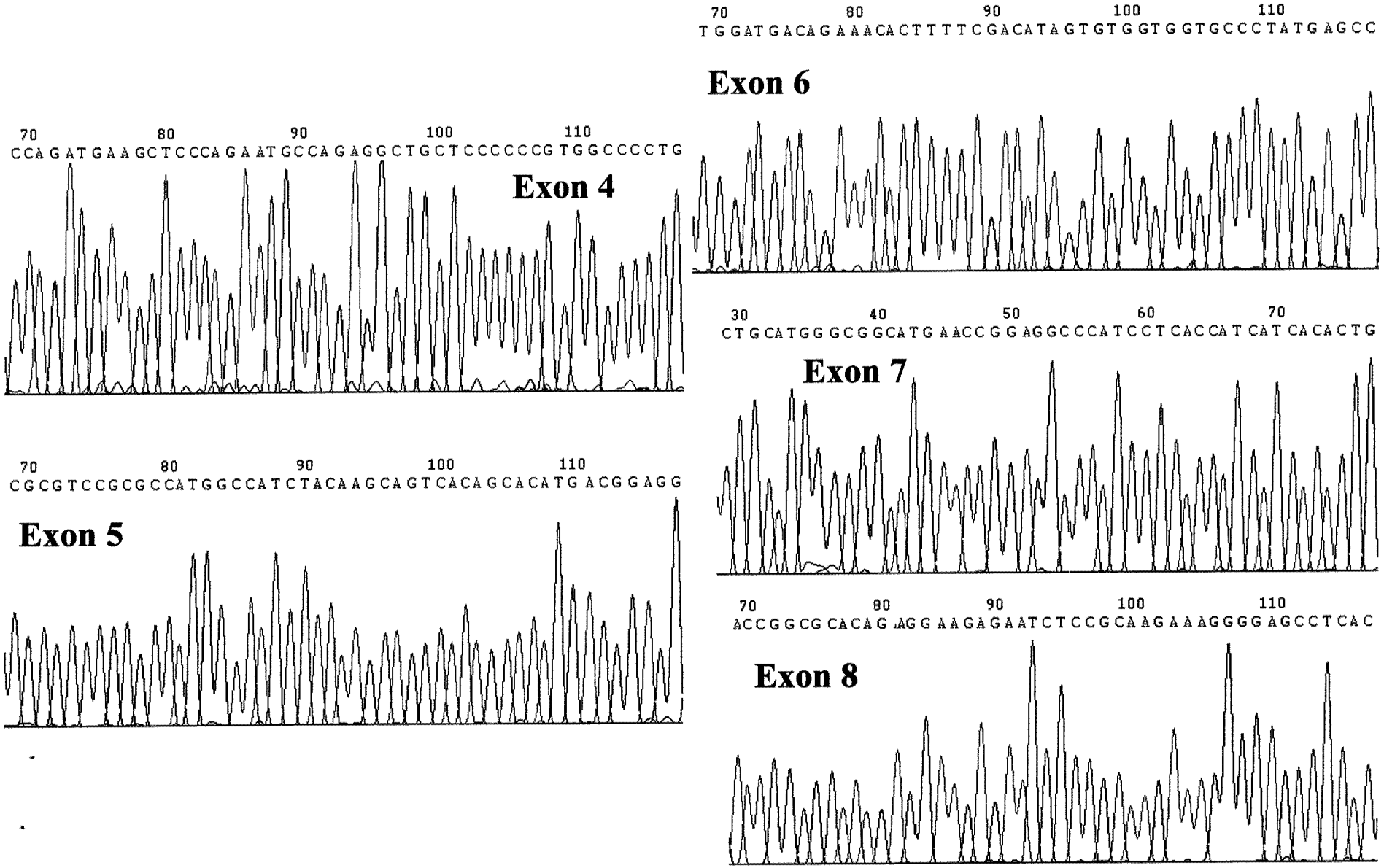

Figure 4. LOH analysis at the *NF1* gene shown for two different patients. The upper panel shows the marker GxAlu. The middle panel shows the marker GATN. The bottom panel shows the marker 28.4.

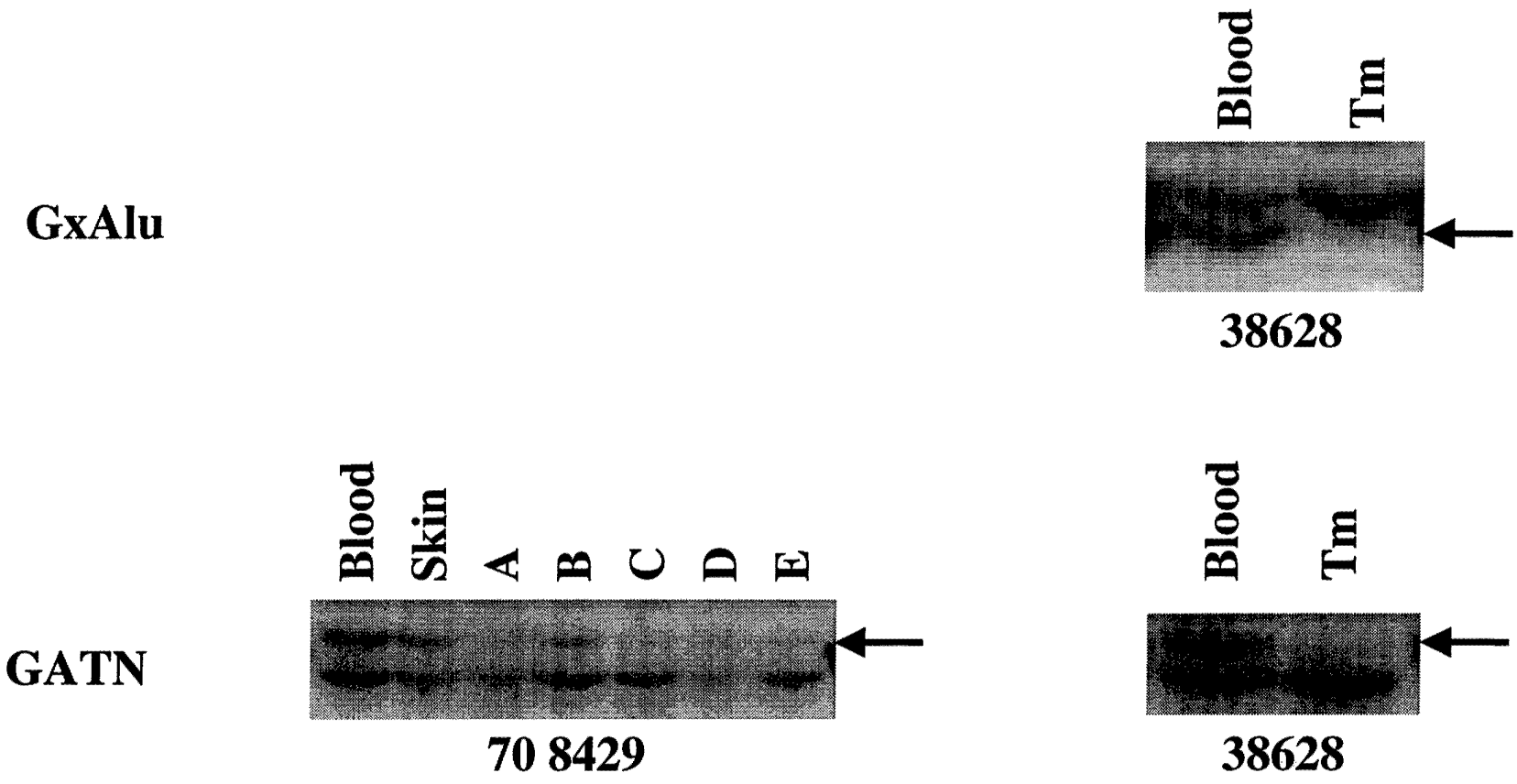

Figure 5. Intra-tumor genetic heterogeneity. A plexiform neurofibroma from patient #708429 showing the 5 different sites in which genetic analysis was carried out on the DNA extracted from the tumor site. The inset in each corner shows the general morphology with H&E staining.

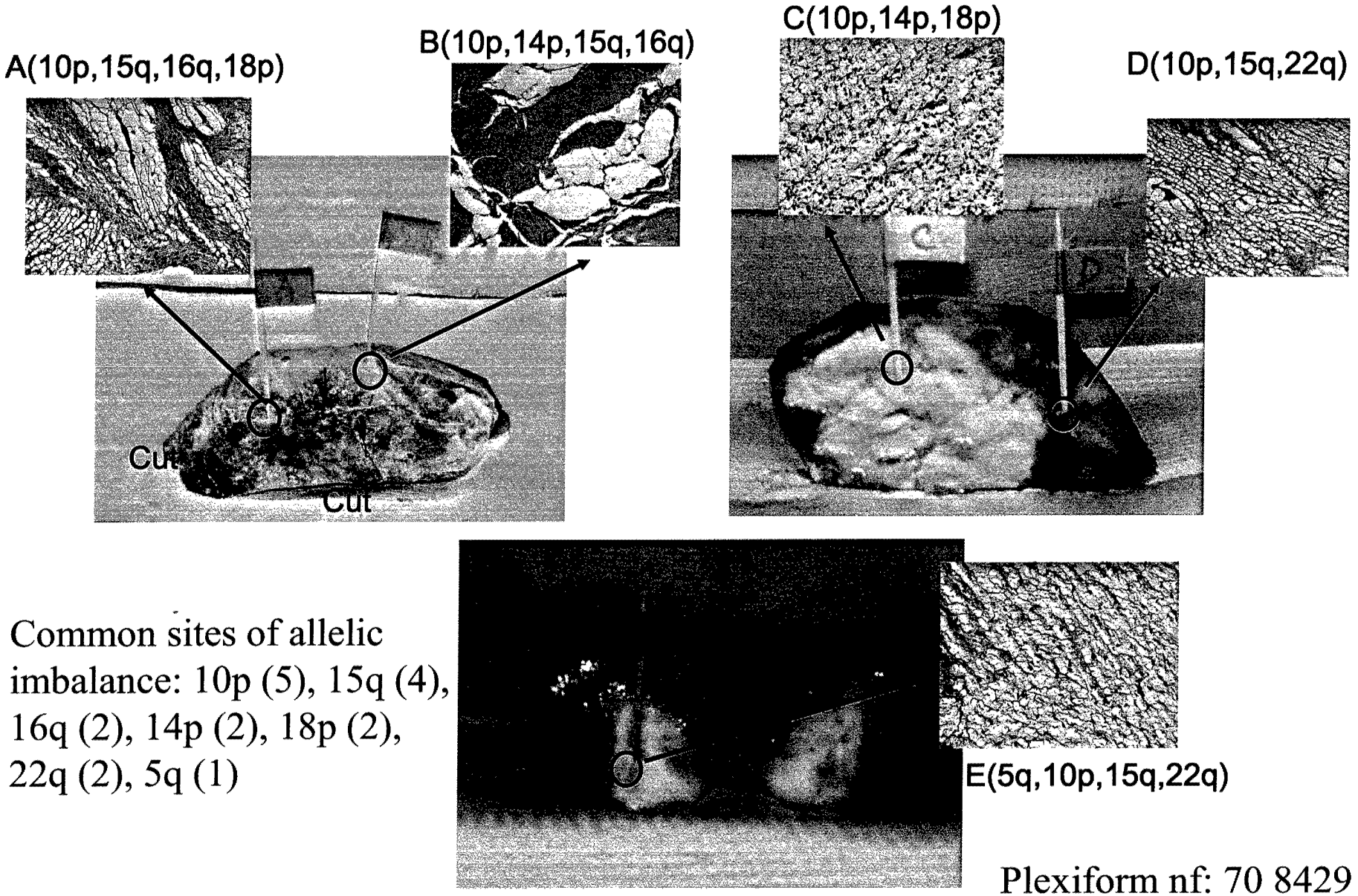

Common sites of allelic imbalance: 10p (5), 15q (4), 16q (2), 14p (2), 18p (2), 22q (2), 5q (1)

Plexiform nf: 70 8429

Figure 6. Immunohistochemical staining of tumor 1 from patient #36670. A) Shows the general morphology of the tumor section with H & E staining. B) - F) are the various immunohistochemical stains for specific antigens as cited. The insert in the corner is the photograph of the tumor after removal.

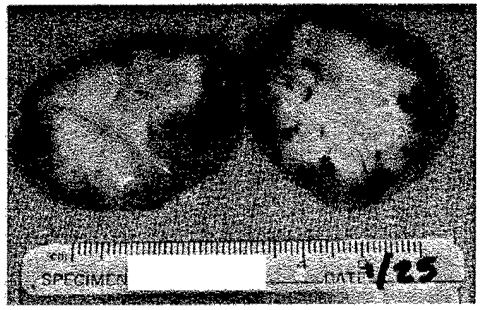

A) H & E

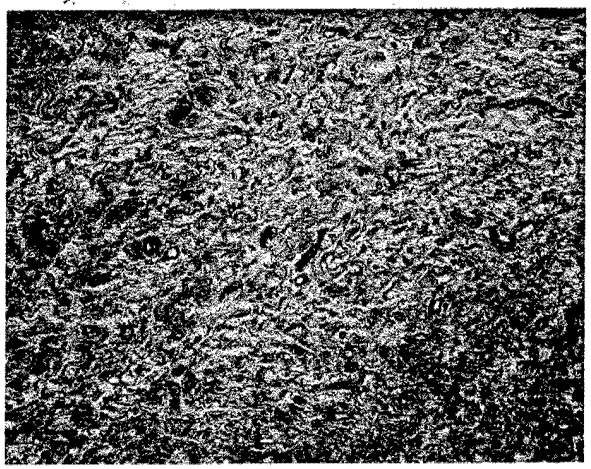

B) Mib-1

C) Topo IIa

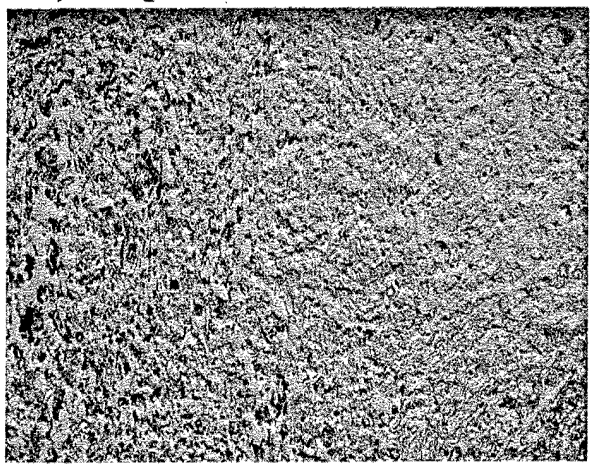

D) p53

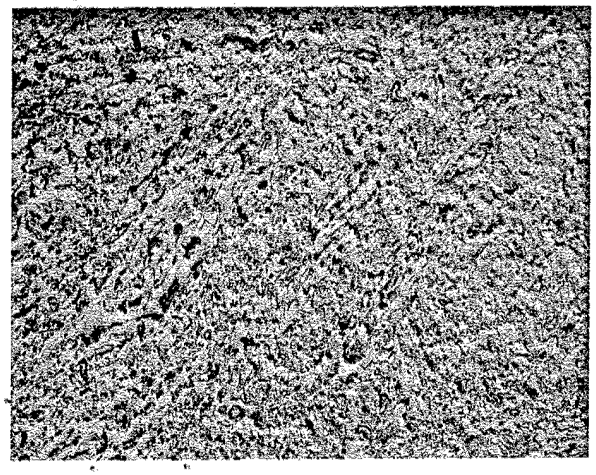

E) p16

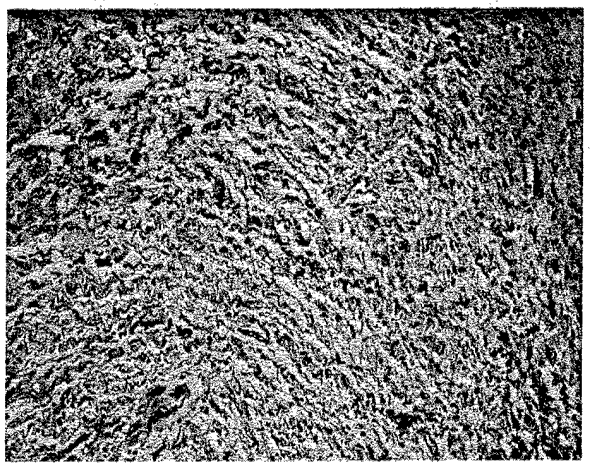

F) p27

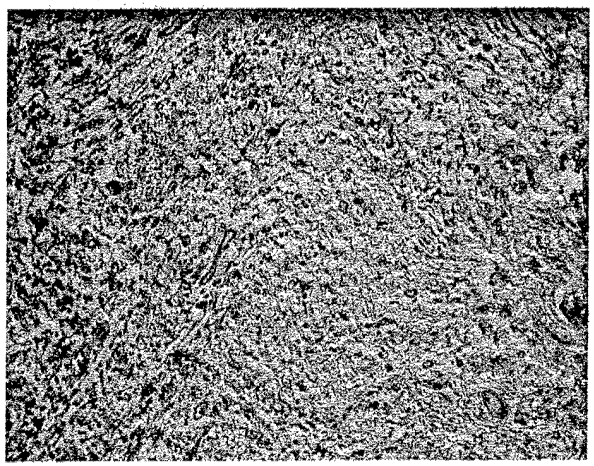

Figure 7. Immunohistochemical staining of tumor C from patient #38628. A) Shows the general morphology of the tumor section with H & E staining. B) - F) are the various immunohistochemical stains for specific antigens as cited. The insert in the corner is a photograph of the tumor after removal.

A) H & E

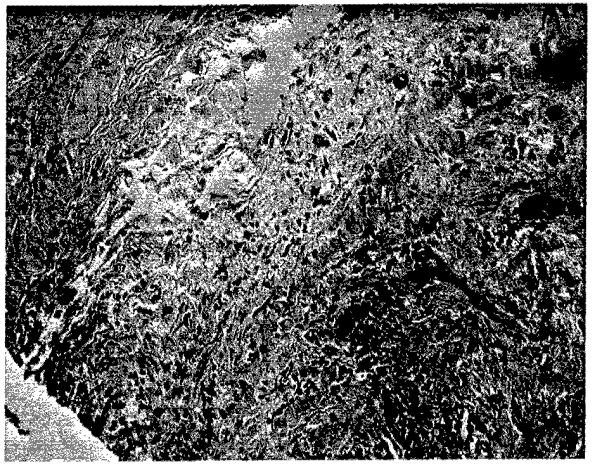

B) Mib-1

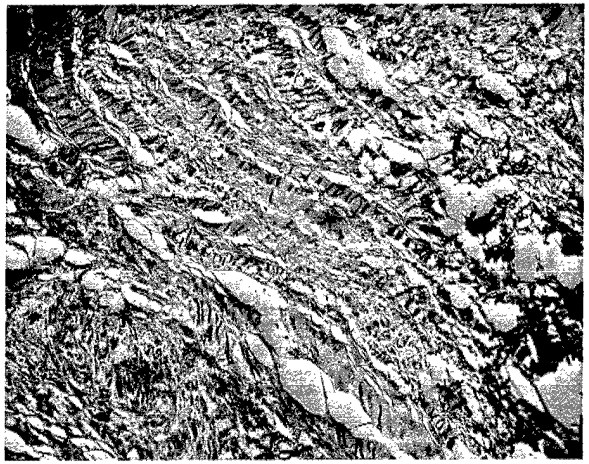

C) Topo IIa

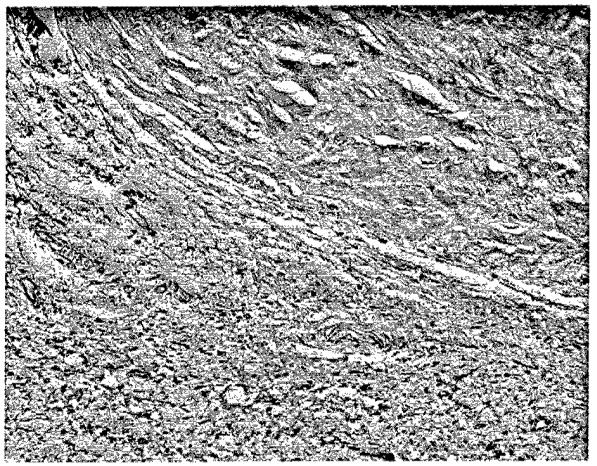

D) p53

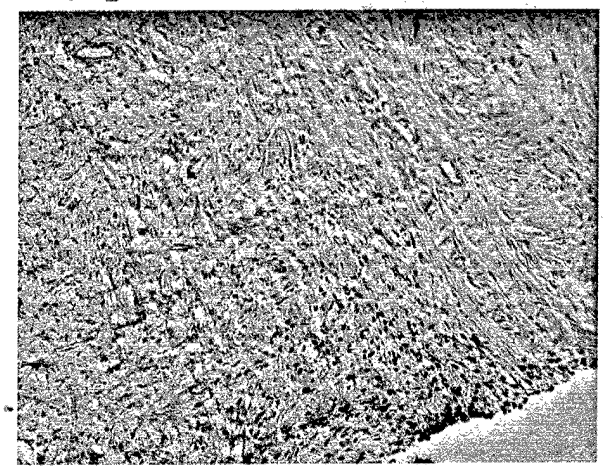

E) p16

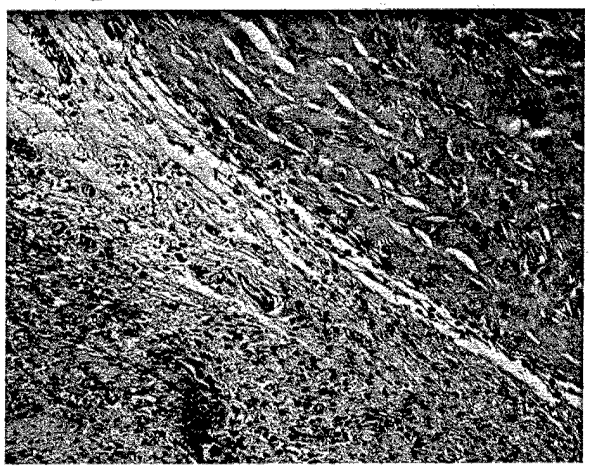

F) p27

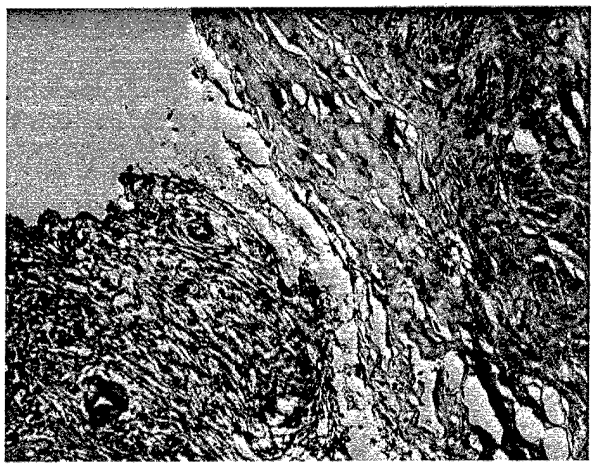

Table 1. Genome-wide screen results using tetra-nucleotide repeats. Blank squares indicates that there is no data available, ○-allelic balance, ● -not informative or homozygous, ●-allelic imbalance and ●-loss of heterozygosity.

			BENIGN PNSTs																										MPNSTs				
PATIENT	36670		588289					595171					708429					U105					U140					U142					38628	306595			
	A	B	A	B	C	D	E	A	B	C	D	E	A	B	C	D	E	A	B	C	D	E	A	B	C	D	E	A	B	C	D	E		A	B	C	D
D1S396	○	○	○	○	○	○	○	●	○	○	○	○	○	○	○	○	○	○	○	○	○	○	●	●	●	●	●	○	○	○	○	○	●	●	●	●	●
D1S517	○	●	○	○	○	○	○	○	○	○	○	○	○	○	○	○	○	●	●	●	●	●	○	○	○	○	○	●	●	●	●	●	●	○	○	○	○
D2S262	○		○	○	○	○	○	○	○	○	○	○	○	○	○	○	○	●	●	●	●	●	○	○	○	○	○	○	○	○	○	○	○	○	○	●	○
D2S1242			○	○	○	○	○	○	○	○	○	○	○	○	○	○	○																	●	●	●	●
D3S1539	○	○	○	○	○	○	○	○	○	○	○	○	○	○	○	○	○	○	○	○	○	○	●	●	●	●	●	○	○	●	○	○	○				
D3S2309	●	●	○	○	○	○	○	○	○	○	○	○	○	○	○	○	○	●	●	●	●	●	●	●	●	●	●	○	○	●	○	○	●	●	●	●	●
D4S2289	○	○	○	○	○	○	○	●	●	●	●	●	○	○	○	○	○	●	●	●	●	●	○	○	○	○	○	○	○	○	○	○	●	○	○	○	○
D4S1529			○	○	○	○	○	○	○	○	○	○	●	●	●	●	●	●	●	●	●	●	○	○	○	○	○	○	○	○	○	○		○	○	○	○
D5S580	●	●	○	○	○	○	○	○	○	○	○	○	○	○	○	○	○	○	○	○	○	○	○	○	○	○	○	○	○	○	○	○	●	○	○	○	○
D5S592	●	●	○	○	○	○	○	○	○	○	○	●	○	○	○	○	●	○	○	○	○	○	○	○	○	○	○	○	○	○	○	○	●	○	○	○	○
D5S1349	○	○	○	○	○	○	○	○	○	○	○	○	○	○	○	○	○	●	●	●	●	●	○	○	●	○	●	○	○	○	○	○	●	○	○	○	○
D6S399	●	●	●	●	●	●	●	●	●	●	●	●	○	○	○	○	○	○	○	○	○	○	●	●	●	●	●	○	○	○	○	○	●	●	●	●	●
D6S392	○	○	○	○	○	○	○	●	●	●	●	●	●	●	●	●	●	○	○	○	○	○	○	○	○	○	○	○	●	○	○	○	●	●	●		●
D7S1506			○	○	○	○	○	○	○	○	○	○	○	○	○	○	○	○	○	●	○	○	○	○	○	○	○	○	○	○	○	○	○	●	●		●
D8S492	●	●	●	●	●	●	●	○	○	○	○	○	○	○	○	○	○	●	●	●	●	●	○	○	○	○	○	○	○	○	○	○	●	●	●	●	●
D8S378	○	○	○	○	○	○	○	○	○	○	○	○	●	●	●	●	●	○	○	○	○	○	○	○	○	○	○	○	○	○	○	○	●	●	●	●	●
D9S759	○	○	○	○	○	○	○	●	●	●	●	●	○	○	○	○	○	○	○	●	○	○	●	●	●	●	●	○	○	○	○	○	●	○	○	○	○
D9S241			●	○	○	○	○	○	○	○	○	○	○	○	○	○	○	○	○	○	○	○	●	●	●	●	●	○	○	○	○	○		○	○	○	○
D9S744	○	○	○	○	○	○	○	○	○	○	○	○	○	○	○	○	○																●	○	○	○	○
D10S526	○	○	●	●	●	●	●	○	○	○	○	○	●	●	●	●	●	○	○	○	○	○	○	○	○	○	○	○	○	○	○	○	●	●	●	●	●
D10S528	○	○	○	○	○	○	○	○	○	○	○	○	○	○	○	○	○	○	○	○	○	○	●	●	●	●	●	○	○	○	○	○	●				

PATIENT	36670		588289					595171					708429					U105					U140					U142					38628	306595			
	A	B	A	B	C	D	E	A	B	C	D	E	A	B	C	D	E	A	B	C	D	E	A	B	C	D	E	A	B	C	D	E		A	B	C	E
D11S1923	●	●	●	●	●	●	●	○	○	○	○	○	○	○	○	○	○	○	○	○	○	○	○	○	○	○	○	●	●	●	●	●	●	○	○	○	C
D11S1298	●	○	○	○	○	○	○	○	○	○	○	○	○	○	○	○	○	○	○	○	○	○	○	○	○	○	○	○	○	○	○	○	●	○	○	○	C
D11S1304		○	●	●	●	●	●	○	○	○	○	○	●	●	●	●	●	○	○	○	○	○	○	○	○	○	○	●	●	●	●	●	●	○	○	○	C
D12S827																		●	●	●	●	●	●	●	●	●	●	●	●	●	●	●	○	●	●	●	●
D12S297	●	●																															●				
D12S807	○	○	○	○	○	○	○	○	○	○	○	●	○	○	○	○	○	●	●	●	●	●	○	○	○	○	○	○	○	○	○	○	●	○	○	○	C
D13S258	●	●	○	○	○	○	○	○	○	○	○	○	●	●	●	●	●	○	○	○	○	○	●	●	●	●	●	○	○	○	○	○	●	○	○	○	C
D14S122	○	○	●	●	○	○	○	●	●	●	●	●	○	●	●	○	○	○	○	○	○	○	○	○	○	○	○	○	○	○	○	○	○	○	○	○	C
D15S195	○	○	○	○	○	○	○	●	●	●	●	●	●	●	○	●	●	○	○	○	○	○	○	○	○	○	○	○	○	○	○	○	●	●	●	●	●
D16S475	○	○	○	○	○	○	○	○	○	○	○	○	○	○	○	○	○	●	●	●	●	●	●	●	●	●	●	○	○	○	○	○	○	○	○	○	C
D16S476	○	○	○	○	○	○	○	○	○	○	○	○	●	●	○	○	○	○	○	○	○	○	●	●	●	●	●	○	○	○	○	○	●	○	○	●	C
D17S695	●	○	○	○	○	○	○	○	○	○	○	○	●	●	●	●	●	●	●	●	●	●	○	○	○	○	○	●	●	●	●	●	●	○	○	○	C
GXAlu	●	●																										○	○	●	○	○	●	●	●		●
D17S960	○	○																										○	○	●	○	○	●	○	○	○	C
GATN													●	●	●		●																●				
D17S722	○	○																															●				
D18S818	●	●	●	●	●	●	●	○	○	●	○	●	●	○	●	○	○	○	○	○	○	○	○	○	○	○	○	○	○	○	○	○		○	○	○	C
D18S380	●	●	●	●	●	●	●	●	●	○	○	○	●	●	●	●	●	●	●	●	●	●	○	○	○	○	○	●	●	●	●	●	●				
D19S581	○	○	○	○	○	○	○	○	○	○	○	○	○	○	○	○	○	○	○	○	○	○	●	●	●	●	●	○	○	○	○	○	○	○	●	●	●
D19S544	○	●	●	●	●	●	●	○	○	○	○	○	●	●	●	●	●	○	○	○	○	○	●	●	●	●	●	●	●	●	●	●	●	○	○	○	C
D20S438	●	●	○	○	○	○	○	○	○	○	○	○	○	○	○	○	○	○	○	○	○	○	○	○	○	○	○	○	○	○	○	○	●	○	○	○	C
D21S1411	○	○	○	○	○	○	○	○	○	○	○	○	○	○	○	○	○	○	○	●	○	○	○	○	○	○	○	●	●	●	●	●	●	●	●	●	●
D22S417	●	●	○	○	○	○	○	○	○	○	○	○	○	○	○	●	●	○	○	○	○	○	○	○	○	○	○	○	○	○	○	○	●	●	●	●	●

Table 2. Genotypes of a PNST tumor and a low-grade MPNST tumor from two different patients. The markers used are indicated along the side of the table, while patient samples are across the top of the table. Symbols used are as follows. = allelic balance; - not determined; F failed sample; I allelic imbalance; LOH loss of heterozygosity; N not informative.

Markers	**PNST (#36670 tumor)**	**Low-grade MPNST (#38628 tumor)**
UT5144-1p	=	LOH
UT5170-1q	=	N
UT595-2p	=	=
UT1360-3p	=	=
UT6129-3q	N	N
UT878-4p	=	I
UT615-5p	N	N
UT5013-5q	N	LOH
UT886-5q	=	N
UT2018-6p	N	I
UT897-6q	=	N
UT5189-7p	F	=
UT5412-8p	N	I
UT909-8q	=	I
UT873-9p	=	LOH
UT913-9q	F	F
UT7422-9q	=	N
UT1699-10p	=	N
UT5419-10q	=	I
UT8115-11p	N	LOH
UT5150-11	LOH	LOH
UT2095-11q	F	LOH
UT5029-12p	N	I
UT6136-12	-	=
UT931-12q	=	N
UT2413-13	N	LOH
UT1392-14	=	=
UT1232-15	=	I
UT581-16p	=	=
UT703-16q	=	I
UT269-17p	I	LOH
UT40-17q	=	I
UT7162-18p	N	F
UT576-18q	N	I
UT5187-19p	=	=
UT1342-19q	=	LOH
UT236-20	N	I
UT1355-20q	=	I
UT1091-22q	N	LOH

Table 3. Summary of genome wide results.

PATIENT NO.	TUMOR TYPE	ALLELIC IMBALANCE	LOH
U100	Dermal	1/39	0/39
U125	Dermal	0/39	0/39
U129	Dermal	1/39	0/39
U135	Dermal	1/39	0/39
58 8289	Plexiform	2/38	0/38
59 5171	Plexiform	7/38	0/38
70 8429	Plexiform	7/38	0/38
U105	Plexiform	4/37	0/37
U140	Plexiform	1/37	0/37
U142	Plexiform	3/37	0/37
36670	Plexiform	3/36	1/36
21508	MPNST	-	7/40
38628	MPNST	12/37	10/37
306595	MPNST	-	**2/37**

Table 4. NF1 genomic sequencing with results from six NF1 patients.

PCR product #	Exon #	PCR product size (bp)	Sequencing Coverage	Patient 38628	Patient 42908	Patient 42907
1	1	1322	optimizing	NA	NA	NA
2	2	1281	single strand	3' sp +300 C to T 3' sp +122 G to A	xx	xx
3	3	1126	double strand	3'sp + 42 -G to A	3'sp + 42 -G/A	3'sp + 42 -G to A
4	4a	1146	double strand	xx	xx	xx
5	4b	1080	double strand	3'sp +89 - c to t	5' sp 90 nts C/T	3'sp +89 - c to t
6	4c & 5	1011	double strand	xx	xx	xx
7	5	1337	single strand	xx	in exon A/T -syn	both bad
8	6	1123	double strand	xx	xx	both dead
9	79	1328	double strand	xx	xx	xx
10	8 & 9	1177	double strand	xx	xx	both dead
11	9	1359	double strand	xx	xx	xx
12	10a	1153	double strand	xx	xx	xx
13	10b	1207	double strand	xx	xx	both dead
14	10c	1184	double strand	xx	3' sp +39 C/T	both dead
15	11	1312	optimizing	NA	NA	NA
16	12a	1072	double strand	xx	xx	marginal
17	12b	1325	optimizing	xx		NA
18	13	1164	optimizing	NA	NA	NA
19	14 & 15	1338	optimizing	NA	NA	NA
20	15	1242	double strand	xx	xx	both dead
21	16	1102	double strand	- C het in exon	Xx	xx
22	17	1222	single strand	xx	both mixed	both mixed
23	18	1209	optimizing	NA	NA	NA
24	19a	1175	optimizing	NA	NA	NA

25	19b	1344	optimizing	NA	NA	NA
26	20 & 21	1358	double strand	xx	both bad	both dead
27	20 & 21	1170	double strand	xx	-G het in exon	xx
28	22 & 23-1	1160	double strand	xx	xx	xx
29	22 & 23-1	1351	single strand	xx	R is dead, 3' sp +39 T to G	xx
30	23-2	1226	single strand	xx	xx	both bad
31		1334	double strand	xx	xx	both mixed
32	24	1361	optimizing	NA	NA	NA
33	25	1333	optimizing	NA	NA	both mixed
34	26	1351	optimizing	NA	NA	NA
35	27a	1188	double strand	xx	xx	xx
36	27b	1141	double strand	5'sp + 52 - C to A	5'sp + 52 - C to A, R read was dead	5'sp + 52 - C to A
37	28	1176	double strand	R is fine, 3' sp +24 T to C	R is fine, 3' sp +24 T/C	both dead
38	29	1295	double strand	3' sp + 20 - T to A	xx	both dead
39	30	1470	double strand	xx	xx	xx
40	31	1273	double strand	xx	both bad	both mixed
41	32 & 33	1361	optimizing	NA	NA	NA
42	33	1267	single strand	xx	xx	-TT/+A +28,29 in runs
43	34 & 35	1279	double strand	3' sp -T in run ~ 240nts	xx	xx
44	35 & 36	1313	double strand	5' sp -2 -T	5' sp -2 -T	5' sp -2 -T
45	36	1174	single strand	xx	both dead	3' sp -A in run ~ 330nts
46	37	1238	double strand	5' sp -A ~230nts	5' sp -A ~230nts	xx
47	38	1253	single strand	G to C in exon, syn,	G to C in exon, syn,	G to C in exon, syn,

				ACG to ACC (Thr)	ACG to ACC (Thr)	ACG to ACC (Thr)
48	39	1341	double strand	xx	xx	xx
49	40	1350	single strand	xx	5' sp +~165 A/T	xx
50	41	1240	double strand	xx	xx	both dead
51	42	1171	double strand	5' sp +28nts G to A	5' sp het +28nts G/A	xx
52	43	1151	single strand	both reads bad	5' sp +225 C to G	5' sp +225nts C to G
53	44 & 45	1230	single strand	xx	xx	both bad
54	44 & 45	1342	double strand	xx	xx	xx

xx = good read and no polymorphism detected; NA = not available, still optimizing the protocol

Table 4 cont.

PCR product #	Exon #	Exon #	PCR product size (bp)	Sequencing Coverage	Patient 42730	Patient 46265	Patient 36670
1	1	1	1322	optimizing	NA	NA	NA
2	2	2	1281	single strand	3' sp +52 het G/C	both dead	5' sp +122 G to A
3	3	3	1126	double strand	3'sp + 42 -G to A	both dead	3'sp + 42 -G/A
4	4a	4	1146	double strand	xx	both dead	xx
5	4b	5	1080	double strand	3'sp +89 - c to t	both dead	3' sp +89 C to T
6	4c & 5	6	1011	double strand	xx	both dead	xx
7	5	7	1337	single strand	both dead	both dead	NA
8	6	8	1123	double strand	both dead	both dead	xx
9	79	9	1328	double strand	xx	xx	xx
10	8 & 9	10	1177	double strand	both bad	xx	xx
11	9	11	1359	double strand	xx	xx	xx
12	10a	12	1153	double strand	xx	xx	G het, 5' sp +99 and 3'sp + 34
13	10b	13	1207	double strand	xx	5'sp +A 21nts, 5'sp	NA

						129nts T to A, 5'sp 32nts C to T	
14	10c	14	1184	double strand	xx	5'sp –A 28nts, 3' sp +40 C/T	xx
15	11	15	1312	optimizing	NA	NA	NA
16	12a	16	1072	double strand	marginal	xx	xx
17	12b	17	1325	optimizing	NA	NA	xx
18	13	18	1164	optimizing	NA	NA	NA
19	14 & 15	19	1338	optimizing	NA	NA	NA
20	15	20	1242	double strand	both dead	both dead	xx
21	16	21	1102	double strand	xx	xx	xx
22	17	22	1222	single strand	xx	incomplete coverage	both bad
23	18	23	1209	optimizing	NA	NA	NA
24	19a	24	1175	optimizing	NA	NA	NA
25	19b	25	1344	optimizing	NA	NA	NA
26	20 & 21	26	1358	double strand	3'sp 34nts C to A	both bad	xx
27	20 & 21	27	1170	double strand	5'sp +85nts C to A	-G het in exon	xx
28	22 & 23-1	28	1160	double strand	xx	xx	xx
29	22 & 23-1	29	1351	single strand	both bad	3'sp +G ~40nts, 3'sp +G ~50nts	xx
30	23-2	30	1226	single strand	both bad	xx	xx
31		31	1334	double strand	marginal	xx	xx
32	24	32	1361	optimizing	NA	NA	NA
33	25	33	1333	optimizing	NA	NA	NA
34	26	34	1351	optimizing	NA	NA	NA
35	27a	35	1188	single strand	xx	xx	
36	27b	36	1141	double strand	5'sp + 52 - C to A	xx	5'sp + 52 - C to A
37	28	37	1176	double strand	xx	xx	xx

38	29	38	1295	double strand	L is fine, R is mixed	both dead	no reads
39	30	39	1470	double strand	xx	xx	xx
40	31	40	1273	double strand	both bad	xx	mixed
41	32 & 33	41	1361	optimizing	NA	NA	NA
42	33	42	1267	single strand	both bad	xx	xx
43	34 & 35	43	1279	double strand	xx	xx	3' sp -T in run ~ 240nts
44	35 & 36	44	1313	double strand	5' sp -2 -T	R is dead	5' sp -2 -T
45	36	45	1174	single strand	xx	xx	3' sp -A in run ~ 330nts
46	37	46	1238	double strand	xx	5' sp -A ~230nts	xx
47	38	47	1253	single strand	G to C in exon, syn, ACG to ACC (Thr)	G to C in exon, syn, ACG to ACC (Thr)	G to C in exon, syn, ACG to ACC (Thr)
48	39	48	1341	double strand	xx	xx	xx
49	40	49	1350	single strand	xx	both dead	xx
50	41	50	1240	double strand	xx	xx	xx
51	42	51	1171	double strand	xx	xx	5' sp het +28nts G/A
52	43	52	1151	single strand	both bad	both mixed	xx
53	44 & 45	53	1230	single strand	xx	both dead	xx
54	44 & 45	54	1342	double strand	xx	xx	xx

xx = good read and no polymorphism detected; NA = not available, still optimizing the protocol

Table 5. Ras acitivity in MPNST in tumor samples from 9 NF1 patients.

Sample ID	Tumor type	GTP (fmol/mg prot)	GTP + GDP (fmol/mg prot)	GTP (GTP+ GDP) (%)
21508	Neurofibrosarcoma	21	359	6
BG8	Dermal neurofibroma	17	660	3
P301	MPNST	39	1817	2
306595	MPNST	82	1746	5
U1001	Plexiform neurofibroma	60	735	8
42908	Plexiform neurofibroma	336	1120	30
U100nf	Dermal neurofibroma	41	1595	3
P309	MPNST	122	1143	11
42907	Plexiform neurofibroma	14	488	3

Malignant Peripheral Nerve Sheath Tumor (MPNST): A comparison of grade, immunophenotype, and cell cycle/growth activation marker expression in sporadic and neurofibromatosis 1 (NF1)-related lesions

Holly Zhou, M.D., Cheryl M. Coffin, M.D., Sherrie L. Perkins, M.D., Ph.D. Sheryl R. Tripp, Michael Liew, Ph.D., David H. Viskochil, M.D, Ph.D.

Departments of Pathology (HZ, CMC, SLP, SRT), Pediatrics (ML, DVH)

University of Utah School of Medicine, Salt Lake City, UT

Corresponding Author: Holly Zhou, M.D. Department of Pathology, Primary Children's Medical Center, 100 N. Medical Drive, Salt Lake City , UT 84113. Phone: (801)-588-3168, Fax(801)588-3169. Email: PCHZHOU@IHC.COM

- Supported by grant from the Department of the Army, DAMD-NF980007(DV)

- Presented in part at the United States and Canadian Academy of Pathology, Chicago, IL, February 25, 2002. Abstract published in Mod Pathol 2002; 15:24A.

Abstract

This study investigates differences in expression of cell cycle/growth activation markers p53, p16 and p27, and their relationship with nerve sheath cell and proliferation markers among plexiform neurofibromas (PNF), NF1-related and non-NF1 MPNSTs of different histological grades and between benign-appearing and malignant areas in the same MPNST. Formalin-fixed, paraffin-embedded archival tissue from PNFs and MPNSTs were immunostained using the avidin-biotin-complex method with antibodies to S100 protein (S100), Leu7 (CD57), CD34, p16, p27, p53, Mib-1, and Topoisomerase II-alpha (TopoIIα), with appropriate controls. All PNFs and most low-grade MPNSTs displayed diffuse or focal reactivity for S100, Leu7, CD34, p16 and p27 and negative reactivity to p53, Mib-1, and TopoIIα. Most high-grade MPNST displayed decreased or negative reactivity to S100, Leu7, CD34, p16, and p27 but increased reactivity to p53 (59%), Mib-1 (72%), and TopoIIα (72%). Our findings suggest that p53; p16 and p27 may be involved in tumor progression in the PNF-MPNST sequence. However, alterations in p53, p16, and p27 do not distinguish between low-grade MPNST and PNF, including PNF adjacent to high-grade MPNST. Although p53, p16 and p27 are unlikely to be reliable markers for early

detection of tumor progression in MPNST. p53 reactivity was more frequent in NF1-associated high-grade MPNST and appeared to be a marker for high tumor grade.

Combing immunohistochemical stains with histoloical grading, by careful examination of mitotic index, may provide insight to the transformation process in peripheral nerve sheath tumors

KEY WORDS: p53, p16, p27, plexiform neurofibroma, malignant peripheral nerve sheath tumor, tumor progression/malignant transformation, immunophenotype.

Introduction

Malignant peripheral nerve sheath tumors (MPNST) often occur in association with neurofibromatosis type 1 (NF1), an autosomal dominant condition resulting from inactivation *NF1* gene mutations (1,2,3). The function of the *NF1* gene product, neurofibromin, is to reduce cell signal transduction by accelerating inactivation of the proto-oncogene p21-ras (4,5, 6). Mutations in *NF1* lead to increase Ras signaling; therefore, individuals with NF1 have an increased risk of developing both benign and malignant tumors, especially peripheral nerve sheath tumors. Approximately 20 to 25% of individuals develop plexiform neurofibroma (PNF), which usually arise at an early age and may undergo malignant transformation and progress to MPNST (7,8). Clinically, MPNST is difficult to detect in NF1 patients and has a poor prognosis because of the high likelihood of local recurrence and distant metastasis. At present, there are no

reliable indicators of early detection of tumor progression or malignant transformation of PNF to MPNST apart from classic histopathologic criteria, which remain somewhat controversial at the low-grade end of the spectrum.

Recent studies suggest that the development of MPNST is a multistage process that may involve a number of altered cell cycle regulators in addition to double inactivation of the *NF1* gene (9-17). Among these cell cycle regulators, *TP53* is known for its critical role in arresting cells in the G1 phase of the cell cycle following DNA damage and negative regulation of cellular proliferation. Deletions involving chromosome 17p, including the *TP53* locus and mutation of the *TP53* gene have been observed in a proportion of MPNST but not in neurofibromas (NF) (9,10, 11). p16, encoded by the *CDKN2A/p16* gene on the short arm of chromosome 9 (9p21), inhibits the function of the cell cyclin kinase CDK4- and CDK6-Cyclin D complexes, thus controlling cell proliferation through the retinoblastoma (pRB) pathway (18-20). Inactivation of *CDKN2A/p16* has been observed in a wide variety of human tumors including MPNST (12-15, 21-24). p27 is a multifunctional cyclin-dependent kinase inhibitor (CDKI) and not only directly inhibits cell proliferation, but also functions as an important promoter of apoptosis and has a role in cell differentiation (25-30). A recent study showed that a significant decrease in or loss of nuclear expression of p27, as described in a large numbers of malignant neoplasms, was present in MPNST but not in plexiform NF (16).

In this study, we compared the immunohistochemical expression of cell cycle regulators p53, p16 and p27 between PNF and both sporadic and NF-1 related low- and high-grade MPNSTs. We also compared the sarcomatous and benign PNF areas in MPNST arising in a PNF. The

expression of nerve sheath cell markers S100 protein, Leu 7, and CD34, and the cell proliferation markers, Mib-1 and TopoIIα, were also assessed. The purposes of this study were to investigate alterations of cell cycle regulators in MPNST of different histologic grades, to assess their relationship to tumor cell cytodifferention and proliferation, and to identify possible markers for early detection of tumor progression and malignant transformation from PNF to MPNST.

Materials and methods

Case Selection

Formalin-fixed, paraffin-embedded archival tissue from 19 PNFs and 27 MPNSTs were obtained from institutional surgical pathology files. The diagnosis was based on the light microscopic examination with H&E and immunohistochemical stains. With an appropriate clinical history and presentation, the diagnosis of a low-grade MPNST was made when atypical features in a plexiform neurofibroma, such as increased cellularity, nuclear atypia, and low levels of mitotic activity, were present (31). The diagnosis of a high-grade MPNST was made when a tumor was composed of pleomorphic, dense fascicles of spindle cells with brisk mitoses, focal necrosis, and histologic or immunohistochemical evidence of focal Schwann cell differentiation with exclusion of other high grade sarcomas (32). Cases with heterologous or epithelial elements were not

included in this study. MPNST grade was classified as low or high, using the Pediatric Oncology Group Non-rhabdomyosarcoma Soft Tissue Sarcoma Grading System (33).

Immunohistochemical study

A representative tissue block for immunohistochemical analysis from each case was selected after all H&E stained sections were reviewed. Immunohistochemical analysis was performed with a Ventana 320 automated stainer (Ventana, Tucson, AZ) with use of a standard indirect avidin-biotin peroxidase detection method. The tissue was cut into 3 μm sections onto silanated slides and incubated at 56°C for 30 minutes. The sections were dewaxed and hydrated through diluted ethanol solutions to distilled water. The dilutions and sources of these antibodies are summarized in Table 1. The sections for S100 and CD 34 antibodies were microwaved for 15 minutes in 10 mM citrate buffer. The sections for Leu7 (CD57) had no pretreatment. The sections for all of the other antibodies received antigen retrieval in an electric pressure cooker for 3 minutes. Sections were then stained against antibodies to S100 protein (S100), Leu7, CD34, p16, p27, p53, Mib-1, topoisomerase II-alpha (TopoIIα, with appropriate controls. p27 also included an amplification kit (Amplification kit from Ventana). Among these antibodies, the expression of S100, CD34, Mib-1, TopoIIa, p53, p16, p27 were further compared and analyzed among PNF and low-grade and high-grade MPNSTs.

The staining patterns of S100, Leu 7, and CD34 were determined by examinations of cellular reactivity in the entire section. Positivity of S100, Leu 7, and CD34 staining was scored as diffuse (majority of cells are positive), focal (individual and focal cluster of cells are positive), or absent (no positive cells are identified). Staining for Mib-1, TopoIIα, p53, p16, and p27 was

scored by average numbers of nuclear reactivity in ten microscopic fields. The following percentage of positive nuclear staining were used as cut-off points (14,16,34,35,36): Mib-1 >5%, TopoIIa >5%, p53 >5%, P16 >10%, and p27 >10%.

Statistical Methods

Chi-square test was used to compare immunohistochemical expression of S100, Leu7, CD34, p16, p27, p53, Mib-1 and TopoIIα among PNF, NF1-related and non-NF1 MPNSTs of different histological grades. Significance of correlation for the presence of p53, p16 and p27 with the Mib-1 labeling index was tested by Fisher's exact test. All comparisons were made at a significance level of $p<0.05$.

Results

Clinic pathologic Data

Of 19 PNFs, 15 were from confirmed NF1 patients and 4 had unknown NF1 status. Of 27 MPNSTs, 13 patients had NF1, and 7 were non-NF1, per extended review of medical records. The NF1 status could not be determined by medical record review in the remaining 7 MPNSTs. The MPNST patients without NF1 (age range 2 to 61 years, mean 35 years) were generally older

than those with NF1 (age range 7 to 21years, mean 16.4 years). The PNF patients had a mean age of 13.4 years (age range 2 to 18 years). Histologically, 5 MPNSTs were low-grade (3 with NF1, 1 without NF1, 1 with unknown NF1 status) and the remaining 22 were high-grade (10 with NF1, 6 without known NF1 and 6 with unknown NF1 status). Six high-grade MPNST specimens had associated PNF.

Immunohistochemical data

Results of immunohistochemical stains are summarized in tables 2 and 3. Distinct differences between PNFs (Figure 1) and high-grade MPNSTs (Figure 2) were noted for S100, Leu7, CD34, Mib-1, TopoIIα, p16, p27 and p53 reactivity. While diffuse S100 and Leu7 staining was present in 89% and 84% of PNFs, it was observed in only 14% and 32% of high-grade MPNSTs ($p<0.001$), respectively. In the remaining high-grade MPNSTs, the S100 and Leu7 staining was focal in 50% and 55%, and absent in 36% and 13% of cases, respectively. In contrast, the pattern and frequency of S100 and Leu7 immunoreactivity was similar between PNFs and low-grade MPNSTs ($p>0.05$ for S100, $p>0.05$ for Leu 7). Similarly, diffuse CD34 positive spindle cells were observed in 95% of the PNFs and 80% of low-grade MPNSTs. In comparison, only 9% of high-grade MPNST displayed diffuse CD34 reactivity ($p<0.001$; for high grade MPNST

versus PNF). Proliferation marker expression differed between PNF and high–grade MPNST, and low-grade MPNST staining was similar to PNF. Mib-1 nuclear staining ranging from 1%-80% was seen in most high-grade MPNSTs. 72% of high-grade MPNSTs had Mib-1 expression in more than 5% of nuclei. In contrast, none of the PNFs had Mib-1 expression in more than 1% of nuclei ($p<0.001$). Although one of five low-grade MPNSTs demonstrated an increased Mib-1 labeling index of 10%, the difference between low-grade MPNSTs and PNFs was not statistically significant ($p>0.05$). TopoIIα reactivity paralleled that of Mib-1. 72% of high-grade MPNSTs had more than 5% of nuclear stain positive for TopoIIα, while none of the PNFs displayed TopoIIα expression in more than 1% nuclei ($p<0.001$). Low-grade MPNSTs and PNFs did not differ significantly in TopoIIα expression ($p>0.05$).

Frequent staining for p53, p16, and p27 was present in high-grade MPNSTs but not in low-grade MPNSTs or PNFs. p53 nuclear reactivity ranging from 5% to > 50% of tumor cells were seen in 59% of high-grade MPNSTs, but in none of 19 PNFs ($p<0.01$). In contrast to the high-grade MPNSTs, only one of the five low-grade MPNSTs showed p53 nuclear staining of more than 5% nuclei. p53 expression between PNFs and low-grade MPNSTs did not differ significantly

($p>0.05$). p16 nuclear staining ranging from 5% to more than 50% of cells was seen in PNFs. p16 positivity in more than 10% nuclei was present in 84% of the PNFs, and only in 46% of high-grade MPNST ($p<0.025$). PNFs and low-grade MPNSTs were similar in their p16 reactivity (84% vs 70%, $p>0.05$). p27 nuclear staining ranging from 5 to 50% of cells was observed in most PNFs. p27 nuclear reactivity in greater than 10% of cells was identified in 68% of PNFs, but only in 14% of high-grade MPNSTs ($p<0.01$) and 40% of low-grade MPNSTs ($p>0.05$). Although occasional cytoplasmic p27 staining was observed in some high-grade MPNSTs, none of these cases had cytoplasmic staining exceeding 10% of cells.

The presence of p53 reactivity correlated with Mib-1 and TopoIIα expression in high -grade MPNSTs ($p<0.01$). No statistically significant correlations, however, were identified between p16 and p27 expression and proliferation markers Mib-1 and TopoIIα.

When high-grade MPNSTs with associated benign PNF in the same histologic sections were analyzed, distinctive intratumoral heterogeneity was observed for S100, CD34, Mib-1, TopoIIα, p53, p16 and p27 staining (Figures 3 and 4). In high-grade MPNSTs where focal PNF areas with

an abrupt transition to MPNST were seen, staining patterns on each side of the transition areas were respectively similar to those seen in the either isolated PNFs or high-grade MPNSTs.

Comparison of p53, p16 and p27 expression between NF1-related and non-NF1 high-grade MPNSTs revealed a higher frequency of p53 immunoreactivity was present in the NF1-related MPNSTs than that in the sporadic cases (89% versus 43%, $p<0.025$). Although p16 immunoreactivity was lower in NF1-related high-grade MPNSTs, it did not reach statistical significance ($p>0.1$). Similarly, no significant differences were present in the expression of S100, CD34, Mib-1, TopoIIa and p27 between NF1-related and sporadic high-grade MPNSTs.

Discussion

Although the neoplastic origin of PNF and MPNST remains unsettled, most studies suggest that Schwann cells that harbor inactivating *NF1* gene mutations in both allels are the primary neoplastic component in both PNF and the majority of MPNSTs (37,38, 39). Using dual-color fluorescence *in situ* hybridization, Perry and associates provided evidence that the S100-positive Schwann cells harbor *NF1* deletions as somatic inactivating mutations ("second hits") in PNFs

derived from patients with NF1 (39). They suggested that S100-negative cells in MPNSTs represent dedifferentiated Schwann cells that lack functional neurofibromin, and this applies to both NF1-associated and sporadic MPNSTs. Our observation that the diffuse S100 protein and Leu 7 expression in PNFs was diminished, or lost, in the majority of high-grade MPNSTs supports the concept that Schwann cell dedifferentiation occurs during MPNST tumor progression. The decreased CD34 reactivity in our study parallels the change in S100 protein, and most likely represents a loss of CD34-positive, fibroblast-like, "dendritic interstitial", cells in the high- grade MPNSTs (40-41). The CD34-positive cell population, which was present in both normal peripheral nerve and benign peripheral nerve sheath tumors, tended to be lost in the MPNSTs, has been previously described by Weiss et al. (42), who suggested that a CD34-positive cell population is a normally occurring nerve sheath cell component and is apparently distinct from fibroblasts and conventional schwann cells. Although the underlying mechanism for significantly decreased CD34-positive cells in the high-grade MPNST remains unknown, the CD34-positive stromal component may play a role in MPNST tumor formation, as suggested earlier by Watanabe and associates (43).

In this study, the high-grade MPNSTs displayed a distinctive pattern of increased proliferation and frequent alterations of the cell cycle regulators p53, p16 and p27. Interestingly, co-expression of proliferation markers Mib-1 and TopoIIa was found in 72% of high-grade MPNSTs. Mib-1 is a monoclonal antibody to a nuclear proliferating antigen Ki-67, which is present in all phases of the cell cycle, except for G0. A high labeling index, greater than 25%, correlated with a reduced survival rate, and has been proposed as a significant indicator for poor prognosis (44). TopoisomeraseII alpha (TopoIIα) is a nuclear enzyme whose reactivity has been linked with cellular dedifferentiation and a potentially aggressive tumor phenotype in various neoplasms (35,36). Notably, the loss of diffuse staining patterns for S100, Leu7, and CD34, and the increased proliferation immunostaining that characterized the malignant phenotype were restricted to the high-grade MPNST areas in those tumors with both MPNST and PNF components. Furthermore, an identical topographical difference in the expression of p53, p27 and p16 between PNF areas with adjacent MPNST was also present. These observations support the hypothesis that altered p53, p16 and p27 protein expression is associated with tumor progression and malignant transformation from PNF to MPNST.

Although the deletions involving chromosome 17p, including the *TP53* locus, and mutation of the *TP53* gene has been observed in few MPNSTs (8,9,10), the underlying mechanism of p53 dysfunction in MPNST is not well understood. In mouse tumor models, inactivation of both the *Nf1* and *Tp53* genes is sufficient for the high likelihood to develop MPNSTs (45,46). Halling and associates, in a study of 28 MPNSTs, showed a shorter survival for MPNST patients with p53 immunohistochemical positivity than among those without p53 reactivity (47). However, other studies failed to demonstrate a correlation between p53 immunoreactivity and prognosis for MPNST (44). Our data, like previous reports, demonstrated that p53 immunohistochemical reactivity in the high-grade MPNSTs was significantly correlated with the proliferation markers Mib-1 (44) and TopoIIα, suggesting that the alteration of p53 might play a role in tumor progression by promoting cell proliferation. However, in our study, significant p53 nuclear expression was absent in the majority of the low-grade MPNSTs or in the PNFs adjacent to high-grade MPNSTs. The lack of p53 alteration in the majority of low-grade MPNSTs and in the PNFs adjacent to MPNST mitigates against the hypothesis that p53 abnormalities are an initial event in tumor progression in humans. This is in contrast to mouse tumor models where double inactivation of *Nf1* and *Tp53* in mice is sufficient to generate MPNSTs.

There are relatively few studies comparing p53 expression in MPNST of different histologic grades. A study of NF1-related and sporadic peripheral nerve sheath lesions in pediatric patients by Liapis and colleagues (34) reported a significant difference in the frequency of p53 with different histologic grades of MPNST, and they suggested that p53 accumulation with secondary *TP53* mutations may be a late event in the course of tumor progression. In studies of 54 MPNSTs, with or without associated PNF, McCarron and Goldblum (48) observed that the immunohistochemical detection of p53 protein is common in malignant areas, but is rare in the PNF regions. Leroy et al. (49) identified *TP53* mutations in 4/6 NF1-related MPNSTs, but considered mutations the *TP53* as late events in MPNST progression. Thus, the lack of *TP53* mutations and the rarity of p53 staining in the PNF regions preclude the use of p53 immunostaining to predict progression to MPNST (48,49).

In the present study, we observed a higher frequency of p53 immunoreactivity in NF1-related versus non-NF1 high-grade MPNSTs (89% vs. 43 %, $p<0.025$). These results are in agreement with the previous study by Liapis and colleagues, who also found p53 accumulation more frequently in NF1-associated MPNSTs (34). In contrast, Halling et al, reported no difference in

the frequency or degree of p53 staining between MPNSTs from patients with or without NF1 (47). Birindelli and colleagues compared p53 protein expression and *TP53* mutations between NF1- related and sporadic MPNSTs and found that the *TP53* mutation, loss of heterozygosity involving the *TP53* locus, and p53 protein overexpression were mainly restricted to sporadic MPNST (16). Although the causes for the discrepancies among different studies are currently unknown, these observations raise the question that different pathways or mechanisms may be involved in the development and progression of MPNST between NF1-related and sporadic cases (16). It is known that despite similar morphologic and immunophenotypic features in MPNST, tumors in patients with NF1 arise in different clinical and genetic contexts (16). NF1 is a familial cancer syndrome whereby haploinsufficiency of the *NF1* gene product, neurofibromin, plays a critical role in predisposing NF1 patients to develop benign and malignant tumors (50,51). Further studies are required to determine the value of p53 immunodetection in peripheral nerve sheath tumors.

Loss of p16 has been reported in 50 to 75% of MPNSTs in different series (16-18). p16 expression, however, has not been compared in MPNSTs of different histologic grades. We demonstrate that a significant loss of p16 expression is present in high-grade MPNSTs, but not in low-grade MPNSTs. This result is similar to our findings for p53. No significant difference was found between p16 expression in PNF and low-grade MPNST or in PNF areas adjacent to high-grade MPNST. Nor was there a significant correlation between the loss of p16 expression in high-grade MPNST and proliferation markers Mib-1 and TopoIIa. It is known that p16, in contrast to p53, regulates the G1-S phase checkpoint of the cell cycle through the pRB pathway (17-19). Although interactions between different pathways in the tumor progression of MPNST

are currently unknown, several recent studies suggest that dysregulation of cell cycle regulators affecting different pathways may act in concert to facilitate tumor progression in MPNST (13). Recent studies also demonstrated that inactivation of *INK4A*, the gene encoding both p16 and p19, was present in 60% to 75% of MPNSTs (13,14). Since p16 and p19 affect the cell cycle through pRB and p53 pathways respectively, this is further evidence that co-inactivation of different pathways may be an important step in tumor progression (13).

In contrast to p53 and p16, the decreased level of p27 protein expression during tumor development and progression does not appear to result from gene mutation, but mainly at the post-translational level with protein degradation by the ubiquitin-proteasome pathway (26). Korea and colleagues recently reported that a nuclear p27 phenotype was observed in 94% of NFs versus only 9% of high-grade MPNST and they suggested that p27 might be involved in tumor progression in the PNF-MPNST pathway (15). We also observed a significant loss of p27 nuclear expression in high-grade MPNSTs, although the significant cytoplasmic p27 expression described by Korea was not noted (16). We also found no significant difference in p27 nuclear expression between PNF and low-grade MPNST, and there was no significant correlation between p27 immunoreactivity and proliferation marker Mib-1. Since p27 is an important promoter of apoptosis and functions as a downstream substrate in the bcl-2 pathway (25-27), perhaps altered p27 promotes tumor progression through mechanisms involving deranged apoptosis rather than increased cell proliferation.

In contrast to our finding of more frequent p53 expression in NF1- associated MPNST, no significant difference was found in the expression of either p16 or p27 in MPNSTs between

NF1-related versus sporadic tumors. Birindelli and colleagues also reported that the incidence of altered p16, represented by either *p16* gene homozygous deletion or LOH at the relative 9p21 locus and lack of p16 immunostaining, was almost equal between NF1-associated and sporadic MPNST (16). There is no previous study comparing p27 expression between NF1-related and sporadic MPNST.

In summary, frequent alterations of cell cycle regulators p53, p16 and p27 are present in high-grade MPNST. The synchronous presence of p53, p16, and p27 alterations, decreased S100 protein, Leu 7, and CD34 immunoreactivity patterns, and increased proliferation markers Mib-1 and TopoIIa in high-grade MPNST supports the concept that these altered cell cycle regulators influence tumor progression in the PNF-MPNST sequence. The p53 expression in high-grade MPNSTs is associated with concomitant expression of the proliferation marker Mib-1, and it appears to be more frequent in NF1-related MPNSTs. However, the lack of significant alterations of these cell cycle regulators in PNF adjacent to high-grade MPNST, or in the majority of low-grade MPNST, indicates that the alterations are unlikely to be initial events in malignant transformation. Therefore, they are not reliable for early detection of tumor progression in MPNST. Recently, DeClue and coworkers report that epithelial growth factor receptor (EGFR), which regulates the cell cycle through both pRB- dependent and independent pathways, might also play an important role in NF1 tumorigenesis and Schwann cell transformation (52). The question remains whether there are as yet unidentified specific genetic events, which may be responsible for initiating progression from PNF to MPNST. A recent study by Zhu and colleagues provided genetic evidence that the *Nf1* haploinsufficient state of the

somatic tissue surrounding peripheral nerve sheath tumors, including fibroblasts and mast cells, provides a functional contribution to tumor formation either though initiation or progression of tumorigenesis (53). Studies are needed on genetic factors that, if detected, could provide insight to critical events that initiate tumor progression and malignant transformation. In the meantime, histologic criteria, though imperfect, remain the basis for clinically distinguishing PNF from MPNST, and determination of p53 reactivity may prove useful to discriminate low-grade and high-grade MPNST in a small biopsy.

Grants and acknowledgments

Work presented was supported by a grant form the Department of The Army Neurofibromatosis Program (DV); DAMD-NF980007

References

1. Cawthon RM, Weiss R, Xu GF, et al. A major segment of the neurofibromatosis type 1 gene: cDNA sequence, genomic structure, and point mutations. *Cell* 1990; 62:193-201.

2. Viskochil D, Buchberg AM, Xu G, et al. Deletions and a translocation interrupt a cloned gene at the neurofibromatosis type 1 locus. *Cell* 1990; 62:187-92.

3. Wallace MR, Marchuk DA, Andersen LB, et al. Type 1 neurofibromatosis gene: identification of a large transcript disrupted in three NF1 patients. *Science* 1990; 249:181-6

4. Xu GF, O'Connell P, Viskochil D, et al. The neurofibromatosis type 1 gene encodes a protein related to GAP. *Cell* 1990;62:599-608.

5. Martin GA, Viskochil D, Bollag G, et al. The GAP-related domain of the neurofibromatosis type 1 gene product interacts with ras p21. *Cell* 1990; 63:843-9

6. Viskochil D, White R, Cawthon R. The neurofibromatosis type 1 gene. *Annu Rev Neurosci* 1993;16:183-205

7. Ferner RE, Gutmann DH. International consensus statement on malignant peripheral nerve sheath tumors in neurofibromatosis. *Cancer Res* 2002; 62:1573-7.

8. Scheithauer BW, Woodruff JM, Erlandson RA. Tumors of the peripheral nervous system. Atlas of Tumor Pathology, third series, fascicle 24. Washington, DC: Armed Forces Institute of Pathology. 1999.

9. Jhanwar SC, Chen Q, Li FP, et al. Cytogenetic analysis of soft tissue sarcomas. Recurrent chromosome abnormalities in malignant peripheral nerve sheath tumors (MPNST). *Cancer Genet Cytogenet* 1994;78: 138-44

10. Legius E, Dierick H, Wu R, et al. TP53 mutations are frequent in malignant NF1 tumors. *Genes Chromosomes Cancer* 1994;10:250-5.

11. Menon AG, Anderson KM, Riccardi VM, et al. Chromosome 17p deletions and p53 gene mutations associated with the formation of malignant neurofibrosarcomas in von

Recklinghausen neurofibromatosis. *Proc Natl Acad Sci, U S A* 1990;87: 5435-9.

12. Cohen JA, Geradts J. Loss of RB and MTS1/CDKN2 (p16) expression in human sarcomas. *Hum Pathol* 199;28: 893-898.

13. Berner JM, Sorlie T, Mertens F, et al. Chromosome band 9p21 is frequently altered in malignant peripheral nerve sheath tumors: studies of CDKN2A and other genes of the pRB pathway. *Genes Chromosomes Cancer* 1999; 26:151-60.

14. Kourea HP, Orlow I, Scheithauer BW et al. Deletions of the INK4A gene occur in malignant peripheral nerve sheath tumors but not in neurofibromas. *Am J Pathol 1999*;155:1855-60.

15. Nielsen GP, Stemmer-Rachamimov AO, Ino Y, et al. Malignant transformation of neurofibromas in neurofibromatosis 1 is associated with CDKN2A/p16 inactivation. *Am J Pathol* 1999;155:1879-84.

16. Kourea HP, Cordon-Cardo C, Dudas M, et al. Expression of p27(kip) and other cell cycle regulators in malignant peripheral nerve sheath tumors and neurofibromas: the emerging role of p27(kip) in malignant transformation of neurofibromas. *Am J Pathol* 1999;155:1885-91.

17. Birindelli S, Perrone F, Oggionni M, et al.Rb and TP53 pathway alterations in sporadic and NF1-related malignant peripheral nerve sheath tumors. *Lab Invest* 2001 Jun; 81(6):833-44.

18. Serrano M, Hannon GJ, Beach D. A new regulatory motif in cell-cycle control causing

specific inhibition of cyclin D/CDK4. *Nature* 1993 Dec 16;366:704-7.

19. Li Y, Nichols MA, Shay JW, et al. Transcriptional repression of the D-type cyclin-dependent kinase inhibitor p16 by the retinoblastoma susceptibility gene product pRb. *Cancer Res* 1994;54(23):6078-82

20. Lukas J, Aagaard L, Strauss M, et al. Oncogenic aberrations of p16INK4/CDKN2 and cyclin D1 cooperate to deregulate G1 control. *Cancer Res* 1995 ;55:4818-23

21. Ueki K, Ono Y, Henson JW Efird JT, von Deimling A, Louis DN: CDKN2/p16 or RB alterations occur in the majority of glioblastomas and are inversely correlated. *Cancer Res* 1996; 56:150-153.

22. Liew CT, Li HM, Lo KW, et al. High frequency of p16INK4A gene alterations in hepatocellular carcinoma. *Oncogene* 1999, 18:789-795.

23. Burns KL, Ueki K, Jhung SL,et al. Molecular genetic correlated of p16, cdk4 and pRb immunohistochemistry in glioblastomas. *J Neuropathol Exp Neurol* 1998, 57:122-130.

24. Caldas C, Hahn SA, da Costa LT, et al. Frequent somatic mutation and homozygous deletions of the p16 (MTS1) gene in pancreatic adenocarcinoma. *Nature Genet* 1994, 8:27-32.

25. Toyoshima H, Hunter T. p27, a novel inhibitor of G1 cyclin-Cdk protein kinase activity, is related to p21. *Cell* 1994;78:67-74.

26. Polyak K, Lee MH, Erdjument-Bromage H, et al. Cloning of p27Kip1, a cyclin-dependent kinase inhibitor and a potential mediator of extracellular antimitogenic signals. *Cell*

1994;78:59-66.

27. Lloyd RV, Erickson LA, Jin L, et al. p27kip1: a multifunctional cyclin-dependent kinase inhibitor with prognostic significance in human cancers. *Am J Pathol* 1999;154:313-23.

28. Katayose Y, Kim M, Rakkar AN, et al. Promoting apoptosis: a novel activity associated with the cyclin- dependent kinase inhibitor p27. *Cancer Res* 1997;57:5441-5.

29. Levkau B, Koyama H, Raines EW, et al. Cleavage of p21Cip1/Waf1 and p27Kip1 mediates apoptosis in endothelial cells through activation of Cdk2: role of a caspase cascade. *Mol Cell* 1998;1:553-63

30. Durand B, Gao FB, Raff M. Accumulation of the cyclin-dependent kinase inhibitor p27/Kip1 and the timing of oligodendrocyte differentiation. *EMBO J* 1997;16:306-17.

31. Weiss SW, Goldblum JR. Benign tumors of peripheral nerves. In: Weiss SW, Goldblum JR eds. Enzinger and Weiss's Soft Tissue tumor. 4th ed. St. Louis: Mosby. 2001;1137-42

32. Weiss SW, Goldblum JR . Malignant tumors of peripheral nerves. In: Weiss SW, Goldblum JR eds. Enzinger and Weiss's Soft tissue Tumor. 4th ed. St. Louis: Mosby. 2001; 1209-63

33. Parham DM, Webber BL, Jenkins JJ 3rd, et al. Nonrhabdomyosarcomatous soft tissue sarcomas of childhood: formulation of a simplified system for grading. *Mod Pathol* 1995 ;8:705-10

34. Liapis H, Marley EF, Lin Y,et al. p53 and Ki-67 proliferating cell nuclear antigen in benign and malignant peripheral nerve sheath tumors in children. *Pediatr Dev Pathol* 1999;

2:377-84.

35. Costa MJ, Hansen CL, Holden JA, et al. Topoisomerase II alpha: prognostic predictor and cell cycle marker in surface epithelial neoplasms of the ovary and peritoneum. *Int J Gynecol Pathol* 2000; 19:248-57.

36. Nakopoulou L, Lazaris AC, Kavantzas N, et al. DNA topoisomerase II-alpha immunoreactivity as a marker of tumor aggressiveness in invasive breast cancer. *Pathobiology* 2000; 68:137-43.

37. Kluwe L, Friedrich R, Mautner VF. Loss of NF1 allele in Schwann cells but not in fibroblasts derived from an NF1-associated neurofibroma. *Genes Chromosomes Cancer* 1999;24:283-5

38. Serra E, Rosenbaum T, Winner U, et al. Human Schwann cells harbor the somatic NF1 mutation in neurofibromas: evidence of two different Schwann cell subpopulations. *Mol Genet* 2000;9:3055-64

39. Perry A, Roth KA, Banerjee R, Fuller CE, Gutmann DH. NF1 deletions in S-100 protein-positive and negative cells of sporadic and neurofibromatosis 1 (NF1)-associated plexiform neurofibromas and malignant peripheral nerve sheath tumors. Am J Pathol 2001;159:57-61.

40. Nickoloff BJ. The human progenitor cell antigen (CD34) is localized on endothelial cells, dermal dendritic cells, and perifollicular cells in formalin- fixed normal skin, and on proliferating endothelial cells and stromal spindle-shaped cells in Kaposi's sarcoma. Arch Dermatol 1991;127:523-9.

41. Suster S, Fisher C, Moran CA. Expression of bcl-2 oncoprotein in benign and malignant spindle cell tumors of soft tissue, skin, serosal surfaces, and gastrointestinal tract. *Am J Surg Pathol* 1998;22:863-72.

42. Weiss SW, Nickoloff BJ. CD-34 is expressed by a distinctive cell population in peripheral nerve, nerve sheath tumors, and related lesions. *Am J Surg Pathol* 1993;17:1039-45.

43. Watanabe T, Oda Y, Tamiya S, et al. Malignant peripheral nerve sheath tumour arising within neurofibroma. An immunohistochemical analysis in the comparison between benign and malignant components. *Clin Pathol* 2001;54:631-6

44. Watanabe T, Oda Y, Tamiya S, et al. Malignant peripheral nerve sheath tumours: high Ki67 labelling index is the significant prognostic indicator. *Histopathology* 2001;39:187-97.

45. Vogel KS, Klesse LJ, Velasco-Miguel S, et al. Mouse tumor model for neurofibromatosis type 1. *Science* 1999;286:2176-9.

46. Cichowski K, Shih TS, Schmitt E, et al. Mouse models of tumor development in neurofibromatosis type 1. *Science* 1999;286:2172-6.

47. Halling KC, Scheithauer BW, Halling AC, et al. p53 expression in neurofibroma and malignant peripheral nerve sheath tumor. An immunohistochemical study of sporadic and NF1-associated tumors. *Am J Clin Pathol* 1996;106:282-8.

48. McCarron KF, Goldblum JR. Plexiform neurofibroma with and without associated malignant peripheral nerve sheath tumor: a clinicopathologic and immunohistochemical

analysis of 54 cases. *Mod Pathol* 1998;11:612-7.

49. Leroy K, Dumas V, Martin-Garcia N, et al. Malignant peripheral nerve sheath tumors associated with neurofibromatosis type 1: a clinicopathologic and molecular study of 17 patients. *Arch Dermatol* 2001;137:908-13.

50. Riccardi VM, Neurofibromatosis: Phenotype, Natural history, and Patholgogenesis. 2nd ed. The Johns Hopkins University Press. 1992

51. Gutmann DH, Collins FS. Von Recklinghausen Neurofibromatosis. In: Dcriver CR, Beaudet AL, Sly WS, Valle D, eds. The Metabolic and Molecular Bases of Inherited Disease. McGraw-Hill, Inc. 1995:677-96

52. DeClue JE, Heffelfinger S, Benvenuto G, et al. Epidermal growth factor receptor expression in neurofibromatosis type 1-related tumors and NF1 animal models. *J Clin Invest* 2000;105:1233-41

53. Zhu Y, Ghosh P, Charnay P, et al. Neurofibromas in NF1: Schwann cell Origin and Role of Tumor Environment. *Science* 2002;296:920-2

Table 1. Antibodies and Sources

Antibody	Working Dilution	Source
S100	1:2000	Dako Corporation, Carpinteria, CA
CD34	1:200	Biosource International, Camarillo, CA
Leu7	!:40	Becton Dickenson
Mib-1	1:200	Dako Corporation, Carpinteria, CA
TopoIIα	1:1000	Joe Holden, MD, Salt Lake City, UT
p53	1:80	Dako Corporation, Carpinteria, CA
p27	1:60	Dako Corporation, Carpinteria, CA
p16	1:100	Santa Cruz Biotechnology, Inc. CA

Table 2. Clinicopathologic Data of 19 Plexiform Neurofibromas (PNFs)

Case#	Age/Sex	Site	NF1	S100	Leu7	CD34	p16	p27	p53	Mib-1	TopoIIα
1	7y M	knee	Yes	D	D	D	P	N	N	N	N
2	12y M	chest	Yes	D	D	D	P	P	N	N	N
3	14y M	C-4	Yes	F	D	D	N	P	N	N	N
4	12y F	thigh	Yes	D	D	F	P	P	N	N	N
5	14y M	nose	Yes	D	D	D	P	N	P	N	N
6	8y F	shoulder	Yes	D	F	D	P	N	N	N	N
7	21y M	neck	Yes	D	D	D	P	P	N	N	N
8	13y M	supraclavicular	Yes	D	D	D	P	P	N	N	N
9	17y F	arm	Yes	F	F	D	N	P	N	N	N
10	19y F	cheek	Yes	D	D	D	P	P	N	N	N
11	15y F	thigh	Yes	D	F	D	P	P	N	N	N
12	12y F	shoulder	Yes	D	D	D	P	N	N	N	N
13	16y F	shoulder	Yes	D	D	D	N	N	N	N	N
14	11y F	arm	Yes	D	F	D	P	N	N	N	N
15	17y F	foot	Yes	D	D	D	P	P	N	N	N
16	9y F	abdominal wall	Un	D	D	D	P	P	N	N	N
17	15y F	back	Un	D	D	D	P	P	N	N	N
18	11y M	hip	Un	D	D	D	P	P	N	N	N
19	14y M	hand	Un	D	D	D	P	P	N	N	N

*Un-Unknown; D-Diffuse; F-Focal; P-Positive; N-Negative

Table 3. Clinicopathologic Data of 27 MPMSTs

	Age/Sex	Site	Grade	NF1	S100	Leu7	CD34	p16	p27	p53	Mib1	TopoIIα
1	3/ F	leg	H	Un	N	D	D	P	P	N	N	N
2	3/F	leg	H	Un	N	D	D	P	P	N	N	N
3	2/F	Unknown	H	No	D	D	N	P	P	N	P	P
4	13/ F	arm	H	Yes	F	F	F	N	N	P	P	P
5	13/ F	arm	H	Yes	F	F	F	N	N	P	P	P
6	11/ F	neck	H	Yes	N	D	N	P	N	N	P	P
7	15/M	thigh	H	Yes	F	F	F	N	N	P	P	P
8	16/ M	shoulder	L	Yes	F	F	D	P	P	N	N	N
9	18/ F	neck	L	Yes	D	D	D	P	P	P	N	N
10	16/M	lung	H	Yes	F	D	N	P	N	P	P	P
11	13/F	neck	L	Yes	D	F	D	P	N	N	N	N
12	15/ M	chest	H	Un	F	F	N	N	N	N	P	P
13	20/ F	Arm	H	Yes	D	F	F	N	N	P	N	N
14	21/M	tibia	H	Yes	F	F	N	N	N	P	P	P
15	27/ F	back	H	Yes	F	F	N	N	N	P	P	P
16	35/ F	knee	H	No	F	F	N	P	N	N	N	N
17	65/ M	neck	H	Un	F	F	N	P	N	N	N	N
18	61/M	back	H	No	N	N	F	N	N	P	P	P
19	30/M	leg	L	No	N	F	N	N	N	N	N	N
20	43/ M	thigh	H	Yes	F	F	F	P	N	P	P	P

Table 3. (Continued)

	Age/Sex	Site	Grade	NF1	S100	Leu7	CD34	p16	p27	p53	Mib1	TopoIIα
21	40/ M	arm	L	Un	D	F	D	P	N	N	N	N
22	59/ F	thigh	H	Un	N	F	N	N	N	N	P	P
23	25/M	neck	H	No	F	D	N	N	N	N	P	P
24	44/M	back	H	No	N	N	N	N	N	P	P	P
25	44/M	back	H	No	N	N	N	N	N	P	P	P
26 2 7 2 7	20/M	Knee	H	Yes	F	D	N	P	N	P	P	P
	Unknown	Unknown	H	Un	D	F	F	P	N	P	N	N

Un-Unknown; D-Diffuse; F-Focal; P-Positive; N-Negative

Figure Legends:

Fig. 1: A PNF (case # 2) displays diffuse staining of S100, CD34, p16, p27 and negative staining for p53 and Mib-1.

Fig. 2: A MPNST (case #15) displays focal staining to S100, CD34, p16, p27 and increased reactivity to p53 and Mib-1.

Fig. 3: Significant intratumoral heterogeneity between PNF and contiguous high-grade MPNST in expression of S100, CD34, and Mib-1.

Fig. 4: Significant intratumor heterogeneity between a PNF and contiguous high-grade MPNST s in expression of p53, p16, and p27.

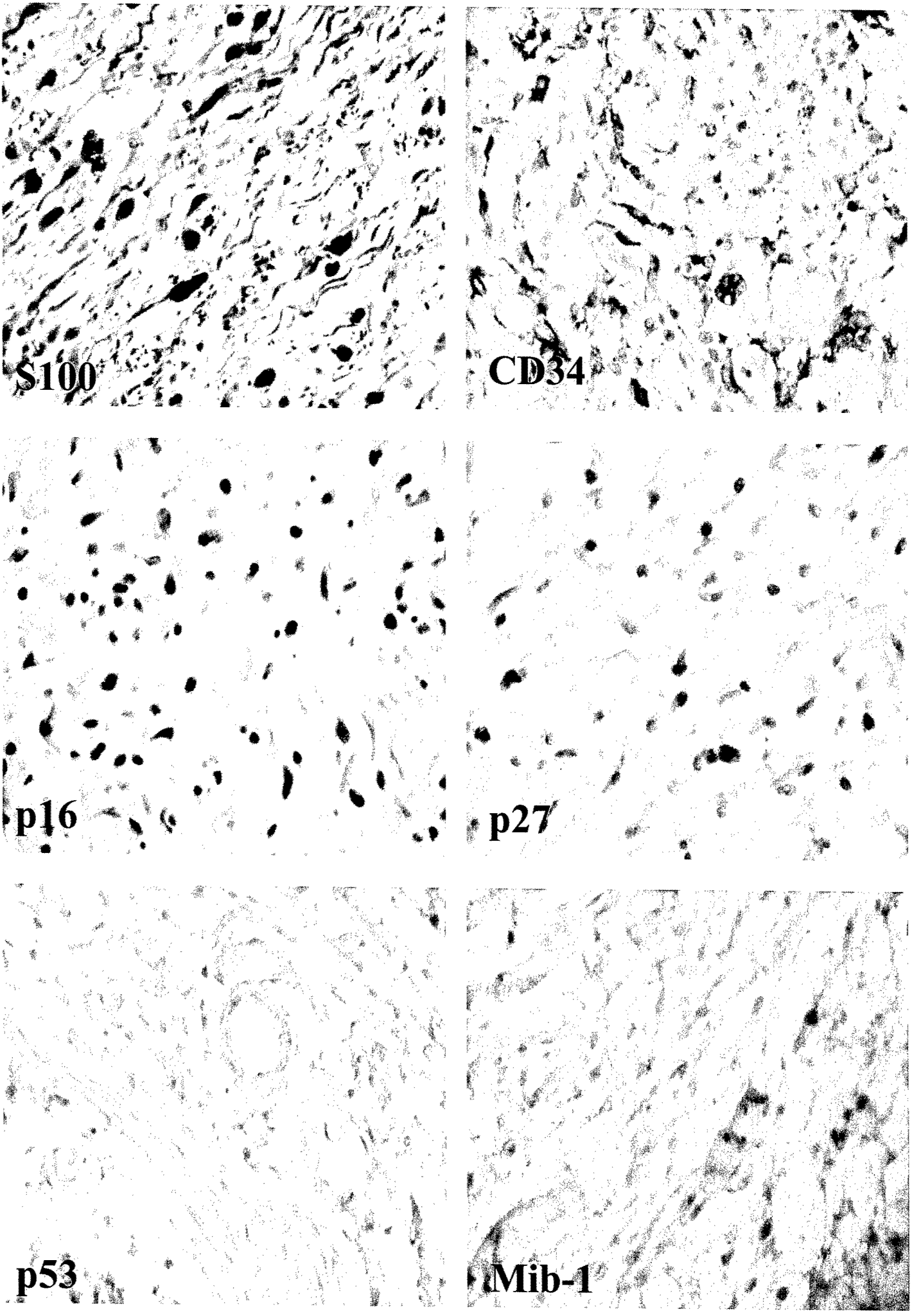
S100
CD34
p16
p27
p53
Mib-1

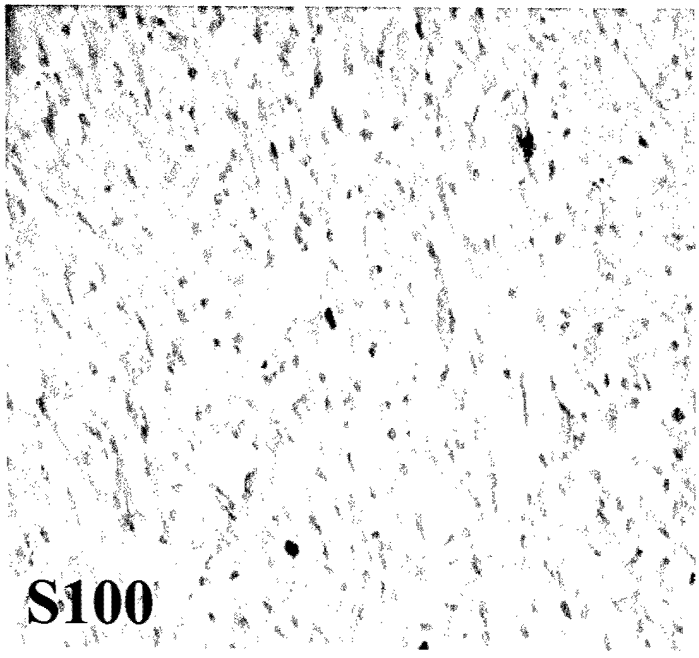
S100

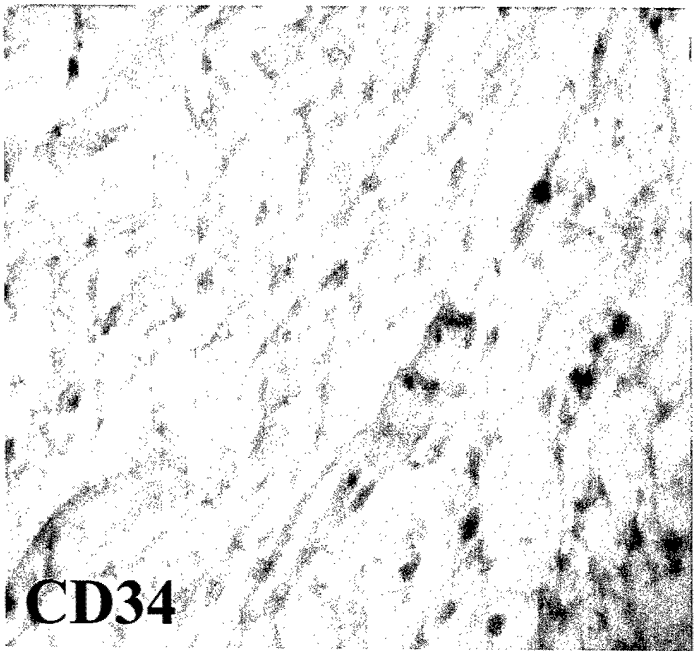
CD34

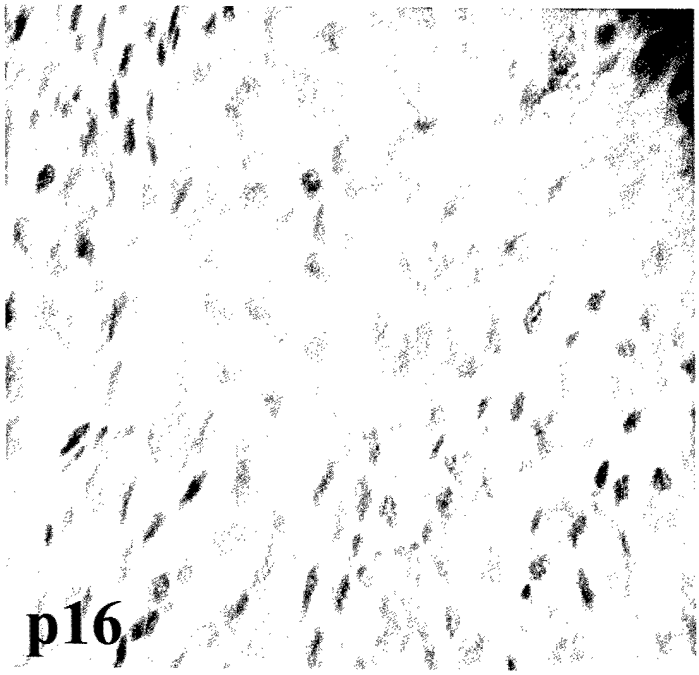
p16

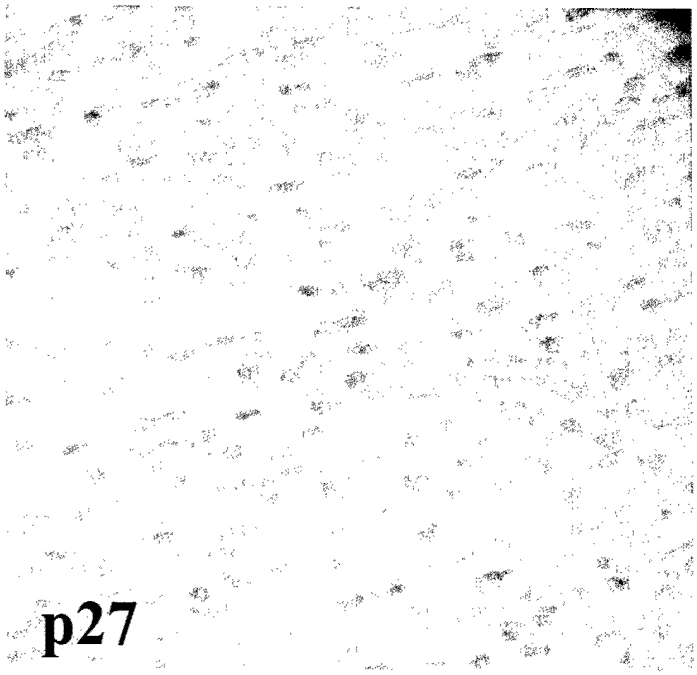
p27

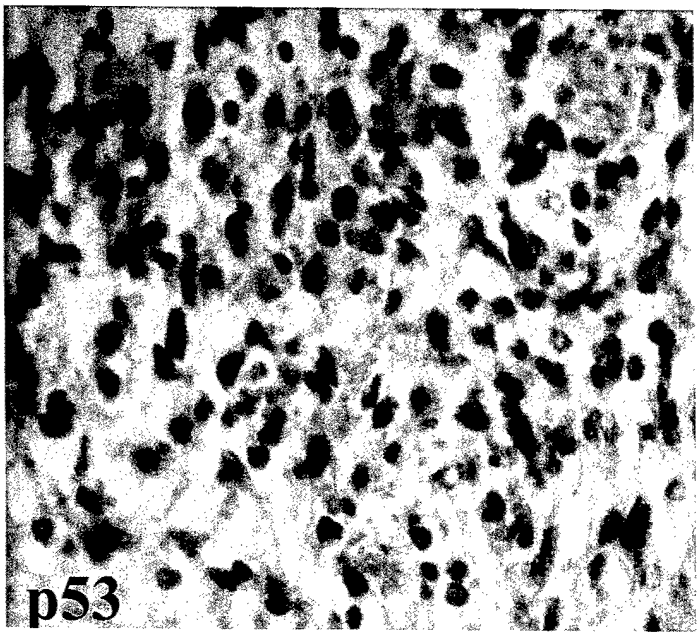
p53

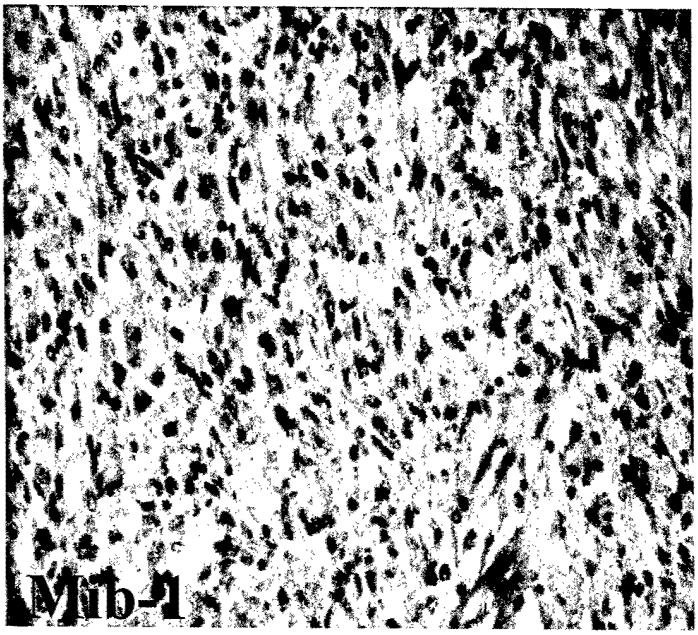
Mib-1

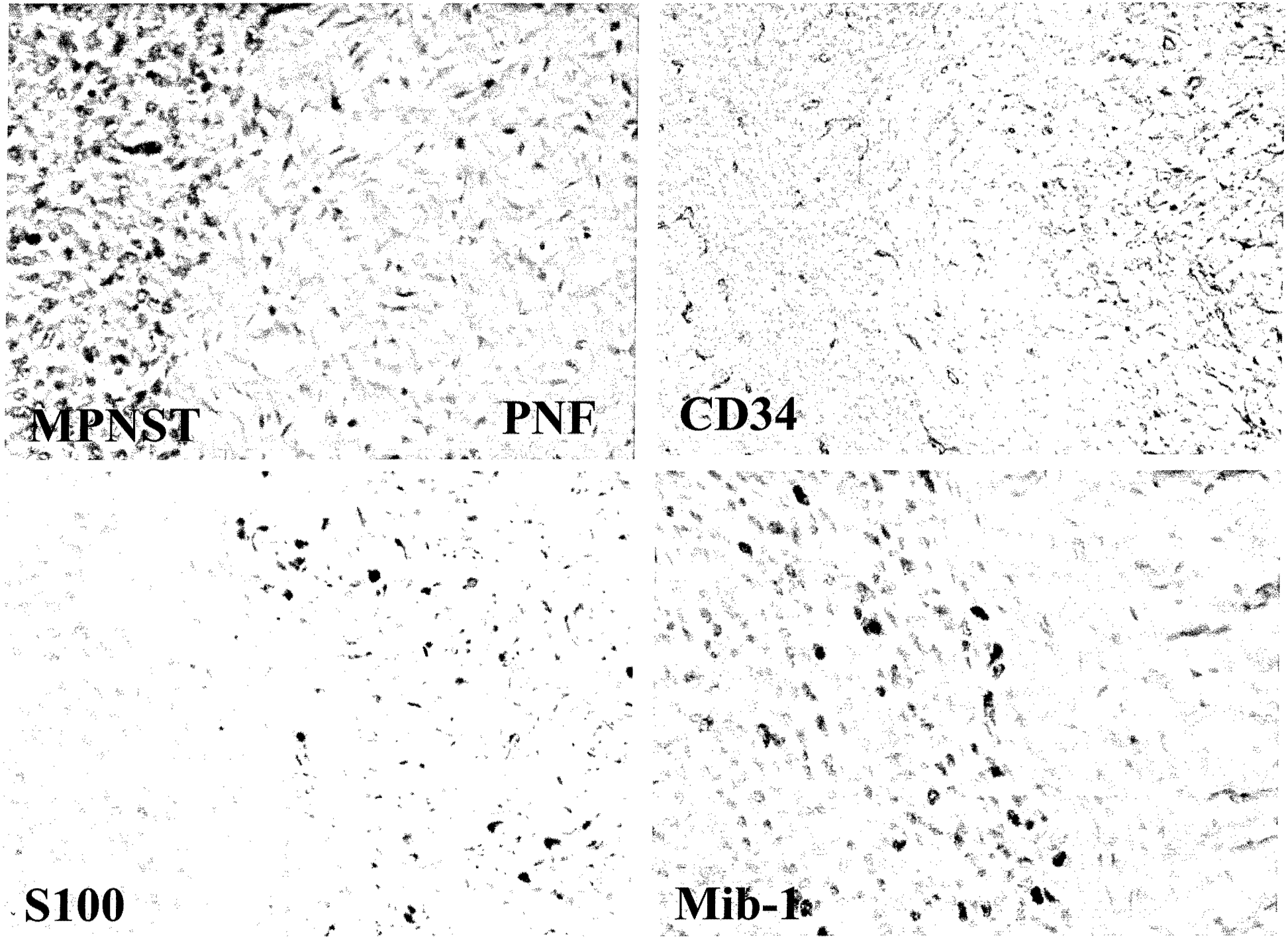
MPNST
PNF
CD34
S100
Mib-1

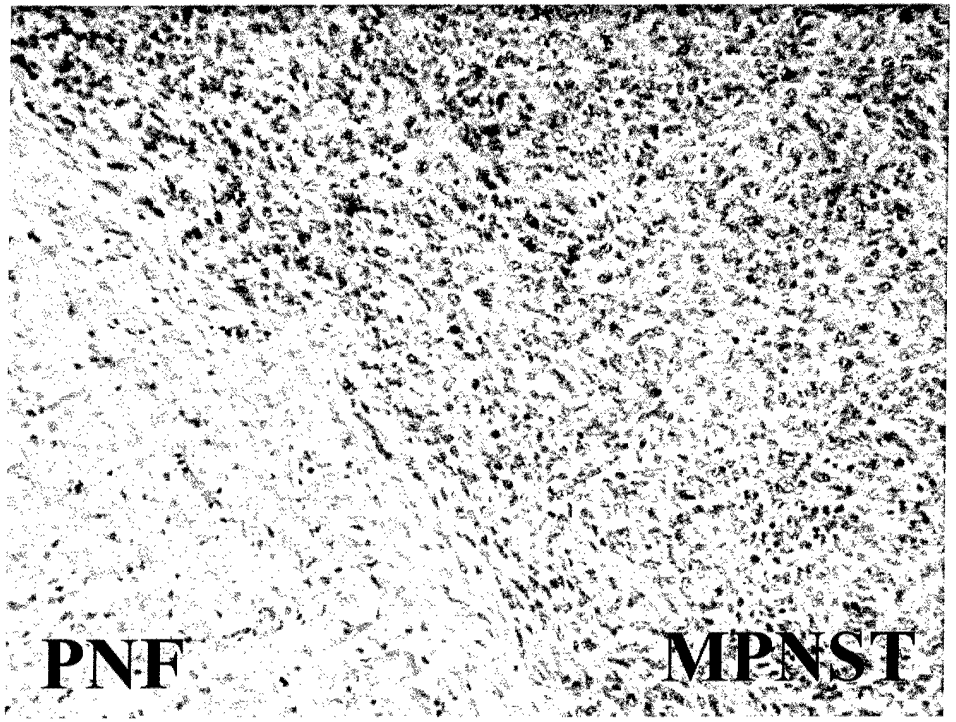
PNF
MPNST

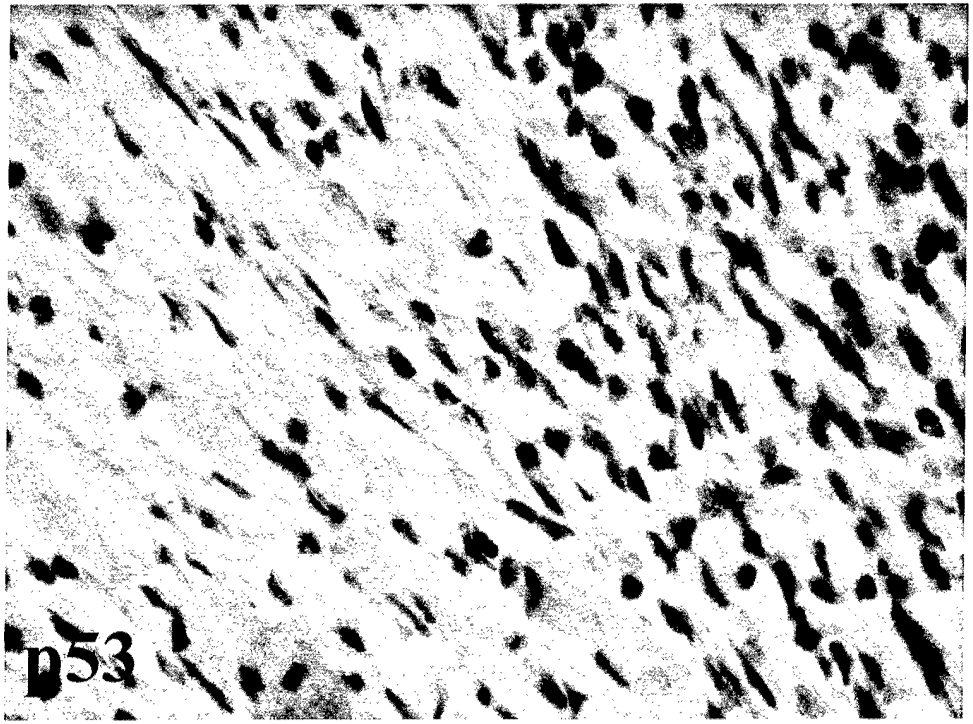
p53

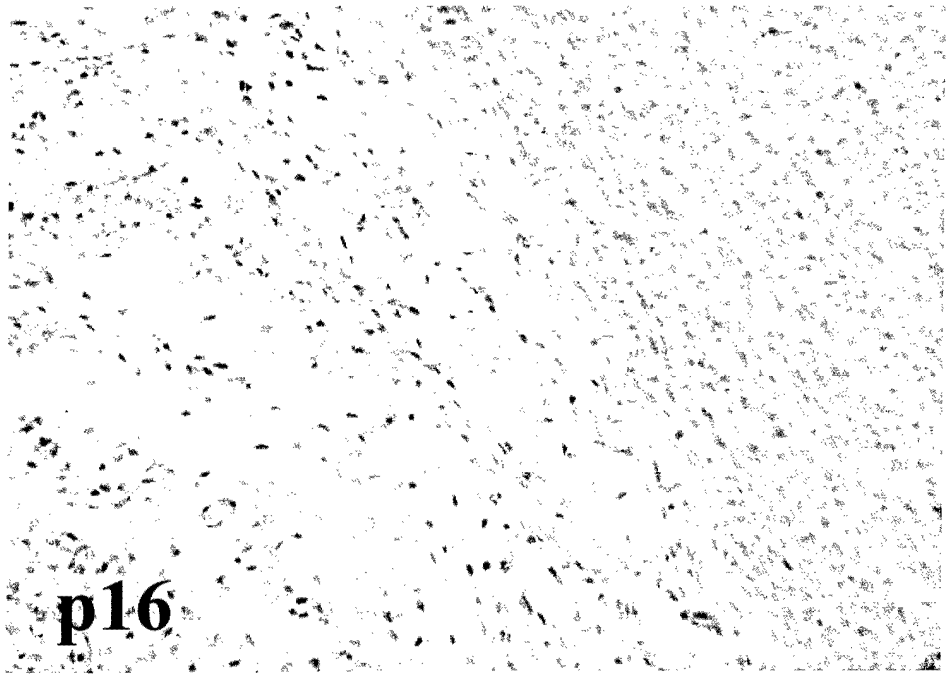
p16

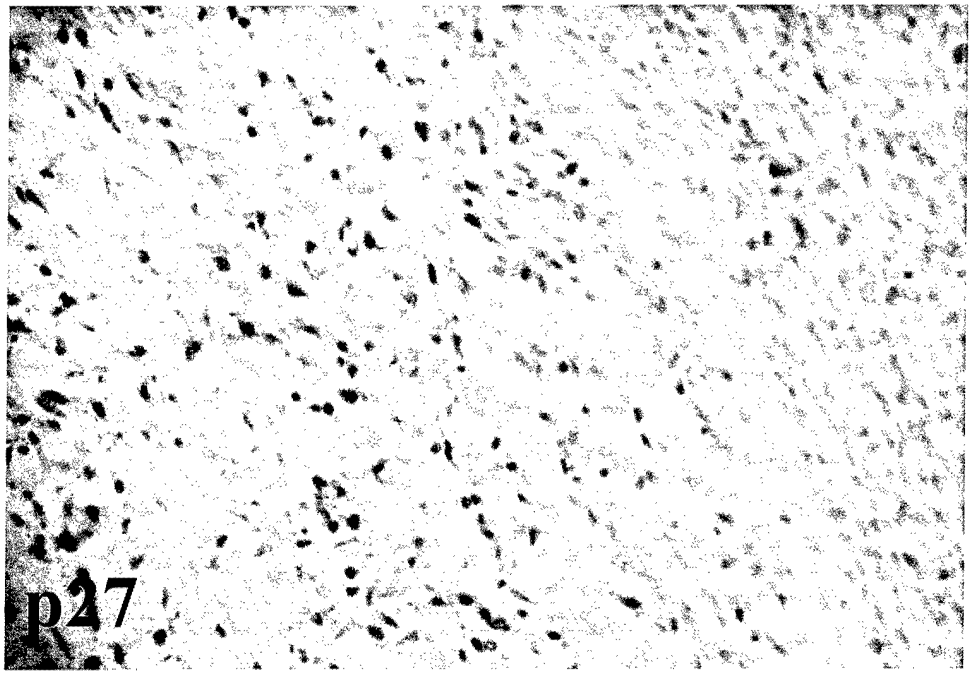
p27

Epidermal growth factor receptor expression in neurofibromatosis type 1–related tumors and NF1 animal models

Jeffrey E. DeClue,[1] Sue Heffelfinger,[2] Giovanna Benvenuto,[1] Bo Ling,[3] Shaowei Li,[1] Wen Rui,[3] William C. Vass,[1] David Viskochil,[4] and Nancy Ratner[3]

[1]Laboratory of Cellular Oncology, National Cancer Institute, Bethesda, Maryland, USA
[2]Department of Pathology, and
[3]Department of Cell Biology, Neurobiology, and Anatomy, University of Cincinnati College of Medicine, Cincinnati, Ohio, USA
[4]Department of Genetics, University of Utah, Salt Lake City, Utah, USA

Address correspondence to: Jeffrey E. DeClue, Laboratory of Cellular Oncology, National Cancer Institute, Building 36, Room 1D-32, Bethesda, Maryland 20892, USA.
Phone: (301) 496-4732; Fax: (301) 480-5322; E-mail: jd99f@nih.gov.

Giovanna Benvenuto's present address is: Department of Cellular and Molecular Biology and Pathology, Faculty of Medicine, University of Naples, Naples, Italy.

Received for publication June 16, 1999, and accepted in revised form March 20, 2000.

We have found that EGF-R expression is associated with the development of the Schwann cell–derived tumors characteristic of neurofibromatosis type 1 (NF1) and in animal models of this disease. This is surprising, because Schwann cells normally lack EGF-R and respond to ligands other than EGF. Nevertheless, immunoblotting, Northern analysis, and immunohistochemistry revealed that each of 3 malignant peripheral nerve sheath tumor (MPNST) cell lines from NF1 patients expressed the EGF-R, as did 7 of 7 other primary MPNSTs, a non-NF1 MPNST cell line, and the $S100^+$ cells from each of 9 benign neurofibromas. Furthermore, transformed derivatives of Schwann cells from *NF1*$^{-/-}$ mouse embryos also expressed the EGF-R. All of the cells or cell lines expressing EGF-R responded to EGF by activation of downstream signaling pathways. Thus, EGF-R expression may play an important role in NF1 tumorigenesis and Schwann cell transformation. Consistent with this hypothesis, growth of NF1 MPNST lines and the transformed *NF1*$^{-/-}$ mouse embryo Schwann cells was greatly stimulated by EGF in vitro and could be blocked by agents that antagonize EGF-R function.

J. Clin. Invest. **105**:1233–1241 (2000).

Introduction

Neurofibromatosis type 1 (NF1) is a dominantly inherited human disease affecting one in 2,500 to 3,500 individuals (1, 2). The NF1 phenotype is highly variable, and its clinical course is unpredictable. Several organ systems are affected, including the bones, skin, iris, and central nervous system (manifested in learning disabilities and gliomas) (3). The hallmark of NF1 is the development of benign tumors of the peripheral nervous system (neurofibromas), which vary greatly in both number and size among patients (1, 4). Neurofibromas are heterogeneous tumors composed of Schwann cells, neurons, fibroblasts and other cells, with Schwann cells being the major (60–80%) cell type (5, 6). Neurofibroma-derived Schwann cells have been demonstrated to possess abnormal properties, including increased invasiveness and the induction of angiogenesis (7). NF1 patients are also at increased risk for the development of certain malignancies, including pheochromocytomas, childhood myeloid leukemias, and in about 5% of patients, malignant peripheral nerve sheath tumors (MPNST) (8–10). Although still a point of some debate, it is widely held that MPNST arise from large (plexiform) neurofibromas and are probably derived from Schwann cells, because many MPNST stain positive for Schwann cell markers such as S100 (4, 11).

The *NF1* gene lies on chromosome 17 (12–14), and the great majority of patient mutations prevent expression of the intact *NF1* product, designated neurofibromin (15). Neurofibromin contains a central domain homologous to a family of proteins known as Ras-GTPase–activating proteins (Ras-GAPs), which function as negative regulators for Ras proteins (16). Ras-GAPs attenuate signaling from Ras, thus blocking the transmission of signals leading to increased growth or differentiation. The role of neurofibromin as a tumor suppressor that inactivates Ras-dependent signals has been confirmed. Primary neurofibromas and cell lines derived from NF1 MPNST show high levels of Ras-GTP, and in MPNST cell lines lacking neurofibromin, elevated Ras-GTP leads to constitutive growth activation (17–19).

Targeted disruption of *NF1* in mice has provided an experimental system for analyzing the role of neurofibromin in growth regulation (20, 21). The importance of Schwann cells to tumor development in NF1 is sug-

gested by the altered properties of Schwann cells from heterozygous (+/-) or homozygous mutant (-/-) embryos (22). Mutant Schwann cells have elevated Ras-GTP, are more invasive than wild-type cells, and when cultured in low serum yield transformed derivatives (TXF) that display altered morphology, reduced growth factor dependence, and reduced adherence (23). These transformed derivatives, which fail to develop in cultures of wild-type (+/+) littermates, retain expression of the Schwann cell markers P75 and S100 (23).

Schwann cell growth in vivo is normally regulated through interactions with neurons (4). The family of small peptides known as heregulins/neuregulins, including glial growth factor (GGF), probably serve as in vivo Schwann cell mitogens. Neuregulins, which robustly stimulate Schwann cell growth in vitro (24), bear homology to EGF and activate transmembrane tyrosine kinase receptors (erbB2, -3, and -4) that are structurally and functionally related to the EGF-R (reviewed in ref. 25). Schwann cells, which express little if any erbB4, use erbB2-3 heterodimers for GGF signaling (26). Stimulation of Schwann cells with GGF in vitro leads to increases in Ras-GTP, demonstrating a link between Ras regulation and Schwann cell proliferation (27).

Both *NF1* alleles are disrupted in MPNST and in at least a proportion of benign neurofibromas (28–30). Whereas mutation or loss of the *p53* gene occurs in about one third of MPNST (31), it is likely that additional alterations are present in these tumors. Here we report evidence indicating that aberrant expression of the EGF-R is associated with tumor development in NF1 and in animal models of NF1, suggesting a role in pathogenesis and representing a novel potential therapeutic target.

Methods

Cell culture and biochemical assays. MPNST lines were grown as described (17), and the embryo-derived mouse Schwann cells and TXF derivatives were isolated and grown as described (22, 23). Agar colony formation assays were carried out as described (17). For MAP kinase assays, cells were grown until confluent, serum-starved for 24 hours, stimulated with mitogen for 5 minutes at 37°C, then lysed, and MAP kinase assays were carried out as described (23). For Western blotting, cells were grown until confluent and lysed. Lysates with 50 µg protein (human) or 100 µg protein (mouse) were subjected to SDS-PAGE using 6% gels. Immunoblotting was carried out as described (17) using the following antibodies from Santa Cruz Biotechnology (Santa Cruz, California, USA): for EGF-R, sc03; for erbB2, sc284; for erbB3, sc285; for erbB4, sc283. Antibodies were used at a dilution of 1:2,000 for human and 1:1,000 for mouse lysates. Blots were developed with an enhanced chemiluminescence detection kit (Kirkegaard & Perry Laboratories, Gaithersburg, Maryland, USA).

Northern blotting. Cells were grown until confluent and lysed, and total RNA was extracted using the RNeasy system (QIAGEN Inc., Valencia, California, USA). Twenty micrograms of total RNA from each line was electrophoresed in an agarose gel and transferred to a nylon filter (Millipore Corp., Bedford, Massachusetts, USA). Human EGF-R probe was derived from the plasmid pCO12 (32) by digestion with *SstII* and *XhoI*. The probe was labeled with ^{32}P in a nick translation system (Promega Corp., Madison, Wisconsin, USA), and hybridization was carried out using Quickhyb buffer (Stratagene, La Jolla, California, USA) with 1.4×10^7 cpm of probe.

Immunohistochemistry. All immunohistochemistry was performed on 4–6-micron paraffin sections using the Ventana ES immunostaining system (Ventana Instruments, Tuscon, Arizona, USA). Following deparaffinization in xylenes and trypsinization (for EGF-R detection), slides were placed in the instrument that adds the primary antibody, the biotinylated anti-mouse or rabbit second antibody, and avidin-conjugated peroxidase or alkaline phosphatase as dictated by a bar code. Primary antibodies were incubated for 32 minutes at 37°C. The instrument performed all washes. Primary antibodies were rabbit polyclonal anti-bovine S100 (Dakopatts Inc., Carpinteria, California, USA) diluted to 1:1000; mouse monoclonal anti-EGF-R 31G7 (1:8; Zymed Inc., South San Francisco, California, USA); or PG-M1, a mouse monoclonal anti-macrophage marker (Dakopatts) diluted to 1:100. Slides were counterstained with hematoxylin or with nuclear fast red by hand. In all cases irrelevant mouse or rabbit immunoglobulin was used instead of a primary antibody as a negative control.

Dissociated cell preparations. Normal human nerves (n = 2) and neurofibroma (n = 3) specimens were digested overnight in enzymes as described (6). Cells (10^6) were washed twice in L15 medium (GIBCO/BRL, Grand Island, New York, USA) then fixed in non-buffered formalin, pelleted, and centrifuged into a cassette (Cytoblock; Shandon Inc., Pittsburgh, Pennsylvania, USA) for embedding.

Patient information. Adult normal nerves were used as controls. When NF1 diagnosis (NF1 dx) was made, it was based on family history, café-au-lait macules, and neurofibromas as described (33). Cutaneous neurofibromas were obtained from: 69-year-old man (non-NF1); 50-year-old woman (non-NF1); adult (non-NF1); 30-year-old woman (NF1). Plexiform neurofibromas were obtained from: 17-year-old man (NF1 dx); 6-year-old boy (NF1 dx); 15-year-old girl (NF1 dx); 14-year-old girl (NF1 dx); and a patient (mid-20s) with segmental NF1. Neurofibromas used for cell dissociation were obtained from: adult woman, cutaneous neurofibroma (NF1 dx); 3-year-old child, cervical neurofibroma (NF1 dx). For MPNST used see Table 1.

Results

NF1 patient tumor lines respond to EGF and express EGF-R. Stimulation of primary Schwann cells with GGF (10 ng/mL) led to a dramatic (approximately 80-fold) activation of mitogen-activated protein kinase (MAP kinase) (Figure 1a), consistent with the role of GGF as

a major Schwann cell mitogen, whereas EGF (50 ng/mL) had no effect. Compared with primary Schwann cells, the basal level of MAP kinase in serum-starved cells was substantially elevated (5–12-fold) in NF1 patient MPNST-derived cell lines (Figure 1a). Surprisingly, treatment of these lines with GGF failed to elicit activation of MAP kinase in two of three lines tested (lines 90-8 and 88-14), whereas only the 88-3 line responded to GGF (three- to fourfold). In contrast to primary Schwann cells, treatment of all three MPNST lines with EGF led to MAP kinase activation (six- to ninefold) (Figure 1a). These results suggested that the NF1 patient lines express the EGF receptor, but only the 88-3 line expresses the GGF receptor. To analyze directly the expression of receptors for EGF and GGF in these cells, we prepared lysates from growing cells and probed them by immunoblotting with antibodies specific for EGF-R and for erbB2, -3, and -4 (Figure 1b). The 88-3, 90-8, and 88-14 lines all expressed a strong band at approximately 170 kDa corresponding to EGF-R and also expressed abundant levels of erbB2, whereas only the 88-3 line expressed

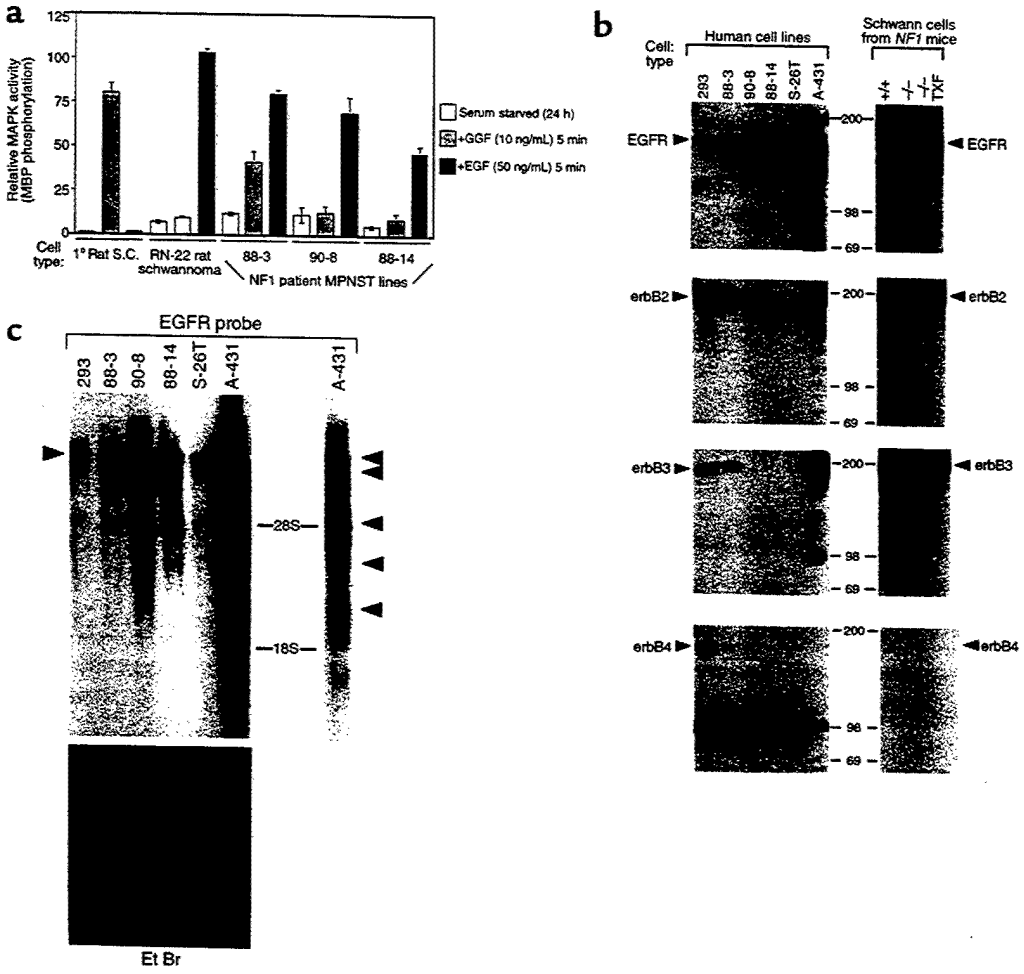

Figure 1

Response of primary rat Schwann cells, RN-22 rat schwannoma line, and human NF1 patient MPNST lines to GGF and EGF, and expression of EGF-R and erbB2, -3, and -4 proteins and *EGFR* mRNA. (**a**) The indicated cells were grown until nearly confluent, serum starved for 24 hours, then left untreated (–) or stimulated with 10 ng/mL recombinant human GGF (G) or 50 ng/mL recombinant human EGF (E) for 5 minutes at 37°C. The cells were lysed and the endogenous MAP kinase activity was assayed. Following the reaction, incorporation of $^{32}P_i$ into exogenous myelin basic protein was determined. Values were normalized to unstimulated primary rat Schwann cells (1.0) and represent the results of two experiments, carried out in duplicate, with error bars shown. (**b**) Expression of EGF-R and erbB2, -3, and -4 proteins in human and mouse cells. Cells were grown until confluent and lysed, and lysates containing 50 μg human or 100 μg mouse cell protein were subjected to analysis by SDS-PAGE and immunoblotting using antibodies specific for each protein indicated (arrows). 293, human embryonic kidney cells; 88-3, 90-8, 88-14, human NF1 MPNST lines; S-26T, human non-NF1 MPNST line; A-431, human epidermoid carcinoma line. Migration of molecular standards (kDa) is indicated at center. A strong nonspecific band of approximately 90 kDa appeared in the erbB4 blot of human but not mouse lysates. (**c**) Expression of *EGFR* mRNA in human MPNST and control cell lines. Cells were grown until confluent and lysed, and 20 μg of total RNA from each line was subjected to electrophoresis, transferred to a filter, and hybridized to a human *EGFR* probe labeled with ^{32}P. The predominant 10.5-kb mRNA is indicated with an arrow at left, as is the approximate location of the 28S and 18S RNAs (top). At right is a shorter exposure of the A-431 line, with arrows designating the different mRNAs detected. The filter was photographed under ultraviolet light before hybridization (bottom).

erbB3. None of the NF1 patient lines expressed significant levels of erbB4. The S-26T line is a S100$^+$ line from a non-NF1 patient (34) that displayed EGF-responsive MAP kinase activation, but this line failed to respond to GGF (G. Benvenuto and J.E. DeClue, unpublished data). This line expressed EGF-R but not erbB2, -3, or -4 (Figure 1b). Control lines included human embryonic kidney cells (line 293), which expressed all four proteins, and A-431 carcinoma cells, which contain amplified and rearranged copies of the *EGFR* gene (35) and expressed very high levels of EGF-R and smaller, related peptides, as well as erbB2 and -3. EGF treatment of all four MPNST lines yielded a 170-kDa tyrosine-phosphorylated band corresponding to the EGF-R, whereas GGF treatment led to the appearance of a 180–190 kDa tyrosine-phosphorylated erbB3 band in lysates from primary Schwann cells and the 88-3 cell line, but not in lysates from the 88-14, 90-8, or S26-T lines (data not shown). We conclude that human NF1 MPNST lines express EGF-R and respond to EGF, whereas only one of the lines expresses erbB3 and responds to GGF. To confirm the expression of EGF-R in these lines at the level of messenger RNA, we carried out Northern analysis using a human *EGFR*-specific probe (Figure 1c). A specific mRNA corresponding to the 10.5-kb, full-length *EGFR* mRNA (36) was detected in each of the MPNST lines (left arrow), as well as in 293, and the intensity of the band provided a striking parallel to the immunoblotting data for EGF-R in Figure 1b. A-431 cells expressed a variety of forms as described previously, including the 10.5-kb band (right panel; top arrow) and a 2.9-kb mRNA resulting from a rearranged copy of the gene (bottom arrow) (35). Based on these results, it is clear that the MPNST lines contain both EGF-R mRNA and protein and display a strong correlation between the levels of mRNA and protein expressed.

The ethylnitrosourea-induced rat schwannoma cell line RN-22, which expresses the Schwann cell marker S100 and normal levels of the neurofibromin, and likely contains a mutation in the *neu* gene encoding rat erbB2, was also analyzed in these experiments (25, 37). Similar to the human NF1 MPNST lines, the elevated basal level of MAP kinase activity in these cells was dramatically stimulated (15-fold) by EGF, whereas GGF had no effect (Figure 1a). Direct immunoblotting of RN-22 lysates with anti-phosphotyrosine antiserum revealed a 170-kDa, EGF-stimulated band, as well as a constitutive 185-kDa band (erbB2) (data not shown). Thus, an alternative route of Schwann cell tumorigenesis in a different species also led to expression of the EGF-R and loss of GGF responsiveness.

Primary benign and malignant NF1 patient tumors express EGF-R. The experiments described above suggest that one of the events leading to malignant tumorigenesis in NF1 is the acquisition of EGF-R expression. To test whether EGF receptors are expressed in primary tumors associated with NF1 disease, and not just in

Table 1
MPNST sections analyzed for EGF-R and S100 expression

Patient information	EGF-R expression	S100β expression
MPNST: 14-year-old girl; NF1 status unknown	Regions of high cellularity robustly EGF-R–positive: other areas EGF-R–negative	S100-negative
MPNST: 42-year-old woman; NF1 status unknown (Figure 2, a and b)	Uniform moderate EGF-R staining in at least 70% of tumor cells	Scattered robustly S100-postive cells (may be macrophages); other areas patch weak S100-positive; some areas S100-negative
MPNST: 31-year-old woman; NF1 status unknown	Multiple foci robustly EGF-R–positive cells	S100-negative
MPNST/Triton tumor: 13-year-old boy; NF1 dx	Robustly EGF-R–positive	S100-negative to uniform trace S100-positive in 1/3 of tumor
MPNST: adolescent Non-NF1	Weak EGF-R–positive staining in up to 10% of cells	Robust S100-positive staining most or all tumor cells
MPNST: 44-year-old man; NF1 dx	Uniform moderate EGF-R–positive staining throughout	S100-negative to uniform trace S100-positive in patches
MPNST: 30-year-old woman; NF1 dx (Figure2, c and d)	Very rare islands of weak EGF-R–positive staining: majority of tumor is negative	Strongly positive throughout

Immunohistochemistry was carried out as described in Methods. Two individuals read each slide (S. Heffelfinger and N. Ratner). In total, only one of seven tumors was almost entirely EGF-R–negative, and even that tumor may have some positive regions. For S100, three of seven are positive, two of seven are negative, and two of seven show trace or no expression. dx: NF1 diagnosis; non-NF1, failed to meet consensus criteria and no evidence of *NF1* mutation.

cultured cell lines, we immunostained sections from normal human nerves, benign neurofibromas, and MPNST with anti-EGF-R or anti-S100. Seven primary MPNST specimens were analyzed for expression of S100 and EGF-R. All seven tumors showed some EGF-R expression, but a range of expression patterns was evident (Table 1). Some tumors showed robust staining in nearly all cells, whereas others contained only rare, weakly positive cells. For example, sections from a tumor in which the majority of the cells showed strong EGF-R immunoreactivity is shown in Figure 2b. This tumor was negative for expression of S100 (Figure 2a). The other extreme example is shown in Figure 2, c and d. The majority of cells in this tumor were negative for EGF-R expression (Figure 2d), whereas many cells were positive for S100 expression (Figure 2c). In another case, focal areas within a single MPNST section had robust EGF-R immunoreactivity, whereas neighboring areas in the same section were negative (data not shown). We conclude that primary MPNST contain varying proportions of cells that express the EGF-R, with some tumors expressing high levels of EGF-R in most of their cells. These results reinforce the findings described above for the MPNST-derived cell lines.

In normal nerves, $S100^+$ cells are found only in the endoneurial compartment (Figure 2e), whereas $EGF\text{-}R^+$ cells (fibroblasts) make up the perineurium (Figure 2f). Sections from nine neurofibromas were analyzed, four from cutaneous neurofibromas, and five from the much larger plexiform neurofibromas. All showed both $S100^+$ cells (Schwann cells) and distinct $EGF\text{-}R^+$ cells (likely fibroblasts) (Figure 2g). In nine of nine neurofibroma specimens, occasional cells appeared to express both antigens. To verify this, we dissociated cells from three additional neurofibromas, isolated the cells, and embedded them in paraffin. Staining sections with anti-S100 and anti-EGF-R demonstrated a population of $S100^+/EGF\text{-}R^+$ cells (Figure 2h). We found that 1.8% of cells expressed both antigens (6/190, 1/110, and 3/216 double-labeled cells in three independent counts). In contrast, normal nerve samples completely lacked double-labeled cells and contained 99% $S100^+$ Schwann cells, and 1% $EGF\text{-}R^+$ cells (fibroblasts/perineurial cells) (Figure 2i). When sections were stained with an anti-macrophage marker (PG-M1) and anti-S100, no double-labeled cells were observed (not shown). We conclude that certain cells in neurofibromas, most likely Schwann cells, express both S100 and EGF-R, whereas such cells are absent in normal nerves.

In vitro transformation of mouse NF1-deficient Schwann cells leads to EGF-R expression. Mice with targeted mutations in the *NF1* gene represent a model system for investigating NF1 tumorigenesis (20, 21). Although homozygous mutant (-/-) embryos die by day 14.5, we have developed techniques to purify Schwann cells from day-12.5 embryos (22, 23). To investigate MAP kinase signaling, these Schwann cells were serum starved, stimulated with GGF, and lysed (Figure 3a). Although Schwann cells lacking one (+/-) or both (-/-) copies of *NF1* have elevated Ras-GTP, there was little or no enhancement of basal MAP kinase activity compared with wild-type cells (Figure 3a). Cells of all genotypes responded to GGF stimulation with large increases in MAP kinase activity. The TXF Schwann cells isolated from (-/-) embryos displayed an increased basal level of MAP kinase activity and responded to GGF.

We hypothesized that the in vitro transformation of *NF1*-deficient mouse Schwann cells might be associated with EGF-R expression. To test this, we examined MAP kinase activity following EGF stimulation of serum-starved (-/-) or TXF cells (Figure 3b). Whereas EGF elicit-

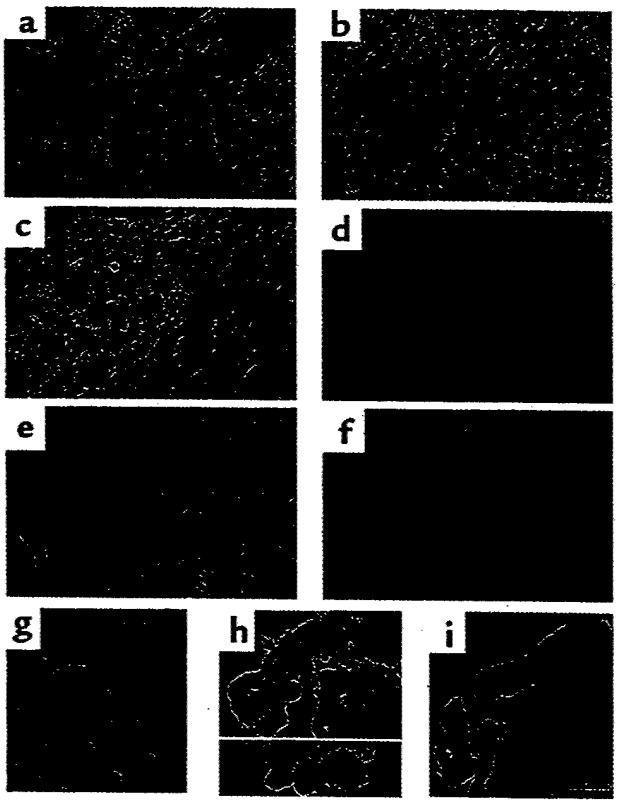

Figure 2
EGF-R expression in NF1 tumor sections. Paraffin sections were stained with anti-EGF-R (**b**, **d**, and **f**) or anti-S100 (**a**, **c**, and **e**) or with both antibodies (**g**, **h**, and **i**). Visualization of single antibodies was with 3'3-diaminobenzidine HCl (DAB; brown) (**a–f**). Double labeling used nitroblue tetrazolium (NBT/BCIP; blue) for anti-S100, and DAB (brown) for anti-EGF-R (**g–i**). In **a**, **b**, and **d–f**, the counterstain is hematoxylin (blue); in **c** and **g–i**, the counterstain is nuclear fast red (pink). (**a–d**) Sections from MPNST. In **a**, the arrow points to a normal nerve within the tumor, containing $S100^+$ cells, whereas the tumor matrix is $S100^-$. An adjacent section from the same tumor in **b** shows that most cells are $EGF\text{-}R^+$. Another MPNST contains $S100^+$ cells (**c**) and is mostly negative for EGF-R (**d**). (**e** and **f**) Sections of normal human nerve (arrow points to perineurium). (**g**) A section of a cutaneous neurofibroma with $EGF\text{-}R^+/S100^+$ cells. (**h**) A section from a dissociated neurofibroma cell preparation. The arrow designates a group of cells double stained by anti-S100 and anti-EGF-R. (**i**) A section from a dissociated normal nerve preparation. No double-labeled cells are detected. **a–g**, bar: 34.2 μm; **h** and **i**, bar: 16.3 μm.

ed no increase in MAP kinase activity in the (-/-) cells, TXF derivatives displayed a dramatic increase, even greater than the response to GGF. Schwann cells from wild-type (+/+) or heterozygous (+/-) embryos failed to respond to EGF (data not shown). To examine the expression of EGF-R and erbB2, -3, and -4, we carried out immunoblotting with antibodies against these proteins (Figure 1b). Lysates of (+/+) and (-/-) cells expressed erbB2 and -3, but not EGF-R. In contrast, the (-/-) TXF cells expressed abundant levels of EGF-R, as well as erbB2 and -3. None of the cells expressed erbB4, consistent with studies published previously (26). Immunoblotting of the lysates from Figure 3b confirmed the activation of EGF-R in the (-/-) TXF cells following EGF treatment, as well as tyrosine phosphorylation of erbB3 in GGF-stimulated lysates from TXF and (-/-) cells (data not shown). We conclude that acquisition of EGF-R expression is associated with in vitro transformation of *NF1*-deficient Schwann cells. These results represent a striking parallel to the results obtained from our analysis of human NF1-related tumors.

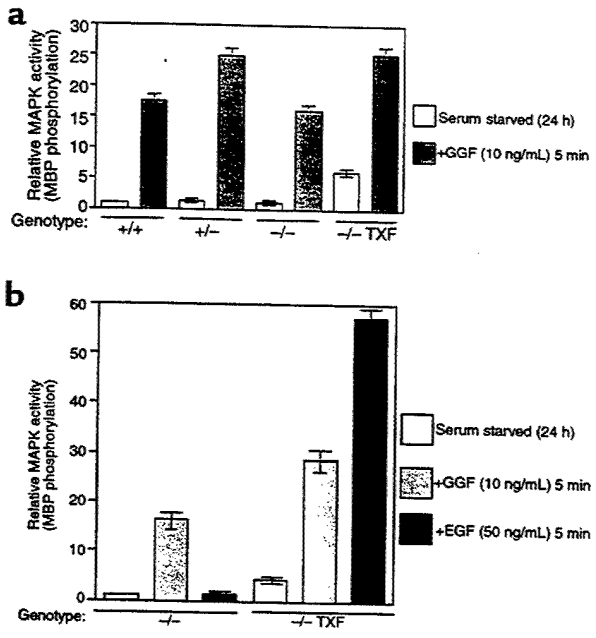

Figure 3

Transformed derivatives of *NF1* (-/-) mouse embryo–derived Schwann cells have elevated basal MAP kinase activity and respond to EGF. (**a**) Mouse Schwann cells were isolated from day 12.5 embryos with wild-type *NF1* (+/+) or targeted disruption of one *NF1* allele (+/-), or both alleles (-/-), and compared with transformed derivatives of (-/-) (TXF). The cells were serum starved for 24 hours, then left untreated or stimulated with GGF, as indicated. Cells were lysed and MAP kinase activity was determined as for Figure 1. Results are the mean of two experiments carried out in duplicate, with error bars shown. Results were normalized to the level of activity present in serum-starved wild-type (+/+) cells (1.0). (**b**) Schwann cells from (-/-) embryos and TXF were treated and assayed as above, except additional samples were prepared after stimulation with 50 ng/mL EGF for 5 minutes. Results are the mean of two experiments carried out in duplicate, with error bars shown. Results were normalized to the level of activity present in serum-starved homozygous null (-/-) cells (1.0).

Growth of NF1 patient tumor lines is EGF dependent and can be blocked by EGF-R antagonists. We wished to determine whether expression of the EGF-R in NF1 tumors and cell lines affected the growth of these cells. When the 88-14 cell line was grown in limiting amounts of FBS (0.1%), cells lacking EGF remained viable (as judged by trypan blue exclusion and replating under growth conditions) but did not grow, whereas cells treated with 10 ng/mL EGF grew at a rapid rate (Figure 4a). The EGF-dependent growth of the 88-14 line suggested that blocking the EGF-R might inhibit the growth of the cells. Therefore, we tested EGF-R antagonists for their ability to suppress growth of 88-14 cells under the same conditions (Figure 4a). Treatment with mAb 225, an antibody that blocks EGF-R activation (38), significantly inhibited cell growth, whereas even more dramatic inhibition was achieved with chemical inhibitors of EGF-R tyrosine kinase activity, the tyrphostins A-25 and AG-1478 (39). All of the EGF-R antagonists displayed significantly greater inhibition than that observed for the potent farnesyltransferase inhibitor B581 (40). Whereas previous studies demonstrated that farnesyltransferase inhibitors slow the growth of the 88-14 line in vitro, most likely by blocking Ras or RhoB activity (41), these results demonstrate that antagonizing the EGF-R also can block their growth.

As an additional test for these agents to antagonize EGF-dependent growth of the 88-14 tumor line, we carried out assays of anchorage-independent growth in soft agar (Figure 4b). When plated in moderate levels (7%) of serum, no significant growth was observed after 4 weeks. However, the presence of 100 ng/mL EGF supported the formation of small- to medium-sized colonies under these conditions (Figure 4b). Furthermore, the presence of mAb 225 or tyrphostin AG-1478 strongly inhibited the formation of such colonies (Figure 4b), whereas B581 had no significant effect (data not shown). We conclude that under limiting conditions, the growth of 88-14 is dependent on EGF and can be blocked by EGF-R antagonists. In other experiments, we found that the addition of EGF dramatically stimulated the growth of (-/-) TXF cells in vitro, and that tyrphostin A-25 could block this effect (data not shown). In contrast, EGF had no effect on nontransformed (-/-) Schwann cells or on Schwann cells from (+/-) or (+/+) embryos (data not shown). We conclude that EGF-R expression has a significant biological effect on the growth of both NF1 patient tumor-derived cells and TXF cells from *NF1*-deficient mice.

The experiments just described were carried out in conditions where exogenous EGF was essential for the growth of the cells. Whereas the availability of EGF-related peptides and other growth factors in the tumor environment is unknown, we nevertheless wished to determine the effect of EGF-R antagonists on the growth of NF1 patient lines under other growth conditions. Therefore, we examined the growth of the 88-14 and the 90-8 MPNST lines in the presence of 2% FBS with no EGF added (Figure 4, c and d). Whereas

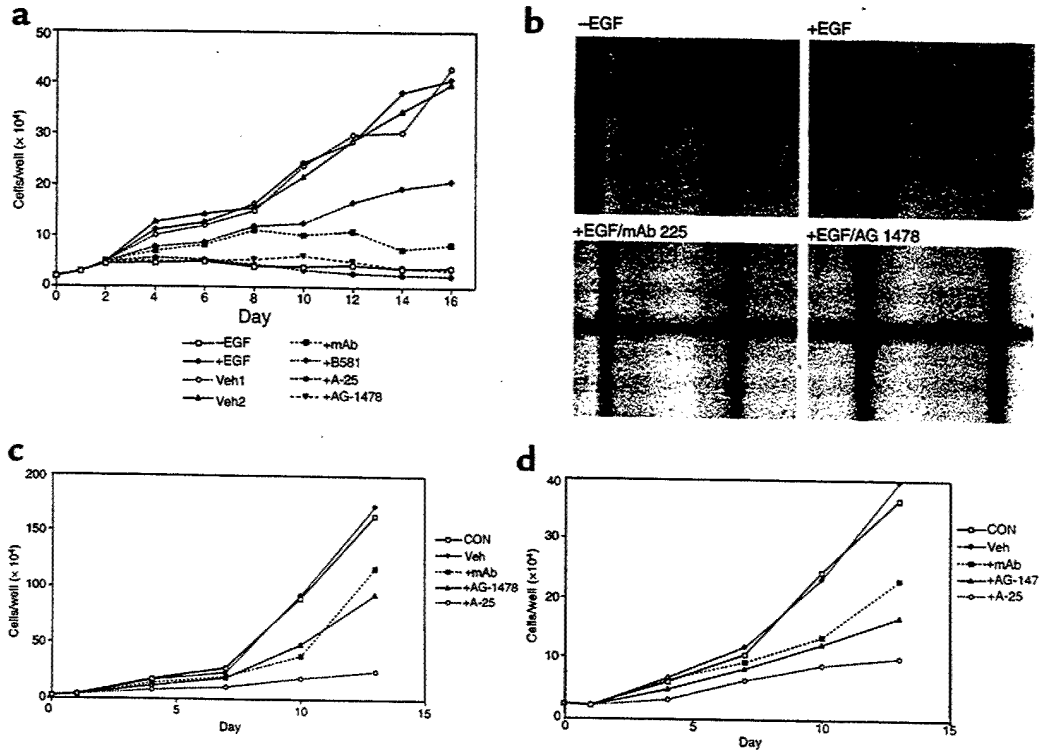

Figure 4

Growth of NF1 patient MPNST lines is EGF dependent and is inhibited by EGF-R antagonists. (**a**) MPNST line 88-14 was plated at 2×10^4 per 35-mm well. The next day (day 1) cells were switched to medium without (–EGF) or with 10 ng/mL EGF (+EGF), and on day 2 cells were switched to medium containing 10 ng/mL EGF and 3% PBS (Veh1); 0.1% DMSO (Veh2); 3 μg/mL mAb 225 in PBS (3% vol/vol; mAb); 40 μM farnesyltransferase inhibitor B581 in water; 10 μM tyrphostin A-25 in DMSO; or 400 nM tyrphostin AG-1478, also in DMSO. Cells were re-fed with medium containing fresh inhibitor and counted in duplicate every 2 days, beginning at day 2. (**b**) Growth of MPNST 88-14 line in soft agar. Cells were plated at 10^5/mL in a 0.4% (wt/vol) agar suspension with 7% FBS with or without 100 ng/mL EGF, as indicated; mAb 225 was included at 5 μg/mL and AG-1478 at 400 nM. Cells were photographed after 4 weeks. × 25. (**c** and **d**) Growth of 88-14 (**c**) and 90-8 (**d**) in 2% serum is inhibited by EGF-R antagonists. Cells were plated as in **a**, and switched on day 1 to medium containing 2% FBS (CON) or 2% serum plus 0.1% DMSO (Veh); 3 μg/mL mAb 225 (mAb); 10 μM tyrphostin A-25; or 400 nM tyrphostin AG-1478. Thereafter, cells were re-fed with medium containing fresh inhibitor every 2 days, and duplicate wells of cells were counted every three days.

the 88-14 line grew much more robustly than 90-8 under these conditions (Figure 4, c and d), the growth of both lines was significantly inhibited by the addition of tyrphostin A-25 and to a lesser extent by tyrphostin AG-1478. The anti-EGF-R mAb also inhibited the growth of these lines in serum, although the effect was somewhat less pronounced (Figure 4, c and d). These results demonstrate that EGF-R expression affects the growth of tumor cell lines derived from NF1 patients under conditions where EGF is not the primary factor driving growth of the cells.

Discussion

Here we have described aberrant expression of the EGF-R in primary tumors from patients with NF1, in cell lines derived from those tumors, in a cell line from a non-NF1 patient with MPNST, in a chemically induced rat schwannoma line, and in in vitro–transformed Schwann cells from mouse embryos lacking an intact *NF1* gene. The congruence of the animal model systems with the results from NF1 patient materials suggests that aberrant expression of the EGF-R might play an important role in the development of peripheral nerve tumors in NF1 patients and that mutation of *NF1* may predispose the tumor progenitor cells to express EGF-R. In the cells tested, we found a perfect correlation between expression of EGF-R and EGF responsiveness and also between expression of erbB2/erbB3 and GGF responsiveness. Additionally, the level of *EGF-R* mRNA in the human MPNST lines correlated well with the level of protein expression. There is a strong precedent for involvement by the EGF-R and other members of the erbB family in human cancer, because over 60% of all solid tumors overexpress at least one of these proteins or their ligands (reviewed in refs. 42 and 43). Furthermore, a negative correlation has been demonstrated between EGF-R expression and survival in certain cancers and with progression to malignancy in others (43). We have found that the growth of cell lines derived from MPNSTs and transformed mouse Schwann cells in vitro was highly EGF dependent and could be blocked by EGF-R antagonists under conditions where EGF was the primary growth factor. This demonstrates that the expressed EGF-R is capable of transmitting

mitogenic signals in these cells. We also found that EGF-R antagonists could block the growth of MPNST lines growing in serum without added EGF. This inhibition may be due to the blocking of potential autocrine growth stimulation pathways in the cells; alternatively, it may indicate that the EGF-R is involved (directly or indirectly) in mitogenic signaling by serum factors that induce growth of the cells.

Other than mutation or loss of the second (normal) *NF1* allele (10), little is known of the specific genetic and epigenetic events involved in the development of NF1-related neurofibromas and MPNSTs. Earlier work suggested a possible involvement of *p53* in NF1-related MPNST formation (31), and it was recently shown that *p53* and *NF1* cooperate in tumor formation in mice (44, 45). Furthermore, the hypothesis of a Schwann cell origin for both benign neurofibromas and MPNSTs remains to be proven. However, our data support other studies suggesting that deregulation of Schwann cell growth is a primary defect driving the development of both benign neurofibromas and MPNST in NF1 patients (4). The immunohistochemical analyses revealed that at some point during or after the formation of neurofibromas, a subset of the ($S100^+$) Schwann cells acquire EGF-R expression. Such cells were not observed in normal control nerves, although a previous analysis of tissue sections of benign schwannomas from non-NF1 patients revealed some EGF-R expression (46). Our analysis of Schwann cells isolated from *NF1*-mutant mouse embryos demonstrated that one of the events occurring concomitant with transformation of (-/-) cells is expression of the EGF-R. The TXF cells, which do not arise from wild-type (+/+) embryos, remained $S100^+$, GGF responsive and expressed other Schwann cell markers (23). Thus both the human and mouse systems indicate that mutational loss of *NF1* may lead to the development of altered Schwann cells with EGF-R expression. It is difficult at present to assess the role of the $EGF\text{-}R^+/S100^+$ cells in the development and progression of benign neurofibromas. Although these cells make up only a small portion of the total population, they may be altered in their interactions with other cells in the tumor environment or may release factors that help drive the growth of benign tumors, which typically undergo periodic bursts of growth. Alternatively, the $EGF\text{-}R^+$ cells may only arise after the benign tumor is formed. Similarly, it is unknown what potential ligands for the EGF-R may be present in benign neurofibromas, although they do contain a rich diversity of cell types, one or more of which may produce an EGF-R ligand. Whereas the vast majority of neurofibromas do not progress to malignancy, they represent the primary burden for many patients, and the role of the $EGF\text{-}R^+/S100^+$ cells in these tumors demands further investigation.

These studies also raise questions about the role of EGF-R in tumor progression, specifically whether EGF-R expression is a necessary step in MPNST formation. All three NF1 patient's MPNST lines expressed EGF-R, and seven of seven primary NF1 MPNST analyzed by immunohistochemistry contained $EGF\text{-}R^+$ cells. However, the relative levels of EGF-R expression in individual cells varied, as did the proportion of cells expressing EGF-R in each tumor. The existence of microdomains defined by EGF-R expression suggests heterogeneity within individual MPNSTs. It is possible that EGF-R expression is transient and occurs at particular stages in tumorigenesis or that expression of the EGF-R represents only one of several routes to formation of MPNST. The significance of EGF-R expression in Schwann cell tumorigenesis is strengthened by our finding that both the $S100^+$, Schwann cell–derived rat RN-22 line and the $S100^+$, non-NF1 human MPNST line S-26T express EGF-R. The finding of EGF-R expression in such a diversity of settings strongly implicates a role for it in the pathogenesis of malignant nerve sheath tumors.

One important distinction between the mouse and human systems was that the three NF1 MPNST lines were $S100^-$, and two of three lacked erbB3 expression and GGF-responsiveness. If these results are interpreted in terms of the Schwann cell origin model, they suggest that subsequent to acquisition of EGF-R expression, the cells begin to dedifferentiate and lose markers such as erbB3 and S100. Such a model may also help explain the general (though not complete) discordance between S100 and EGF-R expression among cells in primary MPNST samples and the fact that 5 of the 7 samples lacked S100 expression. Interestingly, both RN-22 and S-26T were unresponsive to GGF, suggesting that loss of erbB3 may contribute to the dedifferentiation of cells during tumorigenesis even without loss of S100. Our finding that *NF1*-deficient mouse Schwann cells, human $S100^+$ Schwann cells from neurofibromas, and RN-22 cells all express EGF-R leads us to favor the hypothesis that loss of Schwann cell markers is a feature of MPNST formation that can occur subsequent to expression of EGF-R. An alternative model would suggest that the cells giving rise to the $S100^+/EGF\text{-}R^+$ cells in benign neurofibromas and/or to the cells in MPNST, represent a different lineage arising from the neural crest. Such an argument could also be applied to the mouse TXF (-/-) cells. In each case, the loss of *NF1* would lead to a sub-population of cells that acquire EGF-R and various combinations of Schwann cell markers that might change during the evolution of the tumor. This alternative model is being evaluated in our current studies employing microchip gene arrays to compare and contrast the overall pattern of genes expressed in (+/+), (-/-), and TXF (-/-) cells. Another area of future investigation will be to determine the degree to which the EGF-R exerts its mitogenic effects through the Ras pathway. It is interesting that the expression of EGF-R occurs in the context of cells that already have high levels of Ras-GTP because of loss of *NF1*, and this may suggest that the signaling from the EGF-R also involves non-Ras pathways, thereby augmenting the high Ras activity present in the cells.

Acknowledgments

We thank Doug Lowy, Isabel Martinez-Lacaci, and David Salomon for comments and suggestions; Ricardo Dreyfuss for excellent assistance with photography; and Mary Ann Miller for expert assistance with immunohistochemistry. We are grateful to Bruce Korf and Gretchen M. Schneider (Boston Children's Hospital, Boston, Massachusetts, USA) and the University of Miami Human Tissue Bank (Miami, Florida, USA) for providing neurofibromas. We thank Patrick Wood (The Miami Project, Miami, Florida, USA) for normal human nerves, and Diya Mutasim (University of Cincinnati, Department of Dermatology, Cincinnati, Ohio, USA) and Kevin Bove (Cincinnati Children's Hospital, Department of Pathology, Cincinnati, Ohio, USA) for neurofibroma sections. The University of Alabama (Birmingham, Alabama, USA) and the Childhood Cancer Tissue Network (Columbus, Ohio, USA) provided MPNST. N. Ratner is supported by National Institutes of Health grant NS-28840.

1. Huson, S.M., Harper, P.S., and Compston, D. 1988. Von Recklinghausen neurofibromatosis: a clinical and population study in south-east Wales. *Brain.* **111**:1355–1381.
2. Upadhyaya, M., and Cooper, D.N. 1998. *Neurofibromatosis type 1: from genotype to phenotype.* BIOS Scientific Publishers Ltd. Oxford, United Kingdom. pp. 230.
3. Ferner, R.E. 1998. Clinical aspects of neurofibromatosis 1. In *Neurofibromatosis type 1: from genotype to phenotype.* M. Upadhyaya and D.N. Cooper, editors. BIOS Scientific Publishers Ltd., Oxford, United Kingdom. 21–38.
4. Rosenbaum, T., Petrie, K.M., and Ratner, N. 1997. Neurofibromatosis type 1: genetic and cellular mechanisms of peripheral nerve tumor formation. *The Neuroscientist.* **3**:412–420.
5. Stefansson, K., Wollmann, R., and Jerkovic, M. 1982. S-100 protein in soft tissue tumours derived from Schwann cells and melanocytes. *Am. J. Pathol.* **106**:261–268.
6. Peltonen, J., et al. 1988. Cellular differentiation and expression of matrix genes in type 1 neurofibromatosis. *Lab. Invest.* **59**:760–761.
7. Sheela, S., Riccardi, V.M., and Ratner, N. 1990. Angiogenic and invasive properties of neurofibroma Schwann cells. *J. Cell Biol.* **111**:645–653.
8. Ducatman, B.S., Scheithauer, B.W., Piepgras, D.G., and Reiman, H.M. 1984. Malignant peripheral nerve sheath tumors in childhood. *J. Neurooncol.* **2**:241–248.
9. Zoller, M.E., Rembeck, B., Oden, A., Samuelsson, M., and Angervall, L. 1997. Malignant and benign tumors in patients with neurofibromatosis type 1 in a defined Swedish population. *Cancer.* **79**:2125–2131.
10. Side, L.E., and Shannon, K.M. 1998. The *NF1* gene as a tumor suppressor. In *Neurofibromatosis type 1: from genotype to phenotype.* M. Upadhyaya and D.N. Cooper, editors. BIOS Scientific Publishers Ltd. Oxford, United Kingdom. 133–152.
11. Morioka, N., Tsuchida, T., Etoh, T., Ishibashi, Y., and Otsuka, F. 1990. A case of neurofibrosarcoma associated with neurofibromatosis: light microscopic, ultrastructural, immunohistochemical and biochemical investigations. *J. Dermatol.* **17**:312–316.
12. Wallace, M.R., et al. 1990. Type 1 neurofibromatosis gene: identification of a large transcript disrupted in three NF1 patients. *Science.* **249**:181–186.
13. Cawthon, R., et al. 1990. A major segment of the neurofibromatosis type 1 gene; cDNA sequence, genomic structure, and point mutations. *Cell.* **62**:193–201.
14. Viskochil, D., et al. 1990. Deletions and a translocation interrupt a cloned gene at the neurofibromatosis type 1 locus. *Cell.* **62**:187–192.
15. Upadhyaya, M., and Cooper, D.N. 1998. The mutational spectrum in neurofibromatosis 1 and its underlying mechanisms. In *Neurofibromatosis type 1: from genotype to phenotype.* M. Upadhyaya and D.N. Cooper, editors. BIOS Scientific Publishers Ltd. Oxford, United Kingdom. 65–88.
16. Boguski, M.S., and McCormick, F. 1993. Proteins regulating Ras and its relatives. *Nature.* **366**:643–654.
17. DeClue, J.E., et al. 1992. Abnormal regulation of mammalian $p21^{ras}$ contributes to malignant tumor growth in von Recklinghausen (type-1) neurofibromatosis. *Cell.* **69**:265–273.
18. Basu, T.N., et al. 1992. Aberrant regulation of ras proteins in malignant tumour cells from type-1 neurofibromatosis patients. *Nature.* **356**:713–715.
19. Guha, A., et al. 1996. Ras-GTP levels are elevated in human NF1 peripheral nerve tumors. *Oncogene.* **12**:507–513.
20. Jacks, T., et al. 1994. Tumor predisposition in mice heterozygous for a targeted mutation in *NF1*. *Nat. Genet.* **7**:353–361.
21. Brannan, C.I., et al. 1994. Targeted disruption of the neurofibromatosis type-1 gene leads to developmental abnormalities in heart and various neural crest-derived tissues. *Genes Dev.* **8**:1019–1029.
22. Kim, H., et al. 1995. Schwann cells from neurofibromin deficient mice exhibit activation of $p21^{ras}$, inhibition of cell proliferation and morphological changes. *Oncogene.* **11**:325–335.
23. Kim, H.A., Ling, B., and Ratner, N. 1997. *NF1*-deficient mouse Schwann cells are angiogenic and invasive and can be induced to hyperproliferate: reversion of some phenotypes by an inhibitor of farnesyl transferase. *Mol. Cell. Biol.* **17**:862–872.
24. Levi, A.D., et al. 1995. The influence of heregulins on human Schwann cell proliferation. *J. Neurosci.* **15**:1329–1340.
25. Pinkas-Kramarski, R., Alroy, I., and Yarden, Y. 1997. ErbB receptors and EGF-like ligands: cell lineage determination and oncogenesis through combinatorial signaling. *J. Mammary Gland Biol. Neoplasia.* **2**:97–107.
26. Burden, S., and Yarden, Y. 1997. Neuregulins and their receptors: a versatile signaling molecule in organogenesis and oncogenesis. *Neuron.* **18**:847–855.
27. Kim, H., DeClue, J.E., and Ratner, N. 1997. cAMP-dependent protein kinase A is required for Schwann cell growth: interaction between cAMP and neuregulin/tyrosine kinase pathways. *J. Neurosci. Res.* **49**:236–247.
28. Colman, S.D., Williams, C.A., and Wallace, M.R. 1995. Benign neurofibromas in type 1 neurofibromatosis (NF1) show somatic deletions of the *NF1* gene. *Nat. Genet.* **11**:90–92.
29. Sawada, S., et al. 1996. Identification of *NF1* mutations in both alleles of a dermal neurofibroma. *Nat. Genet.* **14**:110–112.
30. Serra, P., et al. 1997. Confirmation of a double-hit model for the *NF1* gene in benign neurofibromas. *Am. J. Hum. Genet.* **61**:512–519.
31. Menon, A.G., et al. 1990. Chromosome 17p deletions and *p53* gene mutations associated with the formation of malignant neurofibrosarcomas in von Recklinghausen neurofibromatosis. *Proc. Natl. Acad. Sci. USA.* **87**:5435–5439.
32. Velu, T.J., et al. 1989. Retroviruses expressing different levels of the normal epidermal growth factor receptor: biological properties and new bioassay. J. Cell. Biochem. **39**:153–166.
33. Gutmann, D.H., et al. 1997. The diagnostic evaluation and multidisciplinary management of neurofibromatosis 1 and neurofibromatosis 2. *JAMA.* **278**:51–57.
34. Dahlberg, W.K., Little, J.B., Fletcher, J.A., Suit, H.D., and Okunieff, P. 1993. Radiosensitivity *in vitro* of human soft tissue sarcoma cell lines and skin fibroblasts derived from the same patients. *Int. J. Radiat. Biol.* **63**:191–198.
35. Merlino, G.T., et al. 1985. Structure and localization of genes encoding aberrant and normal epidermal growth factor receptor RNAs from A431 human carcinoma cells. *Mol. Cell. Biol.* **5**:1722–1734.
36. Merlino, G.T., et al. 1984. Amplification and enhanced expression of the epidermal growth factor receptor gene in A431 human carcinoma cells. *Science.* **224**:417–419.
37. Pfeiffer, S.E., and Wechsler, W. 1972. Biochemically differentiated neoplastic clone of Schwann cells. *Proc. Natl. Acad. Sci. USA.* **69**:2885–2889.
38. Peng, D., et al. 1996. Anti-epidermal growth factor receptor monoclonal antibody 225 up-regulates $p27^{KIP1}$ and induces G_1 arrest in prostatic cancer cell line DU145[1]. *Cancer Res.* **56**:3666–3669.
39. Levitzki, A., and Gazit, A. 1995. Tyrosine kinase inhibition: an approach to drug development. *Science.* **267**:1782–1788.
40. Garcia, A.M., Rowell, C., Ackermann, K., Kowalczyk, J.J., and Lewis, M.D. 1993. Peptidomimetic inhibitors of Ras farnesylation and function in whole cells. *J. Biol. Chem.* **268**:18415–18418.
41. Yan, N., et al. 1995. Farnesyltransferase inhibitors block the neurofibromatosis type I (NF1) malignant phenotype. *Cancer Res.* **55**:3569–3575.
42. Salomon, D.S., Brandt, R., Ciardiello, F., and Normanno, N. 1995. Epidermal growth factor-related peptides and their receptors in human malignancies. *Crit. Rev. Oncol. Hematol.* **19**:183–232.
43. Bridges, A.J. 1996. The epidermal growth factor receptor family of tyrosine kinases and cancer: can an atypical exemplar be a sound therapeutic target? *Curr. Med. Chem.* **3**:167–194.
44. Cichowski, K., et al. 1999. Mouse models of tumor development in neurofibromatosis type 1. *Science.* **286**:2172–2176.
45. Vogel, K.S., et al. 1999. Mouse model for neurofibromatosis type 1. *Science.* **286**:2176–2179.
46. Sturgis, E.M., Woll, S.S., Aydin, F., Marroji, A.J., and Amedee, R.G. 1996. Epidermal growth factor receptor expression by acoustic neuromas. *Laryngoscope.* **106**:457–462.

Title: EXPRESSION OF EPIDERMAL GROWTH FACTOR RECEPTOR AND VASCULAR ENDOTHELIAL GROWTH FACTOR RECEPTOR IN PLEXIFORM NEUROFIBROMA AND MALIGNANT PERIPHERAL NERVE SHEATH TUMORS

H Zhou [1], D H Viskochil [2], S L Perkins [1], S R Tripp [1] and C M Coffin [1]. [1]Pathology, and [2]Pediatrics, University of Utah, Salt Lake City, UT, .

Background: Malignant peripheral nerve sheath tumor (MPNST) may arise in association with neurofibromatosis type I (NF1) or sporadically, and some evidence suggests a role for epidermal growth factor receptor (EGFR) in pathogenesis. EGFR is a transmembrane glycoprotein with intrinsic tyrosine kinase activity. In cancer cells, activation of the EGFR signaling pathway has been linked with increased cell proliferation, aberrant cell differeniation, and angiogenesis through modulation of vascular endothelial growth factor (VEGF) expression. VEGF and its receptor (VEGFR) are implicated in tumor neovascularization, growth and metastasis. This study investigates immunohistochemical expression of EGFR and VEGFR among plexiform neurofibroma (PNF), and NF1-related and non-NF1 malignant peripheral nerve sheath tumor (MPNST).

Design: Formalin-fixed, paraffin-embedded archival tissue from 4 PNFs, and 13 MPNSTs (7 with NF1) were immunostained with monoclonal antibodies to EGFR (Zymed), and VEGFR (Dako) using an automated staining system (Ventana). Positivity was scored semi-quantitatively as 0 to 3. (0=<5%, 1+ =5-25%, 2 + =25-50%, 3 + = >50% positive cells).

Results: All MPNSTs had intense cytoplasmic EGFR staining ranging from 2-3+. Cytoplasmic VEGFR staining ranging from 1-2+ was also observed in both vascular endothelial and tumor cells in these MPNSTs. In PNFs, a subset of S100-positive tumor cells also demonstrated distinct membranous/cytoplasmic EGFR staining. Compared to EGFR-negative tumor cells in the same lesion, the EGFR-positive cells were typically dissociated Schwann cells with vacuolated cytoplasm. In PNF, occasional cytoplasmic VEGFR expression was present in the vascular endothelial cells but absent in the tumor cells.

Conclusion: EGFR is expressed in a high percentage of neoplastic cells in NF1-related and non-NF1 MPNST and in a subset of Schwann cells within PNF. These data indicate that EGFR may play a role in tumor progression of Schwann cell-derived tumors and may be associated with VEGF/VEGFR expression in MPNST. Further studies are needed to determine whether the EGFR-positive Schwann cells in the PNF represent an aggressive cell phenotype that may undergo malignant transformation to MPNST.

TECHNICAL ABSTRACT

Immunohistochemical and Genetic Analyses in Peripheral Nerve Sheath Tumors in NF1
David Viskochil, M.D., Ph.D., Investigator-Initiated Research Award

Background: Malignant peripheral nerve sheath tumor (MPNST) is a sarcoma arising from the peripheral nerve sheath, and its association with neurofibromatosis type 1 (NF1) is well-established. A number of biochemical pathways have been shown to be altered in association with MPNSTs, but the mouse model provides compelling evidence to promote p53 as the most important contributor to malignant transformation. There have been relatively few studies that have focused on the correlation of p53 immunohistochemical staining with *TP53* mutation analysis in human MPNSTs. This correlation needs to be explored, without losing sight of the potential for contributions from other disrupted pathways in malignant transformation. Extensive chromosome analysis, combined with comparative genomic hybridization (CGH), has identified but a few candidate loci harboring candidate genes that may be involved in the altered cellular biology of MPNSTs. A novel technique, CGH microarray, which provides a higher resolution screen of genome imbalances, has not been applied to the study of tumor progression in PNSTs.

Objectives: This project is devoted to the study of peripheral nerve sheath tumors, plexiform neurofibromas and MPSNTs, with respect to NF1. It is divided in 3 parts. The first objective is to develop a better understanding of the role p53 plays in PNST progression. The second objective is to expand our knowledge base of underlying genetic imbalances that arise during "malignant transformation." The third objective is to implement a high-throughput germ-line *NF1* mutation screen to better screen the NF1 population for mutations that may predispose one to develop an MPNST.

Specific Aims: 1.) To determine the immunohistochemical and genetic changes in p53 and *TP53* in the evolution of plexiform neurofibromas to MPNSTs. 2.) To evaluate genomic DNA from PNSTs to identify unbalanced chromosomal regions harboring candidate genes that may contribute to malignant transformation in PNSTs. 3.) To apply high-throughput DNA sequencing to identify *NF1* germline mutations, and to determine if mutation class is associated with an increased risk for MPNST.

Study Design: Archived and prospectively acquired plexiform neurofibromas and MPNSTs will be profiled with a panel of immunohistochemical markers, including a more robust set of p53 antibodies that can distinguish wild-type, mutant and phosphorylated p53. Staining will be correlated with plexiform neurofibromas, low-grade MPNSTs and high-grade MPNSTs. Mutation analysis will be performed on tumor DNA for *TP53* to correlated the presence of mutation with the staining patterns. Spectral Genomics™ has developed a human genome array of 1003 non-overlapping clones that allow quantification of test-DNA hybridization at an average resolution of 3 megabases. CGH microarray analysis will be performed on DNA extracted from plexiform neurofibromas and MPNSTs. Genome imbalances from tumor specimens will be identified and correlated with tumor grades and immunohistochemistry expression profiles. NF1 patients enrolled in this study will be screened with high-throughput cDNA and genomic DNA sequencing protocols for *NF1* mutations. Classes of *NF1* mutations will be correlated with the presence of MPNST.

Relevance: Plexiform neurofibromas are relatively common in NF1, affecting up to 20% of all individuals. Only a subset of these benign tumors undergo malignant transformation, however, neither genetic nor immunohistochemical markers are presently available to signal which plexiform tumors are at risk to evolve into MPSNTs. In addition, there is not an effective surveillance protocol for early detection of MPNST, nor is there effective medical treatment for the malignancy once it has arisen. A better understanding of the pathophysiology of PNSTs is essential for the development of rational adjuvant therapies to complement present day standard of care.

Pediatric and Developmental Pathology 5, 165–169, 2002
DOI: 10.1007/s10024-001-0126-y

Peripheral Nerve Sheath Tumors from Patients with Neurofibromatosis Type 1 Do Not Have the Chromosomal Translocation t(X;18)

MICHAEL A. LIEW,[1]* CHERYL M. COFFIN,[2] JONATHAN A. FLETCHER,[3] MINH-THU N. HANG,[1] KATSUMI TANITO,[1,4] MICHIHITO NIIMURA,[4] AND DAVID VISKOCHIL[1]

[1]Department of Pediatrics, Division of Medical Genetics, University of Utah, 50 North Medical Drive, Salt Lake City, UT 84132, USA
[2]Department of Pathology, Primary Children's Medical Center and University of Utah, 100 North Medical Drive, Salt Lake City, UT 84132, USA
[3]Department of Pathology, Brigham and Women's Hospital, 75 Francis Street, Boston, MA 02115, USA
[4]Department of Dermatology, The Jikei University School of Medicine, Tokyo, Japan

Received July 29, 2001; accepted October 15, 2001.

ABSTRACT

Neurofibromatosis type 1 (NF1) is a common autosomal dominant genetic disorder that is caused by a mutation in the *NF1* gene. Hallmark characteristics include dermal neurofibromas, café-au-lait spots, and learning disabilities. In approximately 25% of NF1 cases, plexiform neurofibromas, or peripheral nerve sheath tumors (PNSTs) that involve large segments of nerve sheath and nerve root, can form, of which a small percentage become malignant (MPNST). Most MPNSTs are composed of spindled neoplastic cells, and they can resemble other spindle-cell sarcomas, including leiomyosarcoma and monophasic synovial sarcoma. Histological diagnosis of MPNST is not always straightforward, and various immunohistochemical and molecular adjuncts can be critical in establishing a correct diagnosis. One example of genetic testing is the assay for the t(X;18) chromosomal translocation, which has been found to be common in synovial sarcomas. The aim of this study was to determine whether MPNSTs contain the t(X;18) chromosomal translocation. To detect the t(X;18) translocation product, SYT-SSX, total RNA was extracted from frozen archival tumors (15 dermal neurofibromas, 4 plexiform neurofibromas, and 7 MPNSTs) using Trizol. The RNA was then subjected to reverse-transcriptase polymerase chain reaction (RT-PCR) to specifically amplify SYT-SSX. None of the dermal neurofibromas, plexiform neurofibromas, or MPNSTs analyzed were positive for SYT-SSX mRNA. The results indicate that the t(X;18) translocation is absent in neurofibromas and is not a marker for MPNST in patients with NF1.

Key words: neurofibromatosis type 1, polymerase chain reaction, synovial sarcoma

INTRODUCTION

Neurofibromatosis type 1 (NF1) is an autosomal dominant disorder that affects approximately 1/3500 individuals. The *NF1* gene was identified as a tumor suppressor and cloned in the early 1990s; it maps to location 17q11.2 and spans 60 exons [1–3]. The *NF1* gene encodes a 2818–amino acid protein called neurofibromin. Hallmark clinical features of this disease are café-au-lait spots, der-

*Corresponding author, at University of Utah, Building 570, BPRB, Room 308, 20S 2030E, Salt Lake City, UT 84112-9454, USA.

was homogenized in 1 ml of TRIZOL reagent and then incubated at room temperature for 5 min. Then 0.2 ml of chloroform was added, followed by vigorous shaking and incubation at room temperature for 2–3 min. The sample was then centrifuged for 15 min at 12,000 × *g* at 4°C for phase separation. After this procedure 0.5 ml of isopropyl alcohol was added to the aqueous phase at room temperature for 10 min, followed by centrifugation at 12,000 × g at 4°C to precipitate out the RNA. The RNA pellet was washed once with 1 ml of 75% (v/v) ethanol and centrifuged at 7,500 × g for 5 min at 4°C. The RNA pellet was then air dried for 10 min at room temperature and dissolved in DEPC-treated distilled water, incubated at 60°C for 10 min, and stored at −70°C.

First-strand cDNA synthesis

First-strand synthesis of cDNA from the isolated total RNA was performed using the reverse transcriptase, Superscript II (Invitrogen, Carlsbad, CA). The following components were combined: 1 μl of random hexamer (1 μg/μl; Pharmacia, Peapack, NJ), 5 μg of total RNA, and sterile distilled water to 12.5 μl. This was then incubated at 70°C for 10 min and then quickly chilled on ice. Then the following components were added: 5 μl of 5 × first-strand buffer, 2 μl of 0.1 mM DTT, 1 μl of 25 mM dNTP (25 mM of each), 0.5 μl of RNasin (Promega, Madison, WI), 1 μl of single-strand DNA binding protein (0.5 μg/μl; USB), and 1.5 μl of water. This was then mixed and incubated at room temperature for 10 min. Then 1.5 μl of SuperScript II Rnase H-Reverse Transcriptase (Invitrogen, Carlsbad, CA) was added. This was then incubated at 37°C for 1 h. The enzyme was then inactivated at 65°C for 10 min and the cDNA was stored at −20°C.

Polymerase chain reaction

The polymerase chain reaction (PCR) method was adapted from O'Sullivan et al. [31]. To ensure the integrity of the cDNA synthesis, β2-microglobulin was amplified using the primers ACCCCCACTGAAAAAGATGA and ATCTTCAAACCTCCATGATG for a predicted product size of 120 base pairs. Contaminating genomic DNA would result in a predicted product size of 730 base pairs. The primers used for the t(X;18) translocation product (SYT-SSX) were AGACCAACACAGCCTGGACCAC and TCCTCTGCTGGCTTCTTG, for a predicted size of 87 base pairs. PCR reactions amplifying β2-microglobulin cDNA were carried out in 25 μl reaction volumes containing 1× PCR buffer, 143 μM dNTP, 200 μM spermidine, 1.5 mM $MgCl_2$, and 0.5 U *Taq* DNA polymerase (Invitrogen, Carlsbad, CA). Thermal cycling conditions for the β2-microglobulin PCR were 94°C for 5 min; 94°C for 40 s, 60°C for 1 min, and 72°C for 30 s, repeated for 38 cycles, followed by 72°C for 5 min. PCR reactions amplifying SYT-SSX cDNA were carried out in 25 μl reaction volumes containing 1 × PCR buffer, 143 μM dNTP, 200 μM spermidine, 0.5 mM $MgCl_2$, and 0.5 U *Taq* DNA polymerase. Thermal cycling conditions for the SYT-SSX PCR were 94°C for 5 min, 94°C for 40 s, 60°C for 1 min, and 72°C for 30 s, repeated for 40 cycles, followed by 72°C for 5 min. The PCR products were electrophoresed on a 2% (w/v, 3:1 Nusieve:Seakem LE) agarose gel.

RESULTS

The integrity of the cDNA synthesis and PCR assays was evident by the presence of amplifiable β2-microglobulin mRNA (Fig. 1a). All samples tested were positive for β2-microglobulin mRNA. When we examined the same samples for the *SYT-SSX* translocation product, the only sample of cDNA that was positive by PCR was from the synovial sarcoma cell line (Fig. 1b). The cDNA from dermal neurofibromas, plexiform neurofibromas, and MPNSTs were negative for the SYT-SSX translocation product.

DISCUSSION

In the study by O'Sullivan et al. [31], which was based on analysis of formalin-fixed, paraffin-embedded tissues, they reported that 2/3 dermal neurofibromas and 15/20 MPNSTs were positive for the t(X;18) translocation. The positive neurofibromas were an atypical neurofibroma and a cellular neurofibroma, which were from patients who did not have clinical features of NF1. Six of the 15 MPNSTs that were positive for the t(X;18) translocation were from patients with NF1, while the remaining 9 patients did not have NF1. In our analysis of frozen tumor samples from NF1 patients, none of the MPNSTs, plexiform neurofibromas, or

2. Wallace MR, Marchuk DA, Anderson LB, et al. Type 1 neurofibromatosis gene: identification of a large transcript disrupted in three patients. Science 1990;249:182–186.
3. Viskochil D, Buchberg AM, Xu G, et al. Deletions and a translocation interrupt a cloned gene at the neurofibromatosis type 1 locus. Cell 1990;62:187–192.
4. Riccardi VM. Neurofibromatosis: Phenotype, Natural History, and Pathogenesis. Baltimore: Johns Hopkins University Press, 1992.
5. Legius E, Marchuk DA, Collins FS, Glover TW. Somatic deletion of the neurofibromatosis type 1 gene in a neurofibrosarcoma supports a tumor suppressor gene hypothesis. Nat Genet 1993;3:122–126.
6. Rasmussen SA, Overman J, Thomson SA, et al. Chromosome 17 loss-of-heterozygosity studies in benign and malignant tumors in neurofibromatosis type 1. Genes Chromosomes Cancer 2000;28:425–431.
7. Schmidt H, Taubert H, Meye A, et al. Gains in chromosomes 7, 8q, 15q and 17q are characteristic changes in malignant but not in benign peripheral nerve sheath tumors from patients with Recklinghausen's disease. Cancer Lett 2000;155:181–190.
8. Birindelli S, Perrone F, Oggionni M, et al. Rb and TP53 pathway alterations in sporadic and NF1-related malignant peripheral nerve sheath tumors. Lab Invest 2001;81: 833–844.
9. Liapis H, Marley EF, Lin Y, Dehner LP. p53 and Ki-67 proliferating cell nuclear antigen in benign and malignant peripheral nerve sheath tumors in children. Pediatr Dev Pathol 1999;2:377–384.
10. Halling KC, Scheithauer BW, Halling AC, et al. p53 expression in neurofibroma and malignant peripheral nerve sheath tumor. An immunohistochemical study of sporadic and NF1-associated tumors. Am J Clin Pathol 1996;106: 282–288.
11. Kourea HP, Orlow I, Scheithauer BW, Cordon-Cardo C, Woodruff JM. Deletions of the *INK4A* gene occur in malignant peripheral nerve sheath tumors but not in neurofibromas. Am J Pathol 1999;155:1855–1860.
12. Kourea HP, Cordon-Cardo C, Dudas M, Leung D, Woodruff JM. Expression of p27(kip) and other cell cycle regulators in malignant peripheral nerve sheath tumors and neurofibromas: the emerging role of p27(kip) in malignant transformation of neurofibromas. Am J Pathol 1999;155: 1885–1891.
13. Dos Santos NR, De Bruijn DRH, Van Kessel AG. Molecular mechanisms underlying human synovial sarcoma development. Genes Chromosomes Cancer 2001;30:1–14.
14. Haagensen CD, Stout AP. Synovial sarcoma. Ann Surg 1944;120:826–842.
15. Pack GT, Ariel IM. Synovial sarcoma (malignant synovioma). A report of sixty cases. Surgery 1950;28:1047–1084.
16. Batsakis JA, Enzinger FM, Tannenbaum M. Synovial sarcomas of the neck. Arch Otolaryngol Head Neck Surg 1967;85:327–331.
17. Roth JA, Enzinger FM, Tannenbaum M. Synovial sarcoma of the neck: a follow-up study of 24 cases. Cancer 1975;35: 1243–1253.
18. Schmookler BM, Enzinger FM, Brannon RB. Orofacial synovial sarcoma: a clinicopathologic study of 11 new cases and review of the literature. Cancer 1982;50:269–276.
19. Witkin GB, Miettinen M, Rosai J. A biphasic tumor of the mediastinum with features of synovial sarcoma: a report of four cases. Am J Surg Pathol 1989;13:490–499.
20. Rosen G, Forscher C, Lowenbraun S, et al. Synovial sarcoma. Uniform response of metastases to high dose ifosfamide. Cancer 1994;73:2506–2511.
21. Limon J, Dal Cin P, Sandberg AA. Translocations involving the X chromosome in solid tumors: presentation of two sarcomas with t(X;18)(q13;p11). Cancer Genet Cytogenet 1986;23:87–91.
22. Kawai A, Woodruff J, Healy JH, et al. *SYT-SSX* gene fusion as a determinant of morphology and prognosis in synovial sarcoma. N Engl J Med 1998;338:153–160.
23. Antonescu CR, Kawai A, Leung DH, et al. Strong association of *SYT-SSX* fusion type and morphologic epithelial differentiation in synovial sarcoma. Diagn Mol Pathol 2000;9:1–8.
24. Tsuji S, Hisaoka M, Morimitsy Y, et al. Detection of SYT-SSX fusion transcripts in synovial sarcoma by reverse transcription-polymerase chain reaction using archival paraffin-embedded tissues. Am J Pathol 1998;153:1807–1812.
25. Nilsson G, Skytting B, Xie Y, et al. The SYT-SSX1 variant of synovial sarcoma is associated with a high rate of tumor cell proliferation and poor clinical outcome. Cancer Res 1999;59:3180–3184.
26. de Leeuw B, Balemans M, Olde Weghuis D, et al. Molecular cloning of the synovial sarcoma–specific translocation (X;18)(p11.2;q11.2) breakpoint. Hum Mol Genet 1994;3: 745–749.
27. Clark J, Rocques PJ, Crew AJ, et al. Identification of novel genes *SYT* and *SSX*, involved in the t(X;18)(p11.2;q11.2) translocation found in human synovial sarcoma. Nat Genet 1994;7:502–508.
28. Crew AJ, Clark J, Fisher C, et al. Fusion of *SYT* to two genes, *SSX1* and *SSX2*, encoding proteins with homology to the Kruppel-associated box in human synovial sarcoma. EMBO J 1995;14:2333–2340.
29. de Leeuw B, Balemans M, Olde Weghuis D, et al. Identification of two alternative fusion genes, *SYT-SSX1* and *SYT-SSX2*, in t(X;18)(p11.2;q11.2)-positive synovial sarcomas. 1995;4:1097–1099.
30. Skytting BT, Nilsson G, Brodin B, et al. A novel fusion gene, *SYT-SSX4*, in synovial sarcoma. J Natl Cancer Inst 1999;91:974–975.
31. O'Sullivan MJ, Kyriakos M, Zhu X, et al. Malignant peripheral nerve sheath tumors with t(X;18). A pathologic and molecular genetic study. Mod Pathol 2000;13:1253–1263.
32. Neurofibromatosis. Natl Inst Health Consens Dev Conf Consens Statement 1987;6:1–7.
33. van de Rijn M, Barr FG, Collins MH, et al. Absence of SYT-SSX fusion products in soft tissue tumors other than synovial sarcoma. Am J Clin Pathol 1999;112:43–49.
34. Hiraga H, Nojima T, Abe S, et al. Diagnosis of synovial sarcoma with the reverse transcriptase-polymerase chain reaction: analyses of 84 soft tissue and bone tumors. Diagn Mol Pathol 1998;7:102–110.
35. Vang R, Biddle DA, Harrison WR, Heck K, Cooley LD. Malignant peripheral nerve sheath tumor with a t(X;18). Arch Pathol Lab Med 2000;124:864–867.

[*Cancer Research* 62, 1573-1577, March 1, 2002]

Meeting Report

International Consensus Statement on Malignant Peripheral Nerve Sheath Tumors in Neurofibromatosis 1[1]

Rosalie E. Ferner[2] and David H. Gutmann[3]
Division of Clinical Neurosciences, Department of Neuroimmunology, Guy's King's and St. Thomas' School of Medicine, London, SE1 1UL United Kingdom

ABSTRACT

Neurofibromatosis 1 (NF1) is an autosomal dominant tumor predisposition syndrome in which affected individuals have a greatly increased risk of developing malignant peripheral nerve sheath tumors (MPNSTs). These cancers are difficult to detect and have a poor prognosis. Because patients may present to specialists from widely differing disciplines, the association with NF1 is often not appreciated, and there is no cohesive pattern of care. A multidisciplinary group of 33 clinicians and scientists with specialist knowledge in MPNST and NF1 reviewed the current published and unpublished data in this field, and distilled their collective experience to produce a consensus summary on MPNST in NF1. The known clinical, pathological, and genetic information on MPNST in NF1 was collated, and a database was established to record information in a uniform manner. Subgroups with a higher risk of developing MPNST were identified within the NF1 population. The consortium formulated proposals and guidelines for clinical and pathological diagnosis, surgical management, and medical treatment of MPNST in individuals with NF1. A multidisciplinary team approach to the management of this complex disorder is advocated. Progress can be made by adopting the guidelines proposed by this consortium and by widespread dissemination of standardized information. Collaborative research should be promoted with the aim of harnessing advances in molecular genetics to develop targeted therapies for MPNST in people with NF1.

Introduction

NF1[4] is an autosomal dominant neurocutaneous disorder, with an estimated birth incidence of 1 in 2500 (1) . The *NF1* gene on chromosome 17q 11.2 was identified by positional cloning, and its protein product, neurofibromin, functions as a tumor suppressor (2, 3, 4) . One of the functions of neurofibromin is to reduce cell proliferation by accelerating the inactivation of the proto-oncogene *p21-ras,* which has a pivotal role in mitogenic intracellular signaling pathways (4) . The cardinal and defining features of NF1 are café au lait macules, neurofibromas, skinfold freckling, iris Lisch nodules, and characteristic osseous dysplasia (5) . The complications of the disorder are legion and may involve any of the body systems (6) .

Individuals affected with NF1 harbor an increased risk of developing both benign and malignant tumors, supporting the classification of NF1 as a tumor predisposition syndrome. The most common tumor in individuals with NF1 is the neurofibroma, a heterogeneous benign peripheral nerve sheath tumor (7 , 8) . Neurofibromas may appear as discrete, dermal neurofibromas, focal cutaneous or s.c. growths, dumbbell-shaped intraforaminal spinal tumors, or nodular or diffuse plexiform neurofibromas. Plexiform neurofibromas are composed of the same cell types as dermal neurofibromas but have an expanded extracellular matrix and often have a rich vascular supply. They develop along a nerve and may involve multiple branches, nerve roots, and plexi. Impingement on surrounding structures may cause functional compromise, and soft tissue and bone hypertrophy may occur (9) .

Plexiform neurofibromas were clinically visible in 30% of 125 NF1 patients in a South Wales population study (10) . Forty four percent of plexiform neurofibromas (32 of 72 patients) were diagnosed before 5 years of age in one clinic-based study (11) suggesting that many plexiform neurofibromas are congenital lesions. Multiple plexiform neurofibromas occur in 9–21% of cases (10, 11, 12) . Although MPNST can develop in individuals in the general population, individuals with NF1 have a significantly increased risk. These tumors arise frequently in preexisting plexiform neurofibromas, which are very uncommon in people who do not have NF1. MPNSTs are often difficult to detect, metastasize to the lung, liver, brain, soft tissue, bone, regional lymph nodes, skin, and retroperitoneum, and have a poor prognosis (13) . Because patients with MPNSTs may present to specialists from widely differing disciplines, the association with NF1 is often not appreciated, and there is no consistent or widely accepted pattern of care.

Aims.

In this unique meeting, the aim was to establish an international, multidisciplinary consortium of experts on MPNST and NF1. The purpose was to collate the known clinical and genetic information about these tumors and to set up a standardized database to record information in a uniform manner. In addition, the goal was to formulate guidelines for clinical and pathological diagnosis, surgical management, and medical treatment. Moreover, strategies were proposed

for developing targeted therapies for NF1-associated MPNSTs, taking into account the recent advances in molecular biology.

Materials and Methods

An international, multidisciplinary group of clinicians and scientists with a specialist interest in soft tissue sarcomas (MPNST) and NF1 was invited. Invitations were sent to clinicians working in specialist soft tissue sarcoma centers or large neurofibromatosis clinics and to individuals with research publications in these fields. The current knowledge in this field was reviewed based on personal expertise and the medical literature. Subsequently, the specialists pooled their collective experience to produce a consensus group summary on MPNST in NF1.

Results

Clinical Consensus Group.

It is generally accepted that MPNSTs occur in about 2–5% of NF1 patients compared with an incidence of 0.001% in the general population (13) . However, there may be differences in cross-sectional *versus* longitudinal determinations of risk for MPNST, and the lifetime risk for MPNST could be as high as 10% (14) . The majority of patients present in the second and third decades of life, and tend to be younger than their counterparts with MPNSTs in the general population (13) . We have also identified MPNSTs in NF1 patients as young as 7 years and as old as 63 years of age. Clinicians should be alerted to the possible diagnosis of MPNST when a patient with NF1 develops unremitting pain not otherwise explained, rapid increase in size of a plexiform neurofibroma, change in consistency from soft to hard, or a neurological deficit.

Most NF1-associated MPNSTs appear to arise within preexisting plexiform neurofibromas. This observation suggests that individuals with NF1 and plexiform neurofibromas warrant increased surveillance for development of MPNST, and those with many or very extensive plexiform neurofibromas may have the highest risk. However, the natural history of plexiform neurofibromas has not been clearly defined, and these tumors may undergo periods of rapid growth followed by periods of relative quiescence. As such, rapid growth is not always a prelude to malignancy. This issue is currently being addressed by an international study using clinical assessment and volumetric MRI (Clinical Coordinator, Bruce Korf, Boston, MA).

There is no evidence that dermal neurofibromas or flat superficial plexiform neurofibromas undergo malignant transformation, and they do not require close monitoring. Nodular plexiform tumors associated with large peripheral nerve sheaths and extensive tumors involving the brachial, lumbar, or sacral plexus may give rise to MPNSTs and, therefore, merit heightened awareness. Plexiform neurofibromas, which are more centrally located and are more extensive, appear to have a higher likelihood of undergoing malignant change. Individuals with a "neurofibromatous" neuropathy might also have an increased risk of developing MPNST, because they develop dermal neurofibromas in early childhood and have diffuse plexiform involvement of the spinal nerve roots and peripheral nerves (15) .

Patients in whom a microdeletion of the *NF1* locus is detected tend to have higher numbers of discrete dermal neurofibromas at earlier ages and might have a higher incidence of MPNST than the overall NF1 population (16) . The increased risk of MPNST in this group could be readily tested by comparing the frequency of *NF1* microdeletions detected by fluorescence *in situ* hybridization of peripheral blood lymphocytes in NF1 patients with and without MPNST.

MPNSTs are often difficult to detect, because the clinical indicators of malignancy may also be features of active, benign plexiform neurofibromas. A MRI should be performed to locate the site, extent, and change in size of the plexiform neurofibroma, but it does not reliably determine malignant transformation. The diffuse nature of the plexiform neurofibroma may preclude total removal because of impingement on surrounding structures and neurological deficit.

PET with the glucose analogue ^{18}FDG is a dynamic imaging technique, which permits the visualization and quantification of glucose metabolism in cells and reflects the increase in metabolism in malignant tumors (17 , 18) . A retrospective study of 18 NF1 patients demonstrated that ^{18}FDG PET is a potentially useful, noninvasive method for detecting malignant change in plexiform neurofibromas (19) . However, the distinction between low-grade MPNSTs and benign plexiform neurofibromas was not clear in all of the cases. It is recommended that a prospective study with clinical, radiological, and pathological correlation be undertaken to evaluate the value of ^{18}FDG PET in the detection of malignant change in NF1. The new tracer ^{18}F-thymidine, which detects DNA turnover, might be helpful in distinguishing low-grade MPNSTs from active, benign plexiform neurofibromas in future PET-based studies.

Scrupulous documentation of information on NF1 patients with MPNST will play a vital part in optimizing the management of this condition. Data should be recorded in a standardized database, which should be circulated to sarcoma units and to specialists in neurology, genetics, surgery, and oncology, who are likely to encounter these patients. Demographic details, confirmation of the diagnosis of NF1, history of cancer in the individual and family, clinical and radiological features of the MPNST, and pathological description of the tumor need to be included. Documentation of treatment modalities and outcome is essential. It is anticipated that molecular analysis of constitutional DNA and tumor material may play a pivotal role in determining therapeutic protocols.

Pathology Consensus Group.

The options for diagnosis include fine needle aspiration, Tru-Cut needle biopsy, open incisional biopsy, and excisional biopsy. Fine needle aspiration is inadequate for the assessment of tumor type and grade, because dissociated tumor cells are obtained and architectural relationships lost. Tru-Cut needle biopsy is the method of choice when undertaken in a multidisciplinary team setting using expert radiological, surgical, and pathological advice. If sufficient tissue cores are taken and the specimen is sent fresh, techniques can be used such as imprint cytology to ensure that tumor tissue is present. Representative fresh tissue cores can be snap frozen in liquid nitrogen for molecular biological studies and research.

An open incisional biopsy provides more tissue for diagnosis and ancillary studies, but the sample is limited to one site. For this reason, it is necessary to ensure that the sample is representative and includes the areas suspected of malignancy. The combination of open incisional biopsy with multiple Tru-Cut needle biopsies from different areas may overcome this difficulty. This technique should be carefully planned so that future surgical resection margins are not compromised. An excisional biopsy should be reserved for small, superficially located tumors, which can be resected with a clear margin. This provides the most material for diagnosis and research. The technique of targeted biopsy using ^{18}FDG PET and magnetic resonance registration is being developed in specialist centers and may be of potential benefit in the management of this group of heterogeneous tumors.

The minimum histological examination should comprise sections stained with conventional tinctorial stains including H&E and reticulin. In addition, immunohistochemical stains for S100 protein, the skeletal muscle markers desmin and myogenin, and a proliferation marker (MIB1) are required. Other spindle cell tumors may be excluded with appropriate immunohistochemical markers. In the future, there might be a place for the routine application of stains for known tumor suppressor genes or oncogenes (*p53, erbB2, p16,* and *p27*), for molecular analysis of NF1 and NF2 expression, and for determination of RAS activity (see "Molecular Biology Consensus Group").

The pathological features of MPNST reveal a fusiform or globoid mass associated with a nerve. Necrosis, pseudocystic change, or hemorrhage may be found. Histologically, the tumor is composed of spindle cells arranged in cellular fascicles (20) . Divergent differentiation may occur, including rhabdomyoblastic change encountered in the malignant triton tumor variant (20 , 21) .

The pathological criteria for malignancy include invasion of surrounding tissues by tumor cells, vascular invasion, marked nuclear pleiomorphism, necrosis, and the presence of mitoses (20) . Even a single mitotic figure may be significant, particularly in a tumor with hypercellularity and nuclear atypia. The significance of the mitoses depends on the prognostic value of increased cell proliferation. Therefore, the most clinically relevant question is how best to determine malignant transformation in these tumors. The methods available for assessing growth rate include direct counting of observed mitotic figures, the estimation of proliferation index using immunostains, flow cytometry, other molecular techniques, or the detection of an imbalance between apoptosis and proliferation. The accurate prediction of biological behavior may depend on the interpretation of a combination of histological and immunohistochemical features.

There is a histological spectrum of peripheral nerve sheath tumors ranging from the clearly benign to the clearly malignant, and it is often possible to distinguish between high-grade and low-grade tumors. However, a significant number of tumors, the so-called "atypical neurofibromas" do not fit into any defined grading system (20 , 22 , 23) . These may be locally aggressive but are less likely to metastasize. In addition, there are a few histologically low-grade tumors that behave aggressively. The application of molecular techniques to determine the gene expression profiles of gene expression in these tumors may help pathologists to predict biological behavior and outcome more accurately. The correlation with new imaging techniques may also help to resolve this issue.

Surgery Consensus Group.

The aim of surgery is complete removal of the lesion with tumor-free margins (13) . Biopsy of the lesion is essential before surgery is undertaken (see "Pathology Group" statement). Small lesions should be widely resected, and larger tumors should be as widely excised as possible (=" src="/math/ge.gif" border=010 cm) to avoid centripetal spread. Reconstruction of the nerve after surgery for brachial and lumboscaral plexus lesions is not advocated, because it does not restore useful function and may compromise the adequacy of the surgical excision. Amputation may be indicated for extensive tumors and for MPNST, which recur after apparently adequate excision.

Patients should have baseline MRI 2–3 months after surgery. Additional imaging studies and their timing will depend on the patient symptoms and the nature of the primary tumor. ^{18}FDG PET might be a useful screening investigation in the future, because it provides both a local and a body-wide scan within a single investigation for this group of "at-risk" patients.

Oncology Consensus Group.

It is not clear whether patients with NF1 and MPNST have a different clinical course or response to treatment compared with their counterparts in the general population. The current management of MPNST should be identical to that of any other soft tissue tumor in that successful treatment depends on complete surgical excision. Radiotherapy provides local

control and may delay the onset of recurrence but has little effect on long-term survival. Adjuvant radiotherapy should be given wherever possible for intermediate- to high-grade lesions and for low-grade tumors after a marginal excision. Chemotherapy for adult soft tissue sarcomas is usually confined to the treatment of metastatic disease. Few drugs have been shown to be effective, and treatment comprises single agent doxorubicin or a combination of doxorubicin and ifosfamide (24) . Although such treatment is not curative, it may achieve useful palliation for many patients, and complete, long-lasting remissions are observed in rare instances. Moreover, it may be useful in the preoperative setting to downstage patients with unresectable primaries.

MPNST appears to be of intermediate chemosensitivity, less responsive than synovial sarcoma, but more chemosensitive than refractory diseases such as alveolar soft part sarcoma. The partial response rate with the best available chemotherapy is likely to be in the range of 25–30% (24) . Controversy surrounds the use of adjuvant chemotherapy. A meta-analysis has shown a significant benefit at 10 years in terms of progression-free survival for both local and distant relapse (25) . However, the magnitude of any overall survival benefit is small (4% and not statistically significant). Chemotherapy might be used to improve local disease control for marginally resected lesions at sites where an adequate dose of radiotherapy is difficult to deliver.

Recent advances in sarcoma therapy have resulted from an improved understanding of the molecular biology of individual diseases. The discovery of mutations in the *c-kit* gene, resulting in overexpression of a constitutively activated c-kit molecule in gastrointestinal stromal tumors, has been of paramount therapeutic importance. This has not only resulted in CD117 overexpression becoming the hallmark diagnostic test for this disease but has lead to a new form of treatment for a disease that was hitherto untreatable. The receptor tyrosine kinase inhibitor STI571 (Glivec) is a potent inhibitor of KIT and has been reported to result in dramatic tumor regressions in these patients, which thus far appear to be durable (26) .

Similarly, it is the hope that new agents, which target the RAS-RAF- mitogen-activated protein/ERK kinase-extracellular signal-regulated kinase pathway, may prove effective against MPNST in NF1. In these tumors, loss of the inhibiting function of neurofibromin results in increased p21-ras signaling. Anti-RAS pathway drugs include farnesyl transferase inhibitors, which block the ability of RAS to reach the membrane where it is activated (27) . However, there are now specific inhibitors of targets downstream of RAS, such as mitogen-activated protein/ERK kinase, that are also being developed for clinical study. Given the success of Glivec, it is clear that tyrosine kinase inhibitors can be developed that are both selective and effective, and hopefully one of these agents will prove effective against MPNSTs.

Molecular Biology Consensus Group.

Significant progress has been made in recent years in elucidating the molecular genetics and biology of MPNST in NF1. Surgical specimens and cell lines from patients with MPNST and NF1 exhibit loss of *NF1* gene (neurofibromin) expression and high levels of RAS activity (28, 29, 30) . Studies of benign neurofibromas from NF1 patients have demonstrated that loss of *NF1* gene expression and increased RAS activation alone is not sufficient for MPNST formation, and that additional genetic alterations (p27-Kip1, p53, and p16) are required for malignant transformation (31, 32, 33, 34, 35) . The generation of mice with targeted mutations in the *NF1* gene has confirmed this notion in that loss of *NF1* expression appears to be sufficient for the formation of tumors with pathological features of plexiform neurofibromas, whereas MPNST development is dependent on functional inactivation of p53 (36 , 37) .

Our ability to more accurately predict tumor behavior and response to therapy is likely to derive from studies aimed at defining the molecular changes seen in these tumors. A variety of different genetic alterations have been reported in MPNSTs, but it is not clear that any of these are causally related to tumorigenesis or malignant progression. Moreover, it is not known whether a subset of these changes will predict the clinical course or define whether a specific form of therapy is likely to be more efficacious. Additional research is required to define the intracellular signaling pathway abnormalities primarily responsible for plexiform neurofibroma or MPNST growth, and to delineate which specific downstream effectors of RAS mediate RAS mitogenic signaling. Similarly, research efforts to define the genetic changes in addition to *NF1* loss that are required for plexiform neurofibroma malignant transformation also may identify additional therapeutic targets for MPNST drug design. These studies have the potential to identify gene expression profiles that are specifically associated with particular MPNST subtypes or plexiform neurofibromas most likely to undergo malignant change ("molecular fingerprint").

The importance of an international tissue bank for MPNSTs to facilitate basic science and translational research cannot be overstated. This would involve storing fresh-frozen specimens, corresponding normal nerve specimens when available, and normal tissue or blood, as well as paraffin sections. These specimens need to be well characterized pathologically and to be linked to molecular, pathological, and clinical-epidemiological patient data. Both NF1-associated and sporadic MPNSTs should be stored in this tumor bank to determine whether the noted molecular and clinical-epidemiological characteristics are similar in these two groups.

Conclusions.

MPNST is a devastating complication of NF1, which should be managed by multidisciplinary teams of clinicians and scientists with expertise in the diagnosis and treatment of this disease. Clinical and molecular genetic studies should identify NF1 patients who are at high risk of developing MPNST. The establishment of an international database will

permit the standardized recording of clinical, pathological, and treatment data, and outcome measures. The development of imaging methods such as PET scanning will aid in distinguishing MPNST from benign plexiform neurofibromas. Recent advances in molecular genetics have provided exciting opportunities to develop targeted therapies for these tumors, which will be helped by the establishment of an international tissue bank. Our ability to translate these advances into rational clinical trials represents the challenge for the immediate future.

Appendix 1

Medical Consensus Group. Gareth Evans, Department of Medical Genetics, St. Mary's Hospital, Manchester, United Kingdom; Rosalie Ferner, Department of Clinical Neurosciences, GKT School of Medicine, Guy's Hospital, London, United Kingdom; Jan M. Friedman, Division of Medical Genetics, University of British Columbia, Vancouver, Canada; Susan Huson, Department of Medical Genetics, Churchill Hospital, Oxford, United Kingdom; Viktor Mautner, Department of Neurology, Klinikum Nord, Ochsenzoll, Hamburg, Germany; Michael O'Doherty, Clinical PET Center, GKT School of Medicine, St. Thomas' Hospital, London, United Kingdom; David Viskochil, Division of Medical Genetics, University of Utah, Salt Lake City, UT.

Surgery Consensus Group. Rolfe Birch, Peripheral Nerve Injury Unit, Royal National Orthopaedic Hospital, London, United Kingdom; Ivo DeWever, Department of Surgical Oncology, University Hospital, Leuven, Belgium; Rheinhard Friedrich, Department of Surgery, University Hospital, Hamburg-Eppendorf, Germany; Henk Giele, Department of Plastic Surgery, Radcliffe Infirmary, Oxford, United Kingdom; Robert Grimer, Department Of Orthopaedics, Royal Orthopaedic Hospital, Birmingham, United Kingdom; Jonathan Lucas, Soft Tissue Tumor Unit, Department of Orthopaedics, Guy's and St. Thomas' Hospitals, London, United Kingdom; Michael Smith, Soft Tissue Tumor Unit, Department of Orthopaedics, Guy's and St. Thomas' Hospitals, London, United Kingdom; Meirion Thomas, Sarcoma and Melanoma Unit, Royal Marsden Hospital, London, United Kingdom.

Pathology Consensus Group. Cheryl Coffin, Division of Pediatric Pathology, University of Utah School of Medicine, Salt Lake City, UT; Susan Robinson, Department of Neuropathology, King's College Hospital, London, United Kingdom; Ann Sandison, Department of Pathology, Charing Cross Hospital, London, United Kingdom; Susan Standring, Division of Neuroscience, Guy's King's and St. Thomas' School of Medicine, London, United Kingdom; Andreas von Deimling, Department of Neuropathology Charité, Humboldt University, Berlin, Germany.

Oncology Consensus Group. Adrian Jones, Department of Radiotherapy, Churchill Hospital, Oxford, United Kingdom; Ian Judson, CRC Center for Cancer Therapeutics, Institute of Cancer Research, Sutton, United Kingdom; Chris Mitchell, Department of Pediatric Oncology, John Radcliffe Hospital, Oxford, United Kingdom; Rif Pamukcu, Cell Pathways, Inc., Horsham, PA; Mike Stevens, Department of Pediatric Oncology, Birmingham Children's Hospital, Birmingham, United Kingdom; Jeremy Whelan, The Meyerstein Institute of Oncology, The Middlesex Hospital, London, United Kingdom.

Molecular Biology Consensus Group. Abhijit Guha, Labatts Brain Tumor Center, The Hospital for Sick Children, Toronto, Ontario, Canada; David Gutmann, Department of Neurology, Washington University School of Medicine, St. Louis, MO; Chris Jones, Department of Pathology, University of Wales College of Medicine, Cardiff, United Kingdom; Eric Legius, Center for Human Genetics, University Hospital, Leuven, Belgium; Anne Mudge, MRC Laboratory for Molecular Biology, University College, London, United Kingdom; Thorsten Rosenbaum, Children's Hospital, Heinrich-Heine University, Dussledorf, Germany; Meena Upadhyaya, Institute of Medical Genetics, University of Wales College of Medicine, Cardiff, United Kingdom.

ACKNOWLEDGMENTS

We thank Bruce Korf for critical insights during the preparation of this document and J. M. Friedman for editorial comments. Susan Huson proposed the topic for this consensus meeting. Rosalie E. Ferner and David H. Gutmann organized the MPNST Consensus Group with assistance from Meena Upadhyaya, David Viskochil, and Roberta Tweedy (British Neurofibromatosis Association).

FOOTNOTES

The costs of publication of this article were defrayed in part by the payment of page charges. This article must therefore be hereby marked *advertisement* in accordance with 18 U.S.C. Section 1734 solely to indicate this fact.

[1] Supported by Wellcome Trust, The British Neurofibromatosis Association, and Cell Pathways, Inc. RFN1RFN1

[2] To whom requests for reprints should be addressed, at Division of Clinical Neurosciences, Department of Neuroimmunology, Second Floor Hodgkin Building, Guy's King's and St. Thomas' School of Medicine, London Bridge, London SE1 1UL, United Kingdom. Phone: 44-207-848-6122; Fax: 44-207-848-6123; E-mail: rosalie.ferner@kcl.ac.uk. RFN2RFN2

[3] D. H. G. was the leader of the following working groups: Medical Consensus Group, Surgery Consensus Group, Pathology Consensus Group, Oncology Consensus Group, and Molecular Biology Consensus Group. Members of the groups are listed in the Appendix. RFN3RFN3

[4] The abbreviations used are: NF1, neurofibromatosis 1; MPNST, malignant peripheral nerve sheath tumor; MRI, magnetic resonance imaging; ^{18}FDG, ^{18}F-fluorodeoxyglucose; PET, positron emission tomography. RFN4

Received 10/ 9/01; accepted 1/ 4/02.

REFERENCES

1. Huson, S. M., Clark, P., Compston, D. A. S., and Harper, P. S. A genetic study of von Recklinghausen neurofibromatosis in South East Wales. 1: prevalence, fitness, mutation rate, and effect of parental transmission on severity. J. Med. Genet., *26:* 704–711, 1991.
2. Viskochil D., Buchberg A. M., Xu G., Cawthon R. M., Stevens J., Wolff R. K., Culver M., Carey J. C., Copeland N. G., Jenkins N. A., White R., O'Connell P. Deletions and a translocation interrupt a cloned gene at the neurofibromatosis type 1 locus.. Cell, *62:* 187-192, 1990.
3. Wallace M. R., Marchuk D. A., Anderson L. B., Letcher R., Odeh H. M., Saulino A. M., Fountain J. W., Brereton A., Nicholson J., Mitchell A. L., Brownstein B. H., Collins F. S. Type 1 neurofibromatosis gene: identification of a larger transcript disrupted in three NF1 patients.. Science (Wash. DC), *249:* 181-186, 1990.
4. Xu G. F., O'Connell P., Viskochil D., Cawthon R., Robertson M., Culver M., Dunn D., Stevens J., Gesteland R., White R., Weiss R. The neurofibromatosis type 1 gene encodes a protein related to GAP.. Cell, *62:* 599-608, 1990.
5. National Institutes of Health Consensus Development Conference Statement Neurofibromatosis. Arch. Neurol., *45:* 575–578, 1988.
6. Ferner R. E. Clinical aspects of neurofibromatosis 1. Upadhyaya M. Cooper D. N. eds. . Neurofibromatosis 1 from Genotype to Phenotype, *:* 21-38, Bios Scientific Publishers Ltd. Oxford 1998.
7. von Recklinghausen, F. D. Über die Multiplen Fibrome der Haut und Ihre Beziehung zu den Multiplen Neuromen. Berlin: A Hirschwald, 1882.
8. Harkin J. C. Pathology of nerve sheath tumors.. Ann. NY Acad. Sci., *486:* 147-154, 1986.
9. Korf B. R., Huson S. M., Needle M., Ratner N., Rutkowski L., Short P., Tonsgard J., Viskochil D. Report of the working group on neurofibroma4-27, The National Neurofibromatosis Foundation, Inc. 1997.
10. Huson S. M., Harper P. S., Compston D. A. S. Von Recklinghausen Neurofibromatosis.. A clinical and population study in South East Wales. Brain, *111:* 1355-1381, 1988.
11. Waggoner D. J., Towbin J., Gottesman G., Gutmann D. H. A clinic-based study of plexiform neurofibromas in neurofibromatosis 1.. Am. J. Med. Genet., *92:* 132-135, 2000.
12. Friedman J. M., Birch P. H. Type 1 neurofibromatosis.. A descriptive analysis of the disorder in 1, *728patients.Am.J.Med.Genet.,70:* 138-143, 1997.
13. Ducatman B., Scheithauer B., Piepgras D., Reiman H. M., Ilstrup D. M. Malignant peripheral nerve sheath tumors: a clinicopathologic study of 120 cases.. Cancer (Phila.), *57:* 2006-2021, 1986.
14. McGaughran J., Harris D. I., Donnai D., Teare D., McLeod R., Kingston H., Super M., Harris R., Evans D. G. R. A clinical study of type 1 neurofibromatosis in North West England.. J. Med. Genet., *36:* 197-203, 1999.
15. Ferner R. E., Upadhyaya M., Osborn M., Hughes R. A. C. Neurofibromatous neuropathy.. J. Neurol., *243:* S20 1996.
16. Leppig K. A., Kaplan P., Viskochil D., Weaver M., Ortenberg J., Stephens K. Familial neurofibromatosis 1 microdeletions: cosegregation with distinct facial phenotype and early onset of cutaneous neurofibromata.. Am. J. Med. Genet., *73:* 197-204, 1997.
17. Strauss, L. G., and Conti, P. S. The applications of PET in clinical oncology. J. Nucl. Med. *32:* 623–648, 1991.
18. Lucas J. D., O'Doherty M. J., Wong J. C. H., Bingham J. B., McKee P. H., Fletcher C. D. M., Smith M. A. Evaluation of fluorodeoxyglucose positron emission tomography in the management of soft tissue sarcomas.. J. Bone Joint Surg. Br. Vol., *80:* 441-447, 1998.
19. Ferner R. E., Lucas J. D., O'Doherty M. J., Hughes R. A. C., Smith M. A., Cronin B. F., Bingham J. B. Evaluation of ^{18}fluorodeoxyglucose positron emission tomography in the detection of malignant peripheral nerve sheath tumors in neurofibromatosis 1.. J. Neurol. Neurosurg. Psychiatry, *68:* 353-357, 2000.
20. Enziger, F. M., and Weiss, S. W. Benign tumors of peripheral nerves: malignant tumors of the peripheral nerves. *In:* W. Sharon, Weiss and J. R., Goldblum (eds.), Soft Tissue Tumors, Ed. 4, pp. 1111–1263. St. Louis, MO: Mosby, 2001.
21. Masson, P. Recklinghausen's Neurofibromatosis. Sensory Neuromas and Motor Neuromas. Libman Anniversary Volumes 2, pp. 793–802. New York: New York International Press, 1932.
22. Lin, B. T-Y., Weiss, L. M., and Medeiros, L. J. Neurofibroma and cellular neurofibroma with atypia. A report of 14 tumors. Am. J. Surg. Pathol., *21:* 1443–1449, 1997.
23. Coffin C. M., Dehner L. P. Cellular peripheral neural tumors (neurofibromas) in children and adolescents: a clinicopathological and immunohistochemical study.. Pediatr. Pathol., *10:* 351-361, 1990.
24. Santoro A., Tursz T., Mouridsen H., Verveij J., Steward W., Somers R., Buesa J., Casali P., Spooner D., Rankin E. Doxorubicin versus CY VADIC verses doxorubicin plus ifosfamide in first-line treatment of

advanced soft tissue sarcomas: a randomized study of the EORTC Soft Tissue and Bone Sarcoma Grou. p. J. Clin. Oncol., *13:* 1537-1545, 1995.

25. Sarcoma Meta-analysis Collaboration. Adjuvant chemotherapy for localised resectable soft-tissue sarcoma in adults: meta-analysis of individual data. Lancet, *350:* 1647–1654, 1997.
26. Van Oosterom A. T., Judson I., Verweij J., Di Paola E., Van Glabbeke M., Dimitrijevic S., Nielsen O. STI571, an active drug in metastatic gastro-intestinal stromal tumors (GIST) an EORTC Phase I study.. Proc. Am. Soc. Clin. Oncol., *20:* 1a 2001.
27. Cox A. D. Farnesyltransferase inhibitors: potential role in the treatment of cancer.. Drugs, *61:* 723-732, 2001.
28. Guha A., Lau N., Huvar I., Gutmann D., Provias J., Pawson T., Boss G. Ras-GTP levels are elevated in human peripheral nerve tumors.. Oncogene, *12:* 507-513, 1996.
29. Basu T. N., Gutmann D. H., Fletcher J. A., Glover T. W., Collins F. S., Downward J. Aberrant regulation of ras proteins in malignant tumor cells from type 1 neurofibromatosis patients.. Nature (Lond.), *356:* 663-664, 1992.
30. DeClue J. E., Papageorge A. G., Fletcher J. A., Diehl S. R., Ratner N., Vass W. C., Lowy D. R. Abnormal regulation of mammalian p21ras contributes to malignant tumor growth in von Recklinghausen's (type 1) neurofibromatosis.. Cell, *69:* 265-273, 1992.
31. Kluwe L., Friedrich R. E., Mautner V. F. Allelic loss of the NF1 gene in NF1-associated plexiform neurofibromas.. Cancer Genet. Cytogenet., *113:* 65-69, 1999.
32. Rutkowski J. L., Wu K., Gutmann D. H., Boyer P. J., Legius E. Genetic and cellular defects contributing to benign tumor formation in neurofibromatosis type 1.. Hum. Mol. Genet., *9:* 1059-1066, 2000.
33. Sherman L. S., Atit R., Rosenbaum T., Cox A. D., Ratner N. Single cell Ras-GTP analysis reveals altered Ras activity in a subpopulation of neurofibroma Schwann cells but not fibroblasts.. J. Biol. Chem., *275:* 30740-30745, 2000.
34. Nielsen G. P., Stemmer-Rachamimov A. O., Ino Y., Moller M. B., Rosenberg A. E., Louis D. N. Malignant transformation of neurofibromas in neurofibromatosis 1 is associated with CDKN2A/p16 inactivation.. Am. J. Pathol., *155:* 1879-1884, 1999.
35. Kourea H. P., Cordon-Cardo C., Dudas M., Leung D., Woodruff J. M. The emerging role of $p27^{kip}$ in malignant transformation of neurofibromas.. Am. J. Pathol., *155:* 1885-1891, 1999.
36. Cichowski K., Shih T. S., Schmitt E., Santiago S., Reilly K., McLaughlin M. E., Bronson R. T., Jacks T. Mouse models of tumor development in neurofibromatosis type 1.. Science (Wash. DC), *286:* 2172-2176, 1999.
37. Vogel K. S., Klesse L. J., Velasco-Miguel S., Meyers K., Rushing E. J., Parada L. F. Mouse tumor model for neurofibromatosis 1.. Science (Wash. DC), *286:* 2176-2179, 1999.

Summary – MPNST Symposium, Aspen, June 7 & 8, 2002

Goal: To develop rational approaches to prevention and effective treatment of malignant peripheral nerve sheath tumors (MPNSTs) in individuals with neurofibromatosis type 1 (NF1).

Objectives:
1. Identify those individuals with NF1 who are at highest risk to develop MPNST.
2. Implement screening protocols for early detection of MPNST in NF1 patients.
3. Evaluate genetic and biologic processes that contribute to the development and progression of peripheral nerve sheath tumors in NF1.
4. Assess the use of neo-adjuvant chemotherapy in the treatment of MPNST.

Strategy: Identify and develop NF1-sarcoma centers with dedicated personnel to identify, screen, and treat individuals with NF1 and MPNST in a uniform way. This would entail the development of protocols, recruitment of patients, application of standards of care, collection of biologic specimens and implementation of treatment protocols. These centers would also be involved in applied and basic research focused on the pathophysiology of MPNSTs, including tissue evaluation, genetic analyses, and the development of animal models. Translational research would include the use of the mouse model for MPNST to develop more effective treatment modalities for MPNST in NF1 patients.

Design:

1. Identify those individuals with NF1 who are at highest risk to develop MPNST.

The prevalence of MPNST among NF1 has been estimated to be 2-to-5% from cross-sectional studies, but recent investigations indicate the lifetime risk is closer to 10%. In addition, there may be subgroups in the NF1 population who are at substantially higher risk, and those not in the high-risk population may have a substantially lower risk. A prospective case-control study is proposed to identify factors that are associated with high risk for MPNST in NF1 patients.

A case-control approach will be used to compare NF1 patients who have confirmed MPSNT to NF1 patients without MPNST. Possible differentiating features that will be evaluated include burden, type and location of plexiform neurofibromas, constitutional large-deletion genotype, family history of sarcoma, therapeutic radiation, and NF1-related neuropathy. NF1-related MPNST cases between 18 and 35 would be recruited for detailed medical and family histories, physical examination, whole-body imaging, and *NF1* mutation analysis to detect large deletion (~10% of NF1 patients). Controls with NF1 but without MPNST would be matched for age and gender. A study that includes 100 cases and 300 controls would have a power of 0.84 to demonstrate a 3-fold increase in the frequency of a factor that occurs in 5% of the controls.

2. Implement screening protocols for early detection of MPNST in individuals with NF1.

At present, histologic evaluation of the entire tumor is the only reliable means of distinguishing MPNSTs from the more common, benign plexiform neurofibromas in individuals with NF1. As with most sarcomas, complete surgical excision predicts better outcome, and this is optimized by early detection. Magnetic resonance imaging locates the site and extent of the lesion, but it does not reliably detect malignancy. Biopsy may miss the site of malignancy or fail to identify the highest grade of malignancy in a heterogenoeous lesion. Recent advances in imaging technology

provide opportunities to evaluate the role of 18Fluorodeoxyglucose positron emission tomography in the diagnosis of MPNSTs. We propose a 5-year, collaborative, prospective study to determine whether ^{18}FDG PET can reliably diagnose MPNST in NF1 patients who have symptoms associated with peripheral nerve sheath tumors..

NF1 patients aged 6-75 years who have a plexiform neurofibroma and 1 or a combination of manifestations (persistent pain lasting more than 1 month, change in texture from soft to hard, rapid increase in size, neurological deficit) will be eligible to enroll in the study. The site and extent of each PNST will be documented by clinical evaluation and MRI scanning. All participants will undergo ^{18}FDG PET. Patients with positive ^{18}FDG PET will undergo tru-cut/open targeted biopsy with MRI and PET registration. The tumor will be excised and the grade will be confirmed on histology. The patient will receive further treatment and follow-up based on the grade of the tumor and clinical need. Individuals with negative ^{18}FDG PET will have tru-cut/open biopsy of the plexiform neurofibroma. If the biopsy is negative for malignancy they will be followed clinically every 6 months for 5 years. Our second goal is to determine whether PET is able to detect asymptomatic second primary tumors in individuals with MPNST and NF1. All participants will undergo ^{11}C-methionine PET in addition to ^{18}FDG PET in centers that have on-site chemistry facilities. Methionine has been useful in detecting low-grade tumors in the central nervous system and may allow a rapid test (within 30 minutes post-injection) to evaluate MPNST formation in plexiform neurofibromas.

3. Evaluate tumor tissue for molecular changes important in malignant transformation of PNSTs.

The factors most important in transforming benign PNST to MPNST have not been identified. In general, both alleles of the *NF1* gene are inactivated in proliferating Schwann cells in benign peripheral nerve sheath tumors. Other molecular changes must occur to transition from the benign to malignant state. A group of studies to evaluate MPNST specimens is proposed.

Immunohistochemical markers and biochemical studies would be performed on all MPNST tissue that has been surgically removed. Peripheral blood lymphocytes, serum, paraffin blocks, fresh frozen tissue, and live cells from the tumor would also be processed for study. These tissue specimens would be stored and distributed through a tissue repository for NF1-related tumors that has already been established at Washington University in St. Louis. This facility would serve as a repository for all biopsy samples and any tumors excised in protocols outlined in objectives 2 and 4.

Specific aims to be addressed focus on the following; determination of molecular markers that distinguish benign versus malignant PNSTs, identification of specific genes that are differentially expressed in MPNSTs, identification of specific genetic changes in MPNSTs that may be associated with clinical outcomes, identification of molecular changes that distinguish MPNST from other spindle cell sarcomas, and determination of molecular markers that distinguish NF1-related MPNSTs from sporadic MPNSTs. The Tissue Core will be comprised of multiple laboratories devoted to the immunohistochemical and molecular analysis of MPNSTs in addition to the pathology lab that will process and store specimens by standard protocols.

4. Assess neo-adjuvant chemotherapy in the treatment of stage III/IV MPNSTs.

Present approaches to treatment of MPNST are not effective, and 5-year survival is currently 40% or less. Among all protocols, surgical excision is the mainstay of therapy. Adjuvant chemotherapies have not been rigorously applied in a coordinated effort. Taking cues from the benefit that has been demonstrated for neo-adjuvant therapy in patients with Ewings sarcoma, we

propose to undertake similar trials for stage III & IV MPNSTs. This study will include MPNST patients who have NF1 as well as those who do not have NF1, because we do not know if the response will differ between these groups.

Patients 18 years or older with high-grade MPNST that is greater than 5 cm in diameter and staged as III or IV will be eligible for this multicenter study. Subjects will be stratified for the presence or absence of NF1. Patients will be treated with 2 cycles of neo-adjuvant chemotherapy (ifosfamide and adriamycin) prior to surgical resection. The primary objective of this trial is to determine the response rate of the tumor based on volumetric imaging studies, dynamic MR, PET scanning, and histology. Responding patients would be continued on therapy, whereas non-responders would proceed to surgical resection with post-operative radiation. Secondary objectives include the identification of molecular differences that correlate with responsive tumors versus non-responsive tumors, and determination of EFS and OS with this regimen.

A diagram outlining the 4 proposed studies is attached. There are 2 cores; an administrative core with clinical coordinators and statistical and database support, and a tissue core for multiple biologic studies. We envision regional academic institutions that can combine successful sarcoma services with NF1 Clinics as regional centers that will carry out the main work effort outlined in the 4 studies. Interaction between each center to rigorously obtain clinical information and perform standard protocols is imperative to the success of the Program. It is likely that subjects would travel to the regional center for initial evaluations and tumor surgery.

The topic of animal models was not discussed in detail at the MPNST Symposium, although presentations from the NNFF International Consortium for the Molecular Biology of NF1 and NF2 (Aspen, June 9-12) clearly demonstrated the development of a model for MPNST in mice. These tumors are highly reproducible, and it could potentially provide a way to screen novel therapies for the treatment and/or prevention of MPNSTs. Correlation between human and murine MPNST is required. Importantly, a rational basis for the selection of candidate therapeutic agents is imperative to optimally screen mice for "breakthrough" therapies, before initiating human protocols. We anticipate linking the NF1-Sarcoma Program described herein with a mouse core(s) in the development and implementation of future protocols.

Chairs

Jan Friedman
David Gutmann
Lee Helman
Rosalie Ferner
David Viskochil

Participants (see attached list)

Michael O'Doherty
Michael Smith
Abhijit Guha
Arie Perry
Cheryl Coffin
Jonathan Lucas
Karen Albritton
Harry Joe
Minesh Mehta
George Demetri
Ian Judson
Bruce Korf
Judy Small
Gareth Evans
Victor Mautner

Acknowlegment: National Neurofibromatosis Foundation, Inc., Peter Bellermann
University of Utah, Kathy Moran

Am. J. Hum. Genet. 70:38–50, 2002

C→U Editing of Neurofibromatosis 1 mRNA Occurs in Tumors That Express Both the Type II Transcript and apobec-1, the Catalytic Subunit of the Apolipoprotein B mRNA–Editing Enzyme

Debnath Mukhopadhyay,[1] Shrikant Anant,[1] Robert M. Lee,[1] Susan Kennedy,[1] David Viskochil,[3] and Nicholas O. Davidson[1,2]

Departments of [1]Medicine and [2]Pharmacology and Molecular Biology, Washington University Medical School, St. Louis; and [3]Department of Pediatrics, Division of Medical Genetics, University of Utah Health Science Center, Salt Lake City

C→U RNA editing of neurofibromatosis 1 (NF1) mRNA changes an arginine (CGA) to a UGA translational stop codon, predicted to result in translational termination of the edited mRNA. Previous studies demonstrated varying degrees of C→U RNA editing in peripheral nerve–sheath tumor samples (PNSTs) from patients with NF1, but the basis for this heterogeneity was unexplained. In addition, the role, if any, of apobec-1, the catalytic deaminase that mediates C→U editing of mammalian apolipoprotein B (apoB) RNA, was unresolved. We have examined these questions in PNSTs from patients with NF1 and demonstrate that a subset (8/34) manifest C→U editing of RNA. Two distinguishing characteristics were found in the PNSTs that demonstrated editing of NF1 RNA. First, these tumors express apobec-1 mRNA, the first demonstration, in humans, of its expression beyond the luminal gastrointestinal tract. Second, PNSTs with C→U editing of RNA manifest increased proportions of an alternatively spliced exon, 23A, downstream of the edited base. C→U editing of RNA in these PNSTs was observed preferentially in transcripts containing exon 23A. These findings were complemented by in vitro studies using synthetic RNA templates incubated in the presence of recombinant apobec-1, which again confirmed preferential editing of transcripts containing exon 23A. Finally, adenovirus-mediated transfection of HepG2 cells revealed induction of editing of apoB RNA, along with preferential editing of NF1 transcripts containing exon 23A. Taken together, the data support the hypothesis that C→U RNA editing of the NF1 transcript occurs both in a subset of PNSTs and in an alternatively spliced form containing a downstream exon, presumably an optimal configuration for enzymatic deamination by apobec-1.

Introduction

Neurofibromatosis type 1 (NF1 [MIM 162200]) is a dominantly inherited disease affecting ~1/3,500 individuals worldwide. The *NF1* gene has been mapped and characterized extensively, and several features of interest have emerged in relation to its altered function in disease. The *NF1* gene spans ~350 kb on chromosome 17q11.2 and encodes 60 exons, which are ubiquitously transcribed (Li et al. 1995). The nuclear NF1 transcript is ~11 kb and encodes neurofibromin, a tumor-suppressor–gene product of 2,818 residues, which contains a region of ~366 amino acids that functions as a GTPase-activating protein (GAP) (reviewed in Cichowski and Jacks 2001). GAP activity has been demonstrated for neurofibromin—more specifically, in the context of Ras activation, both in vitro and in vivo—and is postulated to be an important feature of the loss of function accompanying mutations in the *NF1* gene (Basu et al. 1992; DeClue et al. 1992; Nakafuku et al. 1993; Bollag et al. 1996; Guha et al. 1996; Lau et al. 2000; Sherman et al. 2000).

Although the disorder becomes fully penetrant at a relatively early age, the clinical features of NF1 are quite variable even between affected siblings. In addition, as many as half of the newly diagnosed cases of NF1 represent new mutations, a feature likely accounted for by the high spontaneous-mutation rate at this locus (Andersen et al. 1993; Ars et al. 2000). Taken together, the range of mutations and the phenotypic variability suggest that modifier genes may play a significant role in the natural history of this disease (Skuse and Ludlow 1995). An important consideration in understanding the potential mechanisms for exerting phenotypic variability in this disease is the role of RNA processing of transcripts arising from somatic and germline mutations in the *NF1* gene; for example, alterations in mRNA splicing have been demonstrated to occur in ~50% of pa-

Received August 23, 2001; accepted for publication October 5, 2001; electronically published November 27, 2001.

Address for correspondence and reprints: Dr. Nicholas O. Davidson, Box 8124, Gastroenterology Division, Washington University School of Medicine, 660 South Euclid Avenue, St. Louis, MO 63110. E-mail: NOD@IM.WUSTL.EDU

0002-9297/2002/7001-0006$15.00

tients with NF1 (Park and Pivnick 1998), suggesting an important mechanism for amplifying the phenotypic variability alluded to above.

Another posttranscriptional mechanism, C→U editing of RNA, was postulated for inactivation of the GAP function of NF1 some years ago, by Skuse and colleagues (Skuse et al. 1996; Skuse and Cappione 1997). These investigators identified a C→U change, occurring at nt 3916 in the NF1 transcript, that changes a genomically templated arginine (CGA) to a UGA stop codon in the edited mRNA (Skuse et al. 1996; Skuse and Cappione 1997). The edited transcript encodes a truncated protein product that terminates in the amino-terminal portion of the GAP-related domain and would thus result in functional inactivation of the tumor-suppressor function of neurofibromin (Skuse et al. 1996; Ashkenas 1997; Cappione et al. 1997; Skuse and Cappione 1997). Nevertheless, certain features of these original findings were unexplained. The level of C→U editing of NF1 RNA, for example, was quite variable (4%–17%) among the tumors examined, with a trend suggesting that the more malignant tumors demonstrated higher levels of editing (Skuse et al. 1996; Skuse and Cappione 1997). In addition, the enzymatic factors mediating this C→U change were not identified, and the relationship, if any, to editing of intestinal apolipoprotein B (apoB) (*APOB* [MIM 107730]) mRNA, the prototype example of C→U deamination of nuclear RNA, was not resolved. In particular, C→U editing of mammalian intestinal apoB RNA demonstrates absolute dependence on the expression of the catalytic deaminase, apobec-1 (*APOBEC-1* [MIM 600130]) (Hirano et al. 1996; Morrison et al. 1996), whereas preliminary studies by Skuse et al. (1996) revealed no clear evidence that apobec-1 plays a role in the editing of NF1 RNA.

We have reexamined these questions through analysis of peripheral nerve–sheath tumor samples (PNSTs) from 34 patients with NF1. The majority, 26 of 34, of tumors demonstrated low levels of C→U RNA editing, in the range of 0%–2.5%, with 10 of these 26 demonstrating <1% editing, the limits of reliable detection of the assay. However, the remaining 8 of the 34 tumors demonstrated 3%–12% C→U editing of NF1 RNA, which was reproducible and validated by sequencing of the cDNA products. These tumors demonstrated two distinguishing characteristics. First, these PNSTs express apobec-1 mRNA, the catalytic deaminase of the holoenzyme that edits apoB RNA (Teng et al. 1993; Lau et al. 1994; Yamanaka et al. 1994; Davidson and Shelness 2000), suggesting an important role for apobec-1 in the context of a target beyond apoB RNA. Second, NF1 RNA from these PNSTs contains increased proportions of an alternatively spliced exon, 23A, downstream of the edited base in which editing occurs preferentially. These findings, together with results of both in vivo and in vitro experiments with apobec-1, strongly suggest an important mechanistic linkage between NF1 RNA splicing and C→U editing and provide a basis for understanding the heterogeneity of posttranscriptional regulation of *NF1* expression.

Material and Methods

Tissue Procurement

The use of human tumor and normal adjacent tissue in this investigation was reviewed and approved by the institutional review boards of the University of Chicago Hospitals, the University of Utah Hospital, Massachusetts General Hospital, Harvard University Hospital, and Washington University School of Medicine. Samples of PNSTs were collected from a total of 34 patients with NF1, whose clinical diagnosis was based on National Institutes of Health consensus-conference criteria (National Institutes of Health Consensus Development Conference 1988). No attempt was made to identify familial versus sporadic cases. In addition, paired normal and tumor samples were obtained from 11 patients (without NF1) undergoing surgical resection for colon adenocarcinoma. The majority of these samples were moderately differentiated tumors located in the proximal, mid, or descending colon. Each was snap-frozen in liquid nitrogen and was stored at −80°C until processed. Frozen tissue sections were stained with hematoxylin and eosin to confirm the histological composition of these specimens.

Endogenous Editing of NF1 mRNA

Total RNA and genomic DNA from the NF1 and colon-cancer tissues was isolated by TRIzol reagent (LifeTechnologies). First-strand cDNA was synthesizedby Superscript II reverse transcriptase (RT) (LifeTechnologies) primed with random hexamers. PCR was performed with *Pyrococcus woesei* DNA polymerase (Roche Molecular Biochemicals), to amplify NF1 cDNA flanking the edited base (fig. 1), by primers SA61 (5′- CAAGGAGAACTCCCTATAGCG-ATG-3′; 5′ at nt 3650) and SA64 (5′-CTGTTCTGAGG-GAAACGCTGG-3′; 5′ located at nt 4201). An aliquot of each PCR was analyzed by agarose-gel electrophoresis to monitor yield and the integrity of the product. Typical yield was 0.4–0.5 μg/50 μl PCR. To selectively amplify NF1 mRNA containing exon 23A, primer RML33 (5′-TGTAGCTTTATTCAGTAGGGAGTGG-CAAG-3′; 5′ located at nt 4142) was substituted for SA64, in the PCR (fig. 1). To determine the proportions of NF1 mRNA containing exon 23 A, 10 μCi α[^{32}P]-dCTP (3,000 Ci/mmol) was included in the reaction, and the products were analyzed by 8% native PAGE and were quantitated by phosphorimaging (Molecular Dynamics). Genomic DNA corresponding to exon 22

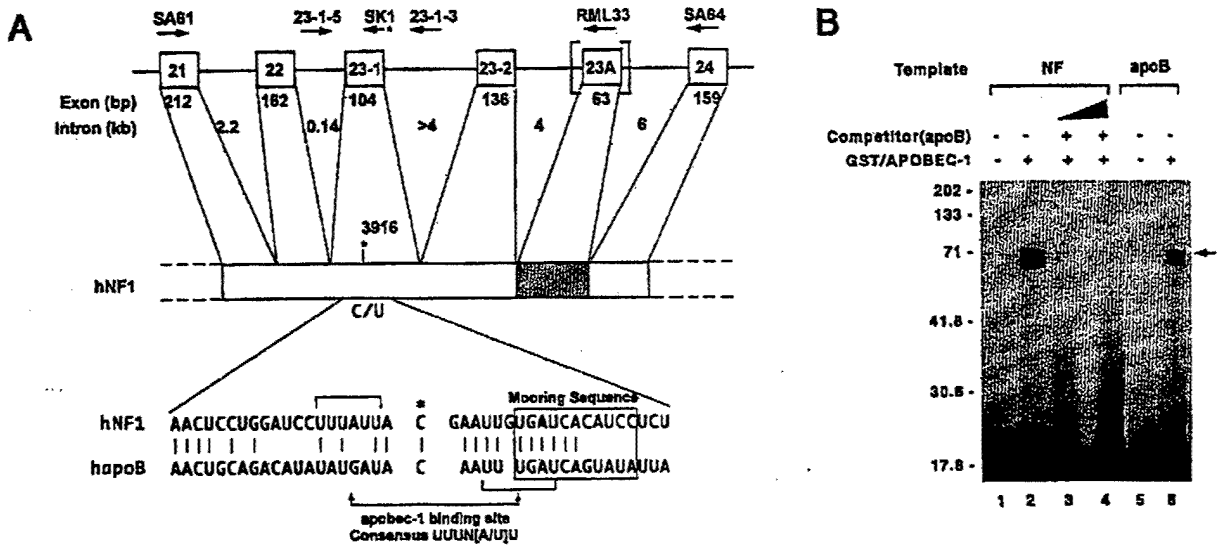

Figure 1 *A*, Organization of *NF1*. *Top*, Exons 21–24 of *NF1*, along with exon and intron sizes. The alternatively spliced exon 23A is within the vertical brackets, and the corresponding region in NF1 mRNA is shaded. Identities, orientations, and locations of the various primers are indicated above the exon and intron designations. *Bottom*, Alignment of 41-nt region (nt 3896–3936) of NF1 mRNA surrounding the edited base, compared to human apoB mRNA (hapoB). The edited C in both sequences is indicated by an asterisk (*), and sequence identity is indicated by vertical lines. The apobec-1 binding site and mooring sequence are indicated by horizontal brackets and a box, respectively. *B*, apobec-1, a NF1 RNA–binding protein. UV cross-linking was performed by incubating 250 ng GST/APOBEC-1 with either a 550-nt [^{32}P]-labeled NF1 RNA (NF [lanes 1–4]) containing exon 23A (nt 3650–4201) or a 105-nt [^{32}P]-labeled apoB RNA (apoB [lanes 5 and 6]), flanking the edited base. After treatment with RNaseT1 and UV irradiation, the cross-linked products were analyzed by 10% SDS-PAGE. For competition analysis, 50- (lane 3) and 100-fold (lane 4) excess of cold apoB RNA was added to the reaction. The results shown are representative of three such experiments. Molecular-weight markers are indicated to the left of the gel, and the location of the cross-linked GST/APOBEC-1 band is indicated by the arrow to the right of the gel.

was amplified by primers 23-1-5 (5′-AAAAACACGGTTCTATGTGAAAAG-3′, located in intron 22) and 23-1-3 (5′-TTTGTATCATTCATTTTGTGTGTA-3′, located in intron 23-1), located in the adjacent introns (fig. 1). Primer-extension analysis was employed to determine the extent of editing of NF1 RNA at nt 3916, by primer SK1 (5′- CATGTTGCCAATCAGAGGATGTG-3′, located at nt 3949) (Skuse et al. 1996), which is complementary to a 23-nt region 12 nt downstream of the edited base. The primer SK1 is that used by Skuse et al. (1996). [^{32}P]-labeled SK1 primer was annealed to 10 ng NF1 cDNA flanking the edited base. Primer extension was conducted in the presence of 0.05 μM each of dATP, dCTP, and TTP and 1.6 μM ddGTP, in the presence of T7 DNA polymerase. In this assay, the radiolabeled primer extends to the first upstream C (at nt 3916) and undergoes chain termination, giving an extension product of 34 nt. If the C at nt 3916 is edited to T, the products extend to the next upstream C, at nt 3908, giving an extension product of 42 nt. The primer-extension products were resolved by PAGE with 10% acrylamide containing 8 M urea, followed by phosphorimaging. We have validated and characterized this assay extensively in the context of editing of apoB RNA (Giannoni et al. 1994; Anant et al. 1998; Madsen et al. 1999). Standardization of the assay was undertaken by use of mixtures of NF1 cDNA containing known quantities of C3916 and T3916 products from sequence-validated templates constructed from previously amplified NF1 cDNA (550 bp), in which a T at nt 3916 was introduced by mutagenesis. Known quantities of PCR product were used to establish the optimal conditions for primer extension. This established that the reliable limits of detection with 10 ng template correspond to 1% U (data not shown). Levels of apparent editing <1% were considered background "primer read through." All assays included a C standard and a T standard, for reference.

In Vitro RNA-Editing Assay

Synthetic templates were prepared to yield transcripts that either included (550 nt) or did not include (487 nt) exon 23A and that contained a C at nt 3916. A 20-fmol sample of each RNA was individually incubated in a buffer containing 20 mM HEPES. HCl pH 7.8, and 100 mM KCl, at 30°C for 4 h, in the presence of 250 ng glutathione-S-transferase (GST)/apobec-1 and 50 μg of

a 30% ammonium sulfate precipitate of bovine liver S-100 extracts (MacGinnitie et al. 1995). The RNA was extracted, subjected to primer extension with [^{32}P]-labeled SK1 primer (see above), and subsequently analyzed, under denaturing conditions, by PAGE with 8% polyacrylamide gel containing 8 M urea. Editing of RNA was quantitated by phosphorimager analysis (Molecular Dynamics).

Protein-Truncation Assay

NF1 cDNA encoding exons 21–24 was amplified by RT-PCR, as described above, with primers NF-PPT-5′ (5′-GGGTGTAATACGACTCACTATAGGCCACC*ATGG-AGCAGAAACTCATCTCTGAA*CAAGGAGAACTCC-CTATAGCGATGGCTC-3′; T7 promoter is underlined, and myc-tag is boldface italic) and SA64. NF-PTT-5′ was designed to contain an upstream T7 promoter and a myc epitope tag, in frame with the NF1 cDNA. These primers were designed so that the region amplified contained the same numbers of methionine residues in the translation products from transcripts either with or without exon 23A. The full-length product (~22 kD) contains six methionine residues, whereas the truncated protein (~11 kD) contains five. The RT-PCR products were subjected to coupled transcription-translation (Promega) with rabbit reticulocyte lysates in the presence of translation-grade [^{35}S]-methionine (Amersham-Pharmacia), according to the manufacturer's recommendations. The translation reaction was subsequently immunoprecipitated with anti-myc monoclonal antibody 9E-10 (Santa Cruz Biotechnology) and was analyzed by gradient 10%–20% SDS-PAGE and autoradiography.

Detection of apobec-1 and apobec-1 Complementation Factor (ACF) mRNA

RT-PCR was conducted by use of primers, listed below, for apobec-1 and ACF. First-strand cDNA synthesis was undertaken as described above, using random-hexamer priming; cDNA amplification used gene-specific primers located in the 5′ and 3′ regions of the coding

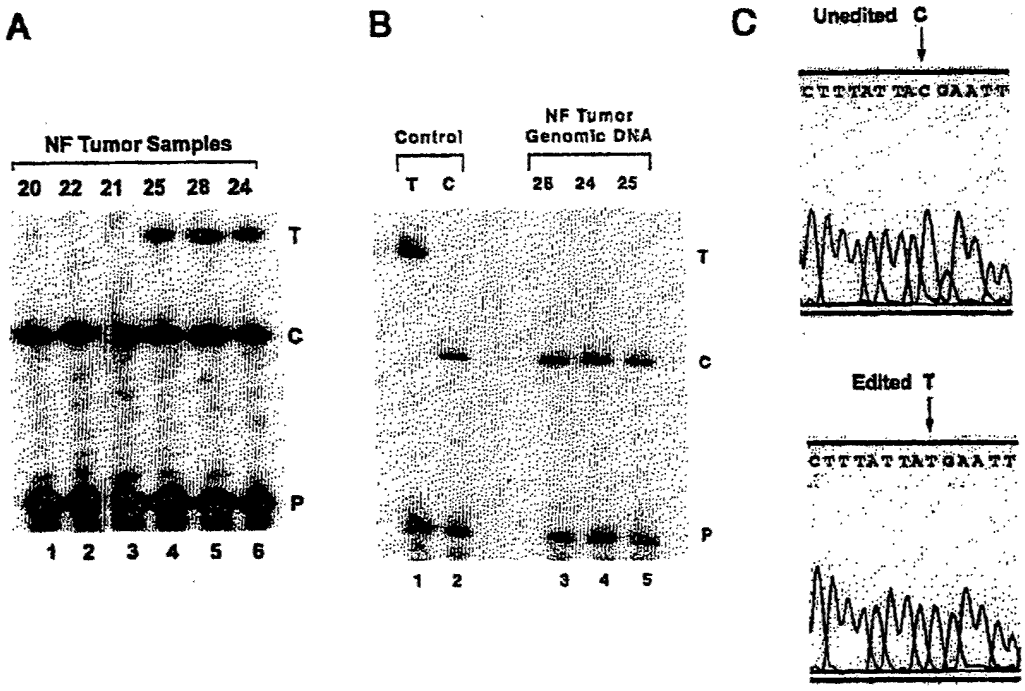

Figure 2 NF1 mRNA undergoing C→U editing in a subset of neurofibromatosis-related PNSTs. *A*, Total RNA extracted from neurofibromatosis tumor tissue—and extent of editing of NF1 mRNA, as determined by primer-extension assay as described in the "Material and Methods" section. The primer-extension products were separated on a gel of 10% polyacrylamide containing urea and were autoradiographed. A representation of experiments performed in triplicate for 34 neurofibromatosis tumor samples is shown. The locations of the primer (P) and of unedited (C) and edited (T) primer-extension products are indicated to the right of the gel. *B*, C→U editing, which is shown not to be a somatic mutation. Genomic DNA flanking exon 23-1 was amplified by PCR using intron-specific primers and subsequently was subjected to primer-extension analysis. As controls, PCR products containing either C or T at nt 3916 of NF1 cDNA were also analyzed. The locations of the primer (P) and of unedited (C) and edited (T) primer-extension products are indicated to the right of the gel. C, Editing at nt 3916 of NF1 RNA, confirmed by sequencing of individual cDNA clones. The locations of the unedited (*Unedited C; top*) and edited (*Edited T; bottom*) nucleotide in a representative clone are indicated by arrows above the gels.

Table 1

C→U Editing of NF1 RNA in PNSTs

Category and Sample	Histology	Editing (%)			Expression	
		Mean	SD	Range ($n = 3$)	apobec-1	ACF
No editing (<1% U):						
NF20	Plexiform	.64	.34	.3–1.0	−	+
NF22	Triton tumor	.65	.35	.3–.9	−	+
NF6	Neurofibroma	.66	.43	.2–1.1	−	+
NF35	Glioblastoma	.68	.22	.45–.9	−	+
NF21	Malignant schwannoma	.69	.65	.2–1.3	−	+
NF3	Neurofibroma	.72	.65	.1–1.4	−	+
NF4	Neurofibroma	.72	.68	.1–1.5	−	+
NF2	Neurofibroma	.86	.65	.75–1.1	−	+
NF18	Malignant schwannoma	.95	.65	.9–1.3	−	+
NF5	Neurofibroma	.99	.56	.95–1.7	−	+
NF7	Malignant schwannoma	1.01	.46	.9–1.5	−	+
NF17	Neurofibroma	1.08	.24	.85–1.5	−	+
NF13	Neurofibroma	1.14	.65	.75–1.8	−	+
NF8	Malignant schwannoma	1.15	.75	.65–1.9	−	+
NF16	Neurofibroma	1.15	.49	.55–1.7	−	+
NF9	Neurofibroma	1.24	.43	.8–1.7	−	+
NF27	Malignant schwannoma	1.35	.36	.9–1.7	−	+
NF23	Neurofibroma	1.37	.54	.75–1.9	−	+
Low editing (<2.5% U):						
NF14	White matter	1.48	.39	1.0–1.9	−	+
NF34	Glioblastoma	1.52	.43	1.1–1.95	−	+
NF11	Neurofibroma	1.57	.54	1.0–2.1	−	+
NF1	Neurofibroma	1.58	.58	1.0–2.2	−	+
NF30	Ganglioneuroma	1.83	.16	1.65–2.1	−	+
NF15	Peripheral nerve	1.85	.86	1.1–2.5	−	+
NF31	Schwannoma	1.99	.38	1.5–2.5	−	+
NF19	Neurofibroma	2.36	1.03	1.33–3.4	−	+
NF10	Neurofibroma	3.16	.98	2.2–4.1	+	+
NF33	Glioblastoma	3.18	.68	2.6–3.9	+	+
NF26	Nonmalignant schwannoma	3.48	.62	2.8–4.2	+	+
NF32	Neurofibroma	5.06	.89	4.1–5.9	+	+
Bona-fide editing (>3% U):						
NF29	Granulomatous cell	5.52	1.08	4.3–6.7	+	+
NF25	Malignant schwannoma	10.35	2.53	8.1–12.5	+	+
NF24	Malignant schwannoma	12.02	3.12	8.9–15.3	+	+
NF28	Ganglioneuroblastoma	12.65	1.65	10.5–14.8	+	+

sequence. PCR cycling conditions for apobec-1 and ACF were 95°C for 3 min, 1 cycle; 95°C for 30 s, 55°C for 1 min, and 72°C for 1 min, 30 cycles; and 72°C for 10 min. As a control, glyceraldehyde-3-phosphate dehydrogenase (GAPDH) mRNA was simultaneously amplified by the indicated primers. The amplified products were sequenced on both strands to confirm their identity. Primers used are as follows: for GAPDH, primers 5′-TCGGAGTCAACGGATTTGGTCG-3′ and GAP 5′-AGGCAGGGATGATGTTCTGGAGAG-3′; for apobec-1, primers SA146 5′-GACGACGACAAGGGATCCATGAGTTCCGAGACAGGC-3′ and SA147 5′-GGAACAAGACCCGTCGACTCATTTCAACCCTGTGGCCCACAG-3′; and, for ACF, primers ACF2 5′-CTCGAGTCAGAAGGTGCCATATCCATC-3′ and ACF6 5′-CAGATATTAGAAGAGATTTGTC-3′. The primer pairs for apobec-1 generate a full-length cDNA, whereas the primers for ACF generate an amplicon of 447 bp. Where indicated in the text, nested PCR was undertaken for apobec-1, by use of the primers listed below, which yield a product of 273 bp (nt 116–388). Primers used for nested PCR were as follows: JM-8 5′-ACCCCAGAGAACTTCGTAAAGAGGCC-3′ and JM-9 5′-CCGAGCTACGTAGATCACTAGAGTCA-3′.

UV Cross-Linking of NF1 and apoB RNAs to apobec-1

NF1 cDNA flanking the edited base (fig. 1) was amplified by primers SA61 and SA64, subcloned into plasmid pGEM-3zf(+) (Promega) and was sequenced to confirm the presence of wild-type sequence. The plasmid was linearized with restriction endonuclease *Kpn*I and was sub-

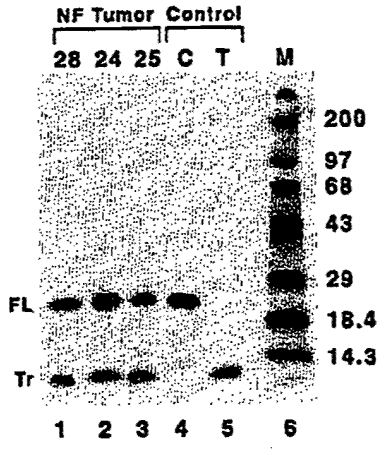

Figure 3 Protein-truncation assay. NF1 cDNA flanking the edited base was amplified by primers NF-PTT-5′ and SA64, as described in the "Material and Methods" section. The RT-PCR products were subjected to in vitro coupled transcription/translation in the presence of [^{35}S] methionine. The translation products were immunoprecipitated with α-myc-tag antibody and were resolved by 10%–20% SDS-PAGE. The locations of the full-length (FL) and truncated (Tr) translation products, which correspond to the unedited and edited NF1 mRNA, respectively, are indicated to the left of the gel. Control reactions were undertaken by use of a synthetic, sequence-validated template containing either C or T at nt 3916. The results shown are representative of three such experiments.

jected to in vitro transcription with SP6 RNA polymerase, in the presence of α[^{32}P]-CTP (3,000 Ci/mmol). The [^{32}P]-labeled NF1 RNA (50,000 cpm, at 4 × 10^8 cpm/μg) was incubated with 25 ng recombinant GST/APOBEC-1 (MacGinnitie et al. 1995) for 15 min at room temperature, in a buffer containing 10 mM HEPES pH 8.0, 100 mM KCl, 1 mM EDTA, 0.25 mM DTT, and 2.5% glycerol. The reaction was then sequentially treated with RNase T1 (final concentration, 1 unit/μl) and heparin (final concentration, 5 mg/ml), followed by UV irradiation (250 mJ/cm^2) in a Stratalinker (Stratagene). As control, RNA binding was performed with a 105-nt rat apoB RNA that previously had been demonstrated to bind apobec-1 (Anant et al. 1995; Nakamuta et al. 1995; Anant and Davidson 2000). Competition analysis was performed with radiolabeled NF1 RNA and 5- and 10-fold excess of cold apoB RNA, as described in detail elsewhere (Anant et al. 1995).

Adenovirus-Mediated Infection of HepG2 Cells

Recombinant adenovirus expressing either rat apobec-1 or a control, lacZ cDNA, were cloned as described elsewhere (Kozarsky et al. 1996) and were titered to a multiplicity of infection (MOI) of 10^9–10^{10} pfu/ml. HepG2 cells were infected with 3 × 10^3–MOI recombinant adenovirus and cell lysates, and total RNA was prepared for analysis after 48 h. Primer-extension analysis was performed to quantitate C→U editing of endogenous NF1 and apoB RNA, as outlined above and as described in detail elsewhere (Giannoni et al. 1994). Cell lysates were analyzed by denaturing SDS-PAGE and western blotting, to demonstrate, as described elsewhere (Anant and Davidson 2000), the presence of apobec-1, by rabbit anti–apobec-1 IgG.

Results

NF1 RNA Sequence Alignment Flanking the Edited Base at nt 3916

The *cis*-acting elements regulating C→U editing of apoB RNA have been extensively characterized and include an AU-rich bulk-RNA context, a mooring sequence 3′ of the edited base, and efficiency elements both upstream and downstream (Shah et al. 1991; Backus and Smith 1992; Driscoll et al. 1993; Backus et al. 1994; Anant et al. 1995; Hersberger and Innerarity 1998; Anant and Davidson 2000). Alignment of an ~40-nt stretch of NF1 RNA sequence flanking nt 3916 reveals ~50% identity with apoB RNA, as has been noted elsewhere (Skuse et al. 1996), including 6 of 11 matches in the region corresponding to the mooring sequence (fig. 1). More recently, a consensus apobec-1 binding motif, UUUN[A/U]U, has been identified in both apoB RNA and other validated targets of high-affinity binding by apobec-1 (Anant and Davidson 2000). Further inspection of the NF1 RNA sequence flanking the edited base reveals this consensus apobec-1 binding site immediately upstream of the targeted cytidine (fig. 1). Therefore, we examined directly the ability of recombinant apobec-1

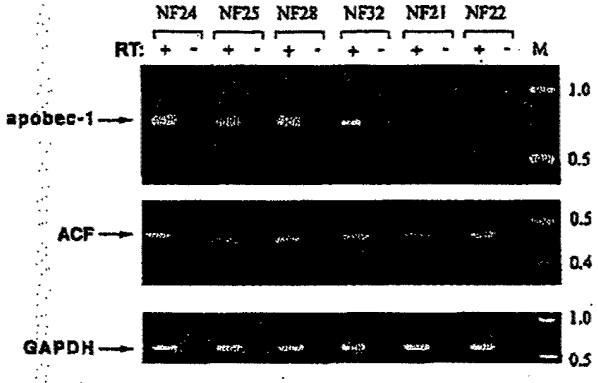

Figure 4 apobec-1 mRNA, expressed in a subset of neurofibromatosis tumors. RT-PCR by gene-specific primers ("+" lanes) was performed to amplify apobec-1, ACF, and GAPDH (*top*, *middle*, and *bottom*, respectively). As a control, PCR without prior RT ("−" lanes) was performed. The locations of molecular-weight standards are indicated to the right of the gel.

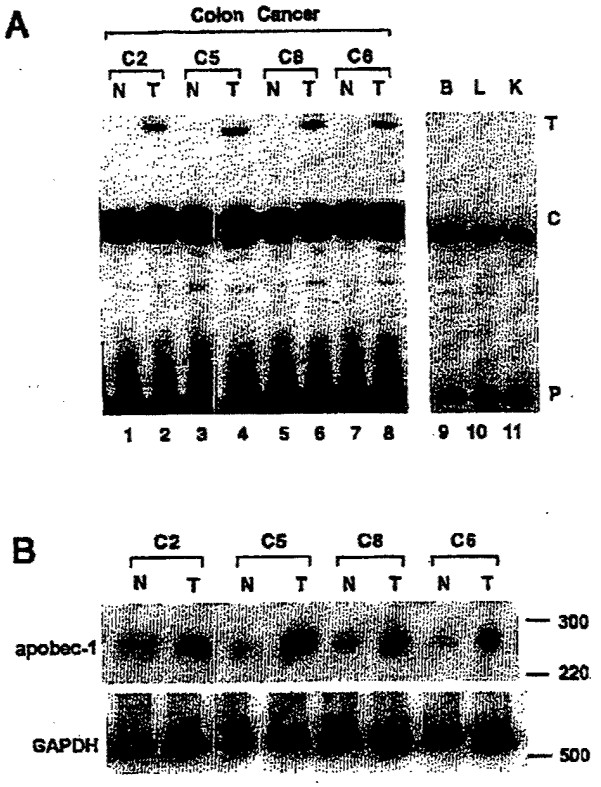

Figure 5 Editing of NF1 mRNA in colon cancers. *A*, Endogenous editing of NF1 RNA, as determined by primer-extension analysis and described in figure 2*A*. The data demonstrate increased editing in colon tumor tissue (lanes T), compared to matched normal control tissue (lanes N). In addition, no editing (<1% U) was observed in NF1 mRNA from normal brain (lane B), liver (lane L), or kidney (lane K). *B*, apobec-1 mRNA expression induced in colon cancers. RT-PCR was performed in the presence of $\alpha[^{32}P]$-dCTP, by use of primers specific for apobec-1 and GAPDH, to amplify a 274- and a 510-bp fragment, respectively. Increased expression of apobec-1 is observed in colon tumor tissue (lanes T), compared to paired normal tissue (lanes N). The locations of the molecular-weight (in bp) markers are indicated to the right of the gel.

to bind synthetic NF1 RNA template, using UV cross-linking. The data demonstrate that apobec-1 binds NF1 RNA (fig. 1*B*) and that this binding is competed by apoB RNA (fig. 1*B*, lanes 3 and 4).

C→U Editing of RNA of NF1 Samples

RNA from 34 PNSTs was subjected to primer-extension assay, to detect C→U editing of NF1 RNA, and the reaction products were analyzed by urea PAGE and phosphorimaging. A representative series of samples is shown in figure 2*A*. Several of the samples (24, 25, and 28; see fig. 2*A*) demonstrated 12%–16% C→U editing of RNA, similar to the values and range noted by Skuse and colleagues (Skuse et al. 1996; Cappione et al. 1997). However, having established, by using synthetic RNA templates (data not shown), the limits of detection, we were able to exclude bona fide editing in samples in which there was less than ~1% U (samples 20–22; see fig. 2*A*). This technical point is also emphasized in the results of primer-extension analysis of genomic DNA from the most extensively edited tumors, in which there is no detectable T in either of the sample lanes or in the control C template (fig. 2*B*). Direct sequencing of the cDNA products confirmed the presence of a T in the edited cDNA, corresponding to nt 3916 (fig. 2C). The cumulative results for the 34 samples assayed are listed in table 1. The findings demonstrate that a subset (8/34) of tumors manifest C→U editing of RNA (defined as >3% U) and that the remainder (26/34) demonstrate either very low levels (1%–2.5% U [in the case of 16/34]) or undetectable (<1% U [in the case of 10/34]) editing activity. These findings suggest that C→U editing of NF1 RNA is not a universal finding in tumors but, rather, appears to be confined to a subset of samples.

C→U Editing of NF1 RNA: Detection by Protein-Truncation Assay

The products of the initial round of RT-PCR were amplified in-frame with a myc-tag and T7 promoter and were used to program a coupled in vitro transcription/translation reaction mixture. Both full-length and truncated products were recovered (fig. 3). The molar incorporation of $[^{35}S]$-methionine into immunoprecipitable protein products revealed the observed proportion of full-length to truncated protein products to be ~10:1, close to the value expected on the basis of C→U editing (i.e., ~10%–15%) of NF1 RNA in the respective sample of origin.

Tumors Demonstrating C→U Editing: Expression of apobec-1 mRNA

The expression of gene products associated with the machinery for editing of apoB RNA was investigated as a potential variable contributing to the heterogeneity observed in C→U editing of NF1 RNA. Two gene products in particular were examined. These correspond to apobec-1, the catalytic deaminase responsible for C→U editing of apoB, and ACF, the competence factor that supports site-specific deamination of apoB RNA by apobec-1 (Teng et al. 1993; Lellek et al. 2000; Mehta et al. 2000). apobec-1 mRNA was detectable in all eight tumors that manifest >3% C→U editing (fig. 4 and table 1). In all cases, the amplification products were sequenced, to confirm the identity of apobec-1 (data not shown). Tumor samples that demonstrated either no C→U editing (samples 21 and 22; see fig. 2*A*) or very low (i.e., ~1%–2%) levels did not yield a detectable product for apobec-1 mRNA (fig. 4 and table 1), even when nested PCR was used. More-

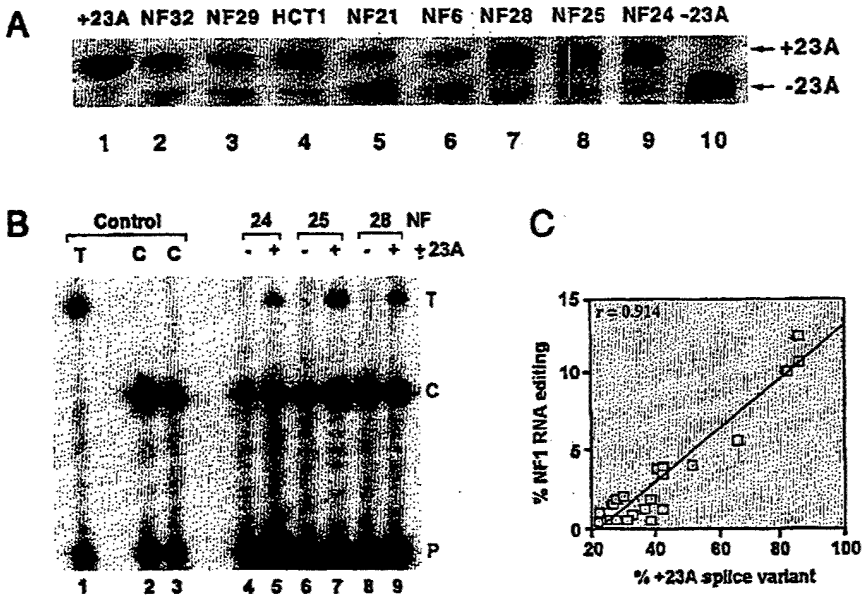

Figure 6 Preferential editing of NF1 mRNA containing exon 23A. *A*, Levels of alternative splicing of exon 23A in various tumor samples, as determined by RT-PCR and described in the "Material and Methods" section. As controls, PCRs were performed with synthetic RNA templates either containing (+23A) or lacking (−23A) exon 23A. The results shown are representative of experiments performed in triplicate, with all the tumor and normal samples. *B*, RT-PCR products of NF1 RNA containing (+23A) and lacking (−23A) the alternatively spliced exon, which were purified by electrophoresis and which subsequently were subjected to primer-extension analysis. As a control, primer-extension analysis was performed with cDNA templates containing only either a C or a T at nt 3916. The results shown are representative of three such experiments. *C*, Correlation between editing of NF1 RNA and inclusion of exon 23A (data are percent of total amount). This correlation was significant ($P < .001$).

over, normal tissue from sites in which apobec-1 is not detectable (e.g., liver, kidney, and brain) demonstrated <1% C→U editing of NF1 RNA (fig. 5). The observation that remains unexplained is the apparent lack of apobec-1 expression in tumors demonstrating very low (i.e., ~1%–2%) levels C→U editing (fig. 4 and table 1). We speculate that this finding may be due to the mixed cellular composition typically found in the PNSTs, in which editing of NF1 RNA occurs in a small subset of cells and in which apobec-1 mRNA is below detection limits. ACF mRNA, by contrast, was detected in all samples (fig. 4 and table 1), a finding consistent with previous reports that its expression is ubiquitous in humans (Lellek et al. 2000; Mehta et al. 2000). As an additional control, all RNA samples supported amplification of GAPDH mRNA (fig. 4).

Non-Neuronal Tumors Expressing apobec-1 and Demonstrating Editing of NF1 RNA

In humans, apobec-1 is normally confined to the luminal gastrointestinal tract (Teng et al. 1993; Yamanaka et al. 1994; Funahashi et al. 1995). Human colorectal cancers, however, have been demonstrated to express increased levels of apobec-1 mRNA, compared to normal adjacent mucosa (Lee et al. 1998). NF1 RNA was amplified from these tumors as well as from the adjacent normal tissue and was subjected to primer-extension assay. The results demonstrate higher levels of C→U editing of RNA in the tumor samples (4%–8% U), compared to paired normal tissue, and confirm the increase in apobec-1 mRNA abundance (1%–3% U) (figs. 5*A* and *B*). These findings suggest that C→U editing of NF1 RNA is not confined to tumors arising from Schwann-like cells but may be a feature of tumors that support apobec-1 expression; however, a more extensive survey of tumors of the gastrointestinal tract will be required, to allow us to formally examine the implications of editing of NF1 RNA, in relation to apobec-1–gene expression.

Editing of NF1 RNA: Occurrence in Transcripts Containing Exon 23A

To further pursue the mechanisms underlying the heterogeneity of C→U editing of NF1, transcripts were selectively amplified (by a strategy reviewed both in the "Material and Methods" section and in fig. 1), to examine alternative splicing of exon 23A, downstream of the edited base. As illustrated in figure 6*A*, these samples reveal a range of proportions of this alternatively spliced

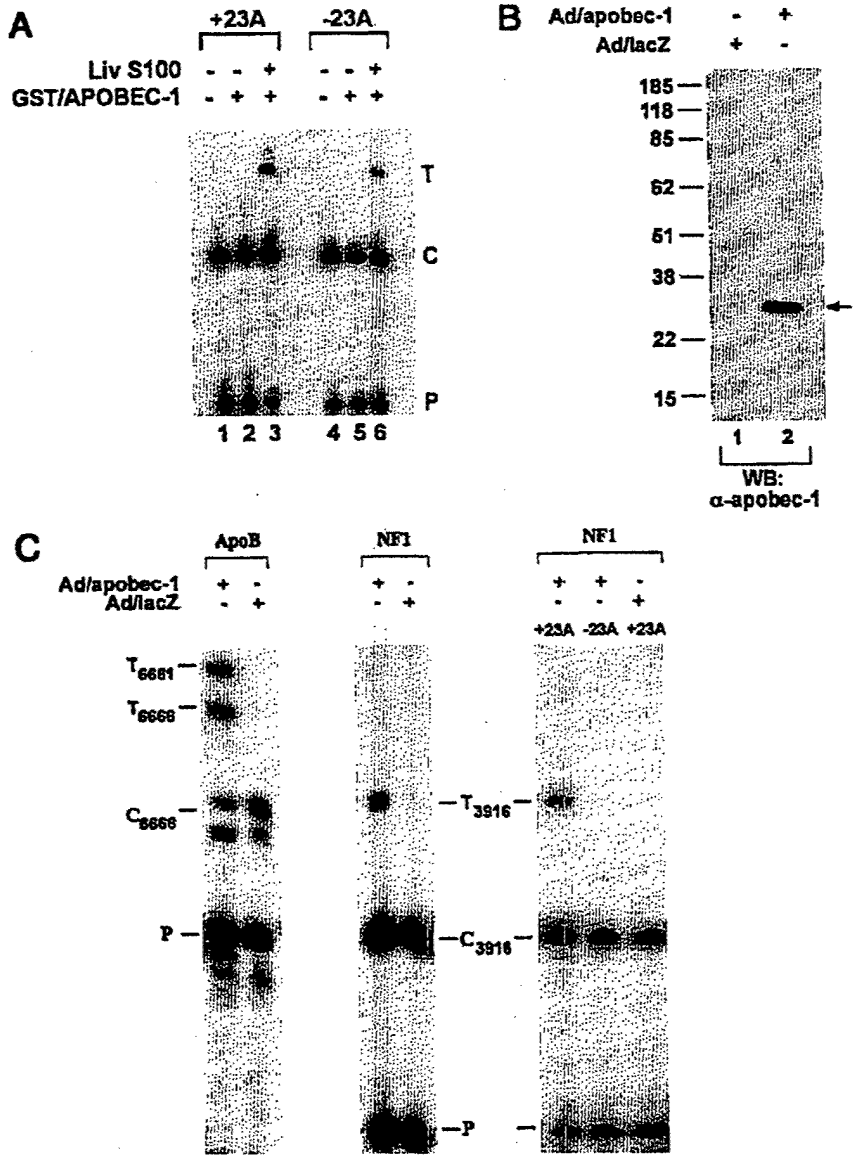

Figure 7 apobec-1 mediation of C→U editing of NF1 RNA. *A*, Assays of in vitro editing of RNA, performed with 20 fmol synthetic NF1 RNA either containing (+23A) or lacking (−23A) exon 23 A, in the presence of 250 ng recombinant GST/APOBEC-1 and 50 μg bovine liver extract (Liv S100). After in vitro incubation, the RNA was extracted, and cDNA was prepared for analysis by primer extension (see the "Material and Methods" section). The mobilities of the primer (P) and of the unedited (C) and edited (T) cDNA are indicated to the right of the gel. *B*, Adenovirus-mediated expression of apobec-1. HepG2 cells, from a human hepatoma cell line, were infected with recombinant adenovirus encoding either apobec-1 (Ad/apobec-1) or the bacterial β-galactosidase (Ad/lacZ). Forty-eight hours after infection, cell lysates were prepared and were subjected to western blot analysis with rabbit α-apobec-1 IgG. Migration of the 27-kD apobec-1 immunoreactive band is indicated by an arrow to the right of the gel, and molecular-weight standards are indicated to the left of the gel. *C*, Total RNA extracted from HepG2 cells infected with either Ad/apobec-1 or Ad/lacZ and subjected to RT-PCR for amplification of apoB (*left panel*) and NF1 (*middle panel*) mRNAs flanking the edited base. Primer-extension analysis was performed and was analyzed by PAGE with 8% acrylamide containing urea. To differentiate the editing of RNA in the two alternatively spliced NF1 transcripts (lanes ±23A), the PCR products were fractionated through agarose gels, and the two products were isolated and were individually subjected to primer-extension analysis (*right panel*). The locations of the primer and of unedited (C) and edited (U) primer-extension products, for both apoB and NF1, are indicated to the left or right of the gels. This is a representative of three independent assays.

exon. These amplicons were individually isolated and were subjected to primer-extension analysis, and the extent of C→U editing was determined. As indicated in figure 6*B*, C→U editing was found only in transcripts containing exon 23A. This approach was applied to the range of tumors studied, and the results demonstrated a strong positive correlation between the relative proportions of exon 23A–containing transcripts and the extent of C→U editing of RNA (fig. 6C). These findings strongly suggest a functional relationship between the presence of exon 23A and the editing of NF1 RNA.

apobec-1 as the Mediator of C→U Editing of NF1 RNA In Vivo and In Vitro

We employed two complementary approaches to confirm the suspected role of apobec-1 in C→U editing of NF1. In the first approach, we incubated synthetic NF1 transcripts that contained the unedited cytidine at nt 3916 and that either included (+23A) or lacked (−23A) the alternatively spliced downstream exon, with apobec-1 and S100 extracts. The results of these assays (fig. 7*A*) reveal that C→U editing of NF1 RNA can be reproduced in vitro and that transcripts containing exon 23A are more extensively edited (12% ± 1.7% U; $n = 3$), compared to transcripts lacking this alternatively spliced exon (3.9% ± 0.8% U; $n = 3$; $P < .001$). In the second approach, we used adenovirus-mediated transduction of apobec-1 to demonstrate a gain of function in cell culture. For this purpose, we turned to HepG2 cells, a human liver–derived cell line that expresses apoB RNA and NF1 mRNA but that does not express endogenous apobec-1 (Giannoni et al. 1994). HepG2 cells were infected with either adenovirus apobec-1 or lacZ, and cell lysates were prepared for protein and RNA extraction 48 h later. The results confirm the efficient induction of editing of apoB RNA after introduction of apobec-1 (see the western blot in fig. 7*B*) and reveal C→U editing at the canonical site (nt 6666), as well as hyperediting of upstream cytidines (C6661), as noted elsewhere (Sowden et al. 1996; Yamanaka et al. 1996) (fig. 7*C*, *left*); RNA from these same cells demonstrated C→U editing of NF1 RNA (fig. 7*C*, *middle*), with no such change, in either transcript, after lacZ transfection. Further analysis of these NF1 RNA species reveals that C→U editing was detectable only in transcripts containing exon 23A (fig. 7*C*, *right*), confirming and extending findings from the tumors analyzed above.

Discussion

Several mechanisms exist for amplification of the repertoire of genes encoded in chromosomal DNA. Posttranscriptional regulation encompasses one such level of control and includes editing of RNA, which has recently emerged as an important restriction point in the species- and tissue-specific modulation of gene expression (Maas and Rich 2000). The central conclusion of the present study demonstrates that C→U editing of NF1 RNA occurs in a subset of tumor samples that have at least two distinguishing characteristics that distinguish them from those tumors in which editing of RNA does not occur; these characteristics are (1) the presence of apobec-1 mRNA and (2) the preferential inclusion of a downstream exon, 23A, in the edited transcript. The findings (*a*) add support to the hypothesis that, in the regulation of mRNA metabolism, apobec-1 may play a role beyond that of its originally identified target, apoB, and (*b*) provide evidence that alternative splicing of NF1 RNA may be an important component of C→U editing of this transcript. Each of these observations merits additional discussion.

apobec-1 is an RNA-specific cytidine deaminase whose expression, in humans, is confined to the luminal gastrointestinal tract (Hadjiagapiou et al. 1994; Lau et al. 1994). apobec-1 functions as a dimeric subunit component of a multicomponent holoenzyme and mediates site-specific deamination of a single cytidine in the nuclear apoB transcript. This C→U RNA-editing reaction results in the production of a truncated protein, apoB48, required for intestinal lipid transport (Chen et al. 1987; Powell et al. 1987; Teng et al. 1993). Accordingly, the finding that apobec-1 mRNA is expressed in neuronal tumors from patients with NF1 represents the first demonstration, in humans, of apobec-1 expression in cells other than epithelial cells lining the gastrointestinal tract (Hadjiagapiou et al. 1994; Lau et al. 1994). apobec-1 mRNA expression is widespread in the mouse and rat, and C→U RNA editing activity can be demonstrated in tissue extracts from numerous organs (Greeve et al. 1993; Nakamuta et al. 1995; Hirano et al. 1997; Qian et al. 1997). Nevertheless, the mechanism by which apobec-1 expression is confined to the gastrointestinal tract in humans has not been clarified. Analyses undertaken by several groups have revealed few informative features of the proximal promoter region of the human *APOBEC-1* gene, and no additional insight has been gained through comparative analyses of the murine, rat, and human loci (Greeve et al. 1993; Nakamuta et al. 1995; Hirano et al. 1997; Qian et al. 1997). apobec-1 mRNA expression has been examined in a number of human carcinomas (Greeve et al. 1999), in light of the phenotype associated with forced overexpression of apobec-1 in transgenic animals, in which promiscuous C→U RNA editing of other target transcripts has been associated with hepatocellular carcinoma (Yamanaka et al. 1996, 1997). These studies, in human cancer tissues, concluded that apobec-1 mRNA is detectable only in cancers arising in the luminal gastrointestinal tract (Greeve et al. 1999), a finding that previously had been noted in normal tissue (Greeve et al. 1993; Hadjiagapiou et al. 1994; Lau et al. 1994). Ac-

cordingly, overexpression of apobec-1 does not appear to be a general feature of malignancy; this said, the factors that permit expression of apobec-1 mRNA in a subset of PNSTs from patients with NF1 will require additional investigation.

In considering the possibility that apobec-1 was involved in C→U editing of NF1, we were intrigued by the earlier observations, by Skuse and colleagues, that the NF1 RNA region flanking the edited base contains only ~50% identity to the canonical apoB RNA sequence, particularly within an 11-nt motif referred to as the "mooring sequence" (Backus and Smith 1992; Skuse et al. 1996). We suspected, as did Skuse and colleagues, that this degree of mismatch would severely impair the efficiency of C→U RNA editing (Skuse et al. 1996). This suspicion is consistent with the finding that C→U editing of NF1 RNA produces ≤20% UGA (edited RNA)—in contrast to the situation with intestinal apoB mRNA, in which, typically, >90% exists in the UAA (edited) form (Chen et al. 1987; Powell et al. 1987). The mechanisms accounting for these quantitative differences remain to be elucidated but include, in addition to structural features of the transcript that are associated with the optimal nucleotide sequence, distinctive requirements for *trans*-acting factors.

The functional significance, if any, of C→U editing of NF1 RNA remains unresolved; in particular, it is widely recognized that second-hit somatic mutations occur in the wild-type *NF1* allele in many PNSTs in patients with neurofibromatosis (reviewed in Cichowski and Jacks 2001). Furthermore, it should be emphasized that, with the exception of C→T changes at nt 3916, we did not systematically exclude somatic mutations in the PNSTs investigated in this study; nevertheless, at least from a theoretical standpoint, the finding that a subset of tumors from patients with NF1 demonstrate C→U RNA editing supports the hypothesis that modifier genes (in this case, apobec-1) may play a role in the heterogeneity of molecular defects. The corollary hypothesis is that C→U editing of NF1 RNA creates a translational stop codon, potentially leading to premature truncation of neurofibromin. We attempted to demonstrate the presence of a truncated protein corresponding to the edited mRNA in cell lysates from clonal intestinal-cancer cell lines supporting >15% C→U editing, but we were successful only in identifying the full-length form of the protein (data not shown). Whether this reflects technical limitations of the reagents or other explanations is currently unknown. Thus, the question of whether the edited NF1 RNA encodes a truncated protein in vivo is still unresolved.

Studies of NF1 mRNA in affected patients have revealed an ~50% incidence of splicing abnormalities (Park and Pivnick 1998). The majority of these splicing defects are predicted to result in protein truncations, and the current findings are certainly consistent with this general expectation; however, the results from this recent survey of splicing abnormalities in NF1 failed to reveal any specific feature associated with exon 23A, nor was there any particular clustering of alternative splice defects, which would favor inclusion of this exon (Costa et al. 2001). Exon 23A itself plays an important role in the function of neurofibromin, as inferred from targeted deletion of this region in mice, which results in a learning deficit (Costa et al. 2001). These findings suggest that there may be important parallels between the murine and human genes for NF1, parallels that could be investigated with surrogate models. Indeed, an important series of questions emerging from current studies concerns the possibility that C→U editing of NF1 RNA may be experimentally approached by murine models. This is an attractive possibility, since our lab and others have generated mutant strains in which apobec-1 has been deleted through homologous recombination. Additionally, the auxiliary subunit of the enzyme that edits apoB RNA recently has been cloned (Lellek et al. 2000; Mehta et al. 2000), and its role in alternative splicing and C→U editing of NF1 RNA will be of interest. In this regard, studies have demonstrated that an apobec-1–related RNA-specific deaminase, ADAR2, which mediates A→I editing of double-stranded RNA, also plays a role in alternative splicing (Rueter et al. 1999); this function will need to be examined in the context of apobec-1 and NF1 RNA. These and other issues related to the molecular mechanisms of posttranscriptional regulation will be the focus of future reports.

Acknowledgments

This work was supported by National Institutes of Health (NIH) grants HL-38180 and DK-56260 and NIH Digestive Disease Research Core Center grant DK-52574 (all to N.O.D.). The authors acknowledge the generous assistance of Drs. David N. Louis (Massachusetts General Hospital, Boston) and Priscilla Short (University of Chicago Hospitals) for their provision of samples for these analyses. In addition, the authors acknowledge their colleagues, Valerie Blanc, Libby Newberry, and Jeffrey Henderson, for their valuable insights and discussion.

Electronic-Database Information

Accession numbers and the URL for data in this article are as follows:

Online Mendelian Inheritance in Man (OMIM), http://www.ncbi.nlm.nih.gov/Omim/ (for NF1 [MIM 162200], APOB [MIM 107730], and APOBEC-1 [MIM 600130])

References

Anant S, Davidson NO (2000) An AU-rich sequence element (UUUN[A/U]U) downstream of the edited C in apolipopro-

tein B mRNA is a high-affinity binding site for Apobec-1: binding of Apobec-1 to this motif in the 3′ untranslated region of c-myc increases mRNA stability. Mol Cell Biol 20: 1982–1992

Anant S, MacGinnitie AJ, Davidson NO (1995) apobec-1, the catalytic subunit of the mammalian apolipoprotein B mRNA editing enzyme, is a novel RNA-binding protein. J Biol Chem 270:14762–14767

Anant S, Yu H, Davidson NO (1998) Evolutionary origins of the mammalian apolipoproteinB RNA editing enzyme, apobec-1: structural homology inferred from analysis of a cloned chicken small intestinal cytidine deaminase. Biol Chem 379:1075–1081

Andersen LB, Fountain JW, Gutmann DH, Tarle SA, Glover TW, Dracopoli NC, Housman DE, Collins FS (1993) Mutations in the neurofibromatosis 1 gene in sporadic malignant melanoma cell lines. Nat Genet 3:118–121

Ars E, Serra E, Garcia J, Kruyer H, Gaona A, Lazaro C, Estivill X (2000) Mutations affecting mRNA splicing are the most common molecular defects in patients with neurofibromatosis type 1. Hum Mol Genet 9:237–247

Ashkenas J (1997) Gene regulation by mRNA editing. Am J Hum Genet 60:278–283

Backus JW, Schock D, Smith HC (1994) Only cytidines 5′ of the apolipoprotein B mRNA mooring sequence are edited. Biochim Biophys Acta 1219:1–14

Backus JW, Smith HC (1992) Three distinct RNA sequence elements are required for efficient apolipoprotein B (apoB) RNA editing in vitro. Nucleic Acids Res 20:6007–6014

Basu TN, Gutmann DH, Fletcher JA, Glover TW, Collins FS, Downward J (1992) Aberrant regulation of ras proteins in malignant tumour cells from type 1 neurofibromatosis patients. Nature 356:713–715

Bollag G, Clapp DW, Shih S, Adler F, Zhang YY, Thompson P, Lange BJ, Freedman MH, McCormick F, Jacks T, Shannon K (1996) Loss of NF1 results in activation of the Ras signaling pathway and leads to aberrant growth in haematopoietic cells. Nat Genet 12:144–148

Cappione AJ, French BL, Skuse GR (1997) A potential role for NF1 mRNA editing in the pathogenesis of NF1 tumors. Am J Hum Genet 60:305–312

Chen SH, Habib G, Yang CY, Gu ZW, Lee BR, Weng SA, Silberman SR, Cai SJ, Deslypere JP, Rosseneu M, Gotto AM, Li WH, Chan L (1987) Apolipoprotein B-48 is the product of a messenger RNA with an organ-specific in-frame stop codon. Science 238:363–366

Cichowski K, Jacks T (2001) NF1 tumor suppressor gene function: narrowing the GAP. Cell 104:593–604

Costa RM, Yang T, Huynh DP, Pulst SM, Viskochil DH, Silva AJ, Brannan CI (2001) Learning deficits, but normal development and tumor predisposition, in mice lacking exon 23a of Nf1. Nat Genet 27:399–405

Davidson NO, Shelness GS (2000) Apolipoprotein B: mRNA editing, lipoprotein assembly, and presecretory degradation. Annu Rev Nutr 20:169–193

DeClue JE, Papageorge AG, Fletcher JA, Diehl SR, Ratner N, Vass WC, Lowy DR (1992) Abnormal regulation of mammalian p21ras contributes to malignant tumor growth in von Recklinghausen (type 1) neurofibromatosis. Cell 69: 265–273

Driscoll DM, Lakhe-Reddy S, Oleksa LM, Martinez D (1993) Induction of RNA editing at heterologous sites by sequences in apolipoprotein B mRNA. Mol Cell Biol 13:7288–7294

Funahashi T, Giannoni F, DePaoli AM, Skarosi SF, Davidson NO (1995) Tissue-specific, developmental and nutritional regulation of the gene encoding the catalytic subunit of the rat apolipoprotein B mRNA editing enzyme: functional role in the modulation of apoB mRNA editing. J Lipid Res 36: 414–428

Giannoni F, Bonen DK, Funahashi T, Hadjiagapiou C, Burant CF, Davidson NO (1994) Complementation of apolipoprotein B mRNA editing by human liver accompanied by secretion of apolipoprotein B48. J Biol Chem 269:5932–5936

Greeve J, Altkemper I, Dieterich JH, Greten H, Windler E (1993) Apolipoprotein B mRNA editing in 12 different mammalian species: hepatic expression is reflected in low concentrations of apoB-containing plasma lipoproteins. J Lipid Res 34:1367–1383

Greeve J, Lellek H, Apostel F, Hundoegger K, Barialai A, Kirsten R, Welker S, Greten H (1999) Absence of APOBEC-1 mediated mRNA editing in human carcinomas. Oncogene 18:6357–6366

Guha A, Lau N, Huvar I, Gutmann D, Provias J, Pawson T, Boss G (1996) Ras-GTP levels are elevated in human NF1 peripheral nerve tumors. Oncogene 12:507–513

Hadjiagapiou C, Giannoni F, Funahashi T, Skarosi SF, Davidson NO (1994) Molecular cloning of a human small intestinal apolipoprotein B mRNA editing protein. Nucleic Acids Res 22:1874–1879

Hersberger M, Innerarity TL (1998) Two efficiency elements flanking the editing site of cytidine 6666 in the apolipoprotein B mRNA support mooring-dependent editing. J Biol Chem 273:9435–9442

Hirano K, Min J, Funahashi T, Davidson NO (1997) Cloning and characterization of the rat apobec-1 gene: a comparative analysis of gene structure and promoter usage in rat and mouse. J Lipid Res 38:1103–1119

Hirano K, Young SG, Farese RV Jr, Ng J, Sande E, Warburton C, Powell-Braxton LM, Davidson NO (1996) Targeted disruption of the mouse apobec-1 gene abolishes apolipoprotein B mRNA editing and eliminates apolipoprotein B48. J Biol Chem 271:9887–9890

Kozarsky KF, Bonen DK, Giannoni F, Funahashi T, Wilson JM, Davidson NO (1996) Hepatic expression of the catalytic subunit of the apolipoprotein B mRNA editing enzyme (apobec-1) ameliorates hypercholesterolemia in LDL receptor-deficient rabbits. Hum Gene Ther 7:943–957

Lau N, Feldkamp MM, Roncari L, Loehr AH, Shannon P, Gutmann DH, Guha A (2000) Loss of neurofibromin is associated with activation of RAS/MAPK and PI3-K/AKT signaling in a neurofibromatosis 1 astrocytoma. J Neuropathol Exp Neurol 59:759–767

Lau PP, Zhu HJ, Baldini A, Charnsangavej C, Chan L (1994) Dimeric structure of a human apolipoprotein B mRNA editing protein and cloning and chromosomal localization of its gene. Proc Natl Acad Sci USA 91:8522–8526

Lee RM, Hirano K, Anant S, Baunoch D, Davidson NO (1998) An alternatively spliced form of apobec-1 messenger RNA is overexpressed in human colon cancer. Gastroenterology 115:1096–1103

Lellek H, Kirsten R, Diehl I, Apostel F, Buck F, Greeve J (2000) Purification and molecular cloning of a novel essential component of the apolipoprotein B mRNA editing enzyme-complex. J Biol Chem 275:19848–19856

Li Y, O'Connell P, Breidenbach HH, Cawthon R, Stevens J, Xu G, Neil S, Robertson M, White R, Viskochil D (1995) Genomic organization of the neurofibromatosis 1 gene (NF1). Genomics 25:9–18

Maas S, Rich A (2000) Changing genetic information through RNA editing. Bioessays 22:790–802

MacGinnitie AJ, Anant S, Davidson NO (1995) Mutagenesis of apobec-1, the catalytic subunit of the mammalian apolipoprotein B mRNA editing enzyme, reveals distinct domains that mediate cytosine nucleoside deaminase, RNA binding, and RNA editing activity. J Biol Chem 270:14768–14775

Madsen P, Anant S, Rasmussen HH, Gromov P, Vorum H, Dumanski JP, Tommerup N, Collins JE, Wright CL, Dunham I, MacGinnitie AJ, Davidson NO, Celis JE (1999) Psoriasis upregulated phorbolin-1 shares structural but not functional similarity to the mRNA-editing protein apobec-1. J Invest Dermatol 113:162–169

Mehta A, Kinter MT, Sherman NE, Driscoll DM (2000) Molecular cloning of apobec-1 complementation factor, a novel RNA-binding protein involved in the editing of apolipoprotein B mRNA. Mol Cell Biol 20:1846–1854

Morrison JR, Paszty C, Stevens ME, Hughes SD, Forte T, Scott J, Rubin EM (1996) Apolipoprotein B RNA editing enzyme-deficient mice are viable despite alterations in lipoprotein metabolism. Proc Natl Acad Sci USA 93:7154–7159

Nakafuku M, Nagamine M, Ohtoshi A, Tanaka K, Toh-e A, Kaziro Y (1993) Suppression of oncogenic Ras by mutant neurofibromatosis type 1 genes with single amino acid substitutions. Proc Natl Acad Sci USA 90:6706–6710

Nakamuta M, Oka K, Krushkal J, Kobayashi K, Yamamoto M, Li WH, Chan L (1995) Alternative mRNA splicing and differential promoter utilization determine tissue-specific expression of the apolipoprotein B mRNA-editing protein (Apobec1) gene in mice: structure and evolution of Apobec1 and related nucleoside/nucleotide deaminases. J Biol Chem 270:13042–13056

National Institutes of Health Consensus Development Conference (1988) Neurofibromatosis: conference statement. Arch Neurol 45:575–578

Park VM, Pivnick EK (1998) Neurofibromatosis type 1 (NF1): a protein truncation assay yielding identification of mutations in 73% of patients. J Med Genet 35:813–820

Powell LM, Wallis SC, Pease RJ, Edwards YH, Knott TJ, Scott J (1987) A novel form of tissue-specific RNA processing produces apolipoprotein-B48 in intestine. Cell 50:831–840

Qian X, Balestra ME, Innerarity TL (1997) Two distinct TATA-less promoters direct tissue-specific expression of the rat apo-B editing catalytic polypeptide 1 gene. J Biol Chem 272:18060–18070

Rueter SM, Dawson TR, Emeson RB (1999) Regulation of alternative splicing by RNA editing. Nature 399:75–80

Shah RR, Knott TJ, Legros JE, Navaratnam N, Greeve JC, Scott J (1991) Sequence requirements for the editing of apolipoprotein B mRNA. J Biol Chem 266:16301–16304

Sherman LS, Atit R, Rosenbaum T, Cox AD, Ratner N (2000) Single cell Ras-GTP analysis reveals altered Ras activity in a subpopulation of neurofibroma Schwann cells but not fibroblasts. J Biol Chem 275:30740–30745

Skuse GR, Cappione AJ (1997) RNA processing and clinical variability in neurofibromatosis type I (NF1). Hum Mol Genet 6:1707–1712

Skuse GR, Cappione AJ, Sowden M, Metheny LJ, Smith HC (1996) The neurofibromatosis type I messenger RNA undergoes base-modification RNA editing. Nucleic Acids Res 24:478–485

Skuse GR, Ludlow JW (1995) Tumour suppressor genes in disease and therapy. Lancet 345:902–906

Sowden M, Hamm JK, Smith HC (1996) Overexpression of APOBEC-1 results in mooring sequence-dependent promiscuous RNA editing. J Biol Chem 271:3011–3017

Teng B, Burant CF, Davidson NO (1993) Molecular cloning of an apolipoprotein B messenger RNA editing protein. Science 260:1816–1819

Yamanaka S, Poksay KS, Arnold KS, Innerarity TL (1997) A novel translational repressor mRNA is edited extensively in livers containing tumors caused by the transgene expression of the apoB mRNA-editing enzyme. Genes Dev 11:321–333

Yamanaka S, Poksay KS, Balestra ME, Zeng GQ, Innerarity TL (1994) Cloning and mutagenesis of the rabbit ApoB mRNA editing protein: a zinc motif is essential for catalytic activity, and noncatalytic auxiliary factor(s) of the editing complex are widely distributed. J Biol Chem 269:21725–21734

Yamanaka S, Poksay KS, Driscoll DM, Innerarity TL (1996) Hyperediting of multiple cytidines of apolipoprotein B mRNA by APOBEC-1 requires auxiliary protein(s) but not a mooring sequence motif. J Biol Chem 271:11506–11510